TABLE OF CONTENTS

12 articles · Pages 1–107

Prenatal Diagnosis and Pediatric Urology 1–13

01. Antenatal Diagnosis of Congenital Urinary Tract Malformations 1–13

TOUABTI Laldja-Souhem; LATRECHE Salah; TOUABTI Nabila; HABCHI Nawel

Pediatric Neurosurgery 14–18

02. Severe Craniocervical Junction Stenosis in Achondroplasia: Two Pediatric Cases and Their Surgical Indications 14–18

BOUDJELOUD Yasmina; HABCHI Nawel; MAHI Naziha; TLIBA Souhil

Neuro-Oncology 19–46

03. Histological Necrosis and IDH Status in Glioblastoma: Contribution of a Prospective Study and VEGFR2 Redocking 19–36

HASSANI Lynda; HABCHI Nawel; TLIBA Souhil

04. Intraventricular WHO Grade 1 Glioneuronal Tumor in a Pediatric Patient: A Rare Third Ventricular Presentation 37–46

OUADI Hayet; HARCHAOUI Nabila; ATROUNE Lynda; YOUSFI Yamina

Spinal Neurosurgery 47–65

05. Spinal Metastases: Clinical Features, Imaging and Prognosis in 52 Patients 47–60

ABDELMALEK Adel; HABCHI Nawel; KARA Samira; TLIBA Souhil

06. Intradural Teratoma of the Cauda Equina in an Adolescent Girl: A Rare Case Report and Review of the Literature 61–65

BELGACEM Ibrahim; DJOUADI Yasmina; ABOUDJABEL Mohamed; IZIROUEL Karim; AIT BACHIR Mustapha

TABLE OF CONTENTS

12 articles · Pages 1–107 · Continued

Pediatric Spinal Trauma 66–70

07. Post-Traumatic Cervicothoracic Spinal Epidural Hematoma in an 18-Month-Old Infant: A Case Report and Literature Review 66–70

HASNAOUI Amina; SIDI MAAMAR Mohamed Amokrane; ABDELMALEK Adel

Spinal Infections 71–79

08. Tuberculous Spondylodiscitis at the Neurosurgery Department of Donka Teaching Hospital in Conakry: Epidemiological, Clinical, Radiological and Therapeutic Aspects — A 27-Case Series 71–79

KOMARA CA; MANSARÉ L; DIALLO B; DIALLO AR; BAH D; BEAVOGUI LK

Neuro-Ophthalmology 80–84

09. Tolosa-Hunt Syndrome: Report of Two Cases 80–84

BEKRALAS Houria

Internal Medicine 85–93

10. Evaluation of Tolerance to Long-Term Corticosteroid Therapy in Patients with Systemic Diseases: A Monocentric Observational Study 85–93

BOUNZIRA Tewfik; BELARBI Nadia; GOUAICH Nesrine Lamia

Renal Epidemiology 94–102

11. Prevalence of Chronic Kidney Disease among Diabetic and/or Hypertensive Patients in the Laghouat District, Algeria: A Cross-Sectional Primary-Care Study 94–102

DJENANE Ahmed

Academic Mental Health 103–107

12. When Supervision Becomes a Source of Distress: A Pilot Study of Academic Mobbing, Anxiety, and Perceived Stress Among Postgraduate Students in Türkiye 103–107

SENGUL Pinar

Prenatal Diagnosis and Pediatric Urology

ANTENATAL DIAGNOSIS OF CONGENITAL URINARY TRACT MALFORMATIONS

TOUABTI Laldja-Souhem[1,*], LATRECHE Salah[1], TOUABTI Nabila[2] and HABCHI Nawel[2]

1: Department of Medicine, University of Sétif 1, Sétif, Algeria. Email:

2: Higher School of Sports Science and Technology (HSSST), Dely-Ibrahim, Algiers, Algeria.
***Corresponding Author:** TOUABTI Laldja-Souhem, Department of Medicine, University of Sétif 1, Sétif, Algeria. Email: souhemtouabti@gmail.com*

***Received:** August 13, 2026 — **Accepted:** September 15, 2026 — **Published:** October 01, 2026*

***Citation:** TOUABTI Laldja-Souhem, LATRECHE Salah, TOUABTI Nabila and HABCHI Nawel. Antenatal Diagnosis of Congenital Urinary Tract Malformations.*
OLCIAS Vol. 3, Issue 2.

ABSTRACT

Congenital urinary tract malformations are the most common congenital malformations in children. Their severity is related to their impact on the kidneys [Macher Ma et al., 1986]. Previously, they were diagnosed when complications developed, generally necessitating intervention because of renal damage. Nowadays, asymptomatic uropathies are detected more frequently, mainly as a result of the widespread introduction of antenatal screening [Bonnin F., Lottman H., 1996]. Management now has two preventive aims: in the short term, to prevent infection, and in the long term, to prevent deterioration of the function of the affected kidney. Fetal ultrasound examination has changed the management of congenital urinary tract malformations. As early as 1958, several authors [Kerzabi K., 1986] published studies on ultrasound examination of the pregnant uterus, the fetus and fetal abnormalities. However, it was not until 1970 that Garret [Garret W. J. et al., 1970] reported the first antenatal diagnosis of a multicystic kidney and fetal ascites.

In our country, congenital urinary tract malformations represent a substantial burden: approximately three-quarters of children receiving dialysis and awaiting transplantation have sequelae of a congenital urinary tract malformation, making this a major public health issue.

***Keywords:** Uropathies – Congenital malformations – Diagnosis*

INTRODUCTION

Why antenatal diagnosis? Failure to recognise these conditions at birth

Only 0.1% of cases are symptomatic at birth. The vast majority become apparent much later, when complications develop, such as pyelonephritis or even renal failure [Dodat H. et al., 2001].

The opportunity to make a therapeutic decision

Medical termination of pregnancy in lethal forms or those associated with severe sequelae, and early neonatal management in other cases [Bonnin F., Lottman H., 1996].

The malformation very often presents as urinary tract dilatation, raising several questions:

- What is the cause of this dilatation?
- Does it reflect simple hypotonia or a genuine obstruction to urinary flow?
- Does it affect fetal development and fetal and postnatal renal function?
- What are the implications for antenatal management?
- Can and should an in utero procedure be proposed?
- Should delivery be brought forward?
- Which postnatal investigations should be performed, and in what sequence?
- In which cases will postnatal surgery be essential?
- In which cases can spontaneous improvement and resolution be expected? [Mahan J. et al., 1982]

The surgical management of congenital urinary tract malformations has evolved in recent years. Treatment is now most often preventive, addressing both infection and the consequences of obstruction. Surgical indications have become more precise, better documented and less routine.

In our country, congenital urinary tract malformations represent a substantial burden: approximately three-quarters of children receiving dialysis and awaiting transplantation have sequelae of a congenital urinary tract malformation, making this a major public health issue.

These considerations prompted us to address this problem and develop a programme covering:

- Antenatal diagnosis of congenital urinary tract malformations in a sample of pregnant women followed at maternal and child health centres (PMI centres), together with screening and follow-up of congenital urinary tract malformations in infants.
- Antenatal diagnosis of congenital uropathies has been widely practised for only about twenty years. Therapeutic decisions require collaboration among paediatricians, surgeons, radiologists, laboratory specialists and bacteriologists. This collaboration should improve a prognosis that remains guarded, making screening a matter of genuine urgency.

RESEARCH METHODOLOGY: SCREENING SURVEY

1. Type of survey

This was a cross-sectional epidemiological survey involving active antenatal screening for congenital urinary tract malformations in a population of pregnant women in the Sétif health district during the year 2000.

2. Objectives

The objectives of the study were:

- To estimate the incidence of urinary tract malformations through antenatal diagnosis in pregnant women during the third trimester of pregnancy.
- To assess the kidneys, monitor their development, and evaluate the progression of lesions and the outcomes of management.
- To establish a protocol for antenatal screening and management of antenatally diagnosed congenital urinary tract malformations.

3. Study method

3.1. Target population

The target population comprised all pregnant women attending primary healthcare facilities in the Sétif health district during the third trimester of pregnancy as part of antenatal follow-up activities in 2010.

3.2. Study population

The study population was a representative sample of the target population, comprising 500 pregnant women in the third trimester of pregnancy.

4. Study protocol

Antenatal screening will be conducted in a representative sample of pregnant women attending PMI centres.

An ultrasound examination is performed during the third trimester, and the findings are confirmed by a second ultrasound examination 15 days to one month later. If the second examination is positive, an ultrasound examination will be performed after birth, on day 7, together with a diagnostic work-up. If the postnatal examination is negative, another ultrasound examination will be performed at one month to avoid false-negative findings.

5. Conduct of the survey

After prior authorisation had been obtained from the relevant authorities, a work plan was drawn up to launch the survey. Information and explanatory meetings were organised with the participation and coordination of the heads of the PMI centres. A working session was also held with the heads of radiology and obstetrics and gynaecology to agree on a schedule and organise radiological and ultrasound examinations without disrupting routine daily activities. To encourage active participation, a conference on congenital urinary tract malformations was held. At the end of this process, two liaison forms were developed.

Administrative arrangements: Approval from the supervisory authority was obtained following submission of an explanatory request outlining the relevance and value of this two-part survey.

Practical arrangements: Our approach involved contacting PMI centres to raise awareness among pregnant women at 37 weeks of gestation and encourage them to undergo repeated obstetric ultrasound examinations.

RESULTS

6. Results of antenatal screening

A representative sample of 500 women underwent systematic ultrasound examination during the third trimester of gestation. Detection of a urinary tract malformation will be confirmed by a second ultrasound examination 15 days to one month later. If the second examination is positive, the newborn undergoes ultrasound on day 7, followed by a complete work-up if the abnormality is confirmed.

6.1. Parental age

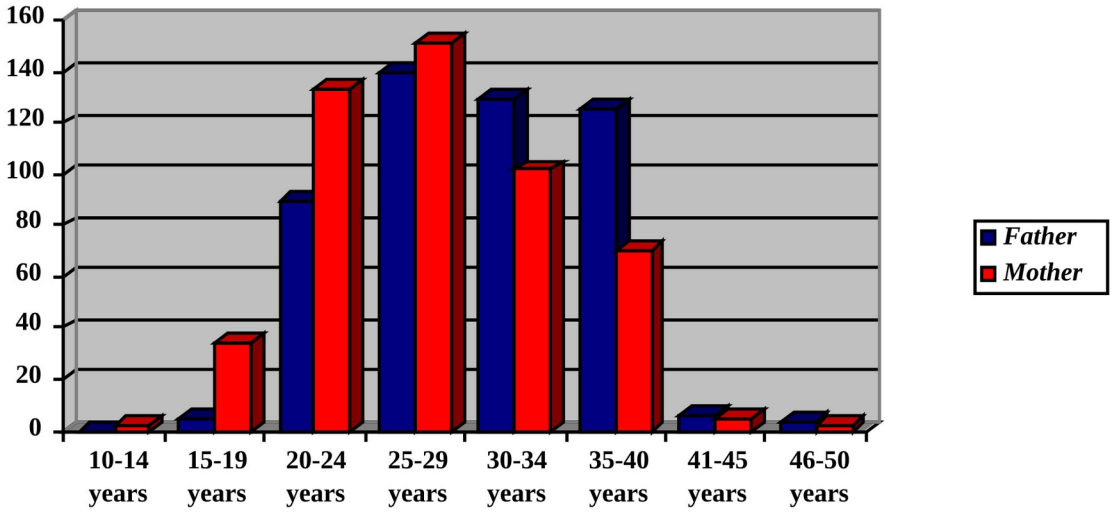


Figure 1: Parental age.

Maternal age lay within the 18–34-year range, corresponding to reproductive age:

2 women were aged 14 years.
33 women were aged 15–19 years.
133 women were aged 20–24 years.
152 women were aged 25–29 years.
102 women were aged 30–34 years.
77 women were older than 35 years.

Paternal age lay within the 25–40-year range:

90 men were aged 20–24 years.
140 men were aged 25–29 years.
130 men were aged 30–34 years.
126 men were aged 35–40 years.

6.2. Gestational age

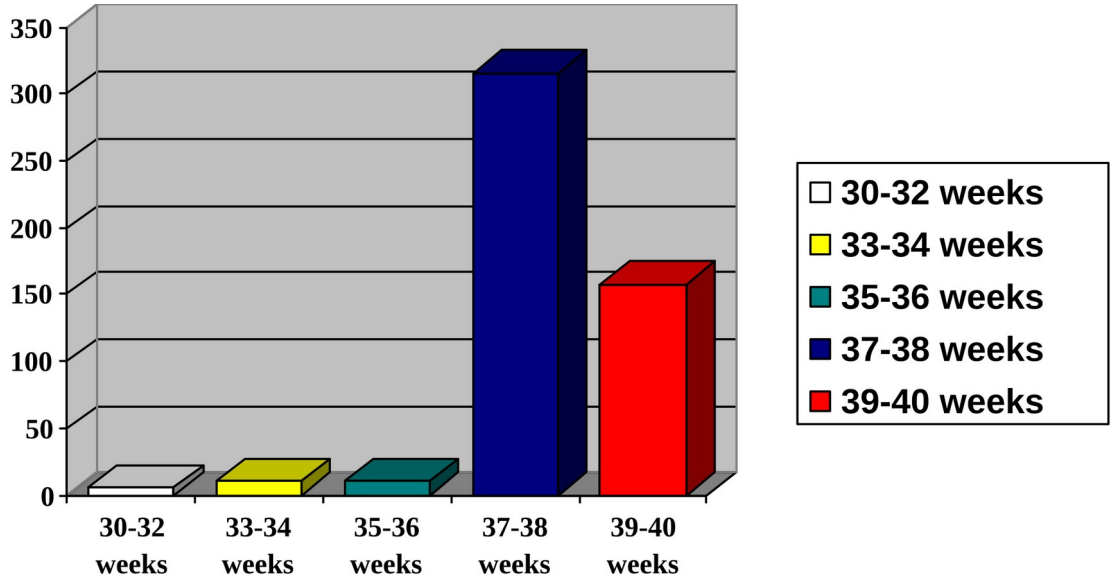


Figure 2: Gestational age.

Screening for congenital urinary tract malformations is performed during routine obstetric ultrasound examinations at the beginning of the third trimester of pregnancy, at 32 weeks of gestation.

6 ultrasound examinations were performed at 30–32 weeks of gestation.
10 ultrasound examinations were performed at 33–34 weeks of gestation.
10 ultrasound examinations were performed at 35–36 weeks of gestation.

To increase the detection rate, screening was intensified during the last month of gestation:

316 ultrasound examinations were performed at 37–38 weeks of gestation.
158 ultrasound examinations were performed at 39–40 weeks of gestation.

6.3. Gestational age and distribution of normal and abnormal ultrasound examinations during antenatal screening

Table I: Gestational age and distribution of normal and abnormal ultrasound examinations.

Gestational age (weeks)	Normal ultrasound	Abnormal ultrasound	Total examinations
30–32	5	1	6
33–34	6	4	10
35–36	5	5	10
37–38	301	15	316
39–40	144	14	158
TOTAL	**461**	**39**	**500**

Antenatal ultrasound detected 39 malformations from the 30th week of gestation onwards:

30–32 weeks: one urinary tract malformation.
33–34 weeks: 4 malformations, comprising 2 urinary tract and 2 neurological malformations.
35–36 weeks: 5 malformations, comprising 3 urinary tract and 2 neurological malformations.
37–38 weeks: 15 malformations, comprising 7 urinary tract and 8 neurological malformations.
39–40 weeks: 14 malformations, all neurological.

Detection of abnormalities of the urinary collecting system was best during the last month of pregnancy. Each abnormality was reassessed by a second ultrasound examination performed 15 days to one month later.

6.4. Malformations detected antenatally

Table II: Malformations detected antenatally.

Malformations	Number	Percentage	95% confidence interval
Neurological malformations	26	5.2	3.3–7.1
Urinary tract malformations	13	2.6	1.3–3.9
TOTAL	**39**	**7.8**	**6.4–10.2**

Thirty-nine abnormalities were detected in 500 fetuses. These comprised 26 neurological abnormalities, including 11 cases of anencephaly and 15 cases of hydrocephalus, giving an incidence of 26/500 = 5.2% (95% confidence interval: 3.3%–7.1%).

Thirteen urinary tract abnormalities were detected, giving an incidence of 13/500 = 2.6% (95% confidence interval: 1.3%–3.9%).

The overall incidence of the malformations encountered was 39/500 = 7.8% (95% confidence interval: 6.4%–10.2%).

Among the 13 urinary tract abnormalities, 2 deaths occurred at birth, and postnatal confirmation was not possible.

One false-positive finding was recorded, with a normal postnatal ultrasound examination confirmed by repeat examination one month later.

The incidence of confirmed urinary tract malformations was 10/500 = 2% (95% confidence interval: 0.8%–3.4%).

With 1,048 births per year in Sétif, approximately 21 urinary tract malformations per year can be expected.

This antenatal screening survey raised awareness among the population and obstetricians. Since then, obstetricians have referred all pregnant women whose ultrasound examination reveals a urinary tract abnormality.

A further 20 cases were detected in this way. Our study therefore covers all antenatally detected congenital urinary tract malformations, comprising 33 cases.

6.5. Urinary tract malformations detected at the first ultrasound examination

Table III: Urinary tract malformations detected at the first ultrasound examination (N = 33).

Urinary tract malformations	**Number**
Hydronephrosis	15
Hydroureteronephrosis	13
Multicystic kidneys	5
TOTAL	**33**
Amniotic fluid	
Oligohydramnios	16
Polyhydramnios	2

The first antenatal ultrasound examination detected 33 cases of congenital urinary tract malformations: hydronephrosis in 15 cases, hydroureteronephrosis in 13 cases and multicystic kidneys in 5 cases. Assessment of amniotic fluid most often revealed oligohydramnios, which was identified in 16 cases.

6.6. Progression of renal lesions on antenatal ultrasound examinations

Table IV: Progression of renal lesions on antenatal ultrasound examinations.

Progression of lesions	**Number**
Stable lesions	26
Worsening hydronephrosis	1
Worsening hydroureteronephrosis	3
Increasing bladder dilatation	3
Amniotic fluid	
Worsening oligohydramnios	5
Worsening polyhydramnios	1
New-onset oligohydramnios	1

Follow-up ultrasound performed 15 days to one month later showed stable findings in 26 cases, worsening hydroureteronephrosis in 3 cases, worsening hydronephrosis in 1 case and increasing bladder dilatation in 3 cases.

Amniotic fluid findings were abnormal in 18 cases and remained stable in 11. The following changes were observed:

• Worsening oligohydramnios in 5 cases.

• Worsening polyhydramnios in 1 case.

In addition, one new case of oligohydramnios was recorded.

6.7. Antenatally diagnosed hydronephrosis

Table V: Hydronephrosis (N = 15).

Unilateral involvement	11 cases
Bilateral involvement	4 cases
Oligohydramnios	10 cases
Polyhydramnios	0 cases

Antenatal ultrasound detected 15 cases of pelvicalyceal dilatation, including 11 with unilateral involvement.

Amniotic fluid was normal in 5 cases. Oligohydramnios was the most frequent finding, occurring in 10 cases.

6.8. Antenatally diagnosed hydroureteronephrosis

Table VI: Hydroureteronephrosis (N = 13).

Unilateral involvement	4 cases
Bilateral involvement	9 cases
Oligohydramnios	9 cases
Polyhydramnios	2 cases

Antenatal ultrasound detected 13 cases of ureteropelvic dilatation, including 9 with bilateral involvement. Oligohydramnios was the most frequent amniotic fluid abnormality, occurring in 9 cases. Polyhydramnios was found in 2 cases, and amniotic fluid was normal in 2 cases.

6.9. Antenatally diagnosed multicystic kidneys

Table VII: Multicystic kidneys (N = 5).

Unilateral involvement	0 cases
Bilateral involvement	5 cases
Oligohydramnios	5 cases

Five cases of multicystic kidneys were diagnosed antenatally. Bilateral involvement and oligohydramnios were present in all cases.

6.10. Agreement between antenatal and postnatal ultrasound examinations

Any urinary tract abnormality detected in utero should lead to an ultrasound examination after birth to confirm or exclude the finding. If the ultrasound examination is positive, further uroradiological and radionuclide investigations allow more precise characterisation of the abnormalities.

Table VIII: Agreement between antenatal and postnatal ultrasound examinations.

Antenatal ultrasound	Postnatal ultrasound	Number of cases
Hydronephrosis	Same appearance	9
Hydronephrosis with contralateral renal agenesis	Same appearance	1
Hydroureteronephrosis	Same appearance	9
Hydroureteronephrosis with contralateral renal agenesis	Same appearance	1
Bilateral multicystic kidneys	Bilateral hydroureteronephrosis	3
Bilateral multicystic kidneys	Bilateral hydronephrosis	1
Bilateral multicystic kidneys	Right hydronephrosis	1
Left hydronephrosis	Left hydroureteronephrosis	2
Unilateral hydronephrosis	Bilateral hydroureteronephrosis	2
Right hydronephrosis	Right hydroureteronephrosis	1
Hydroureteronephrosis	Normal kidney	1
Bilateral hydroureteronephrosis	Death at birth	2

The antenatal diagnosis of urinary tract dilatation was confirmed postnatally in 20 cases. In 10 cases, the diagnosis was incomplete or inaccurate. The most frequent diagnostic confusion was between multicystic kidneys and hydroureteronephrosis, reflecting the severity of the uropathy. Two deaths occurred at birth, and postnatal confirmation was not possible. A single false-positive finding was recorded: a case of hydroureteronephrosis in which postnatal ultrasound was normal, as confirmed by repeat examination one month later.

Among the 31 newborns assessed postnatally, agreement between the ultrasound findings was reported in 60.6% of cases.

6.11. Definitive postnatal aetiological diagnosis

The definitive diagnosis was established within a few days to a few weeks after birth.

Table IX: Definitive aetiological diagnosis.

Definitive aetiological diagnosis (30 cases)	Number
Ureteropelvic junction obstruction	12
Megaureter	9
Vesicoureteral reflux	2
Right bladder diverticulum with hydroureteronephrosis	1
Posterior urethral valves	3
Duplex collecting system	2
Megacystis–megaureter	1

DISCUSSION

The detection of a uropathy in utero primarily raises the issues of identifying the abnormality and determining its severity. Ultrasound examination seeks to answer three questions:

• At what anatomical level is the abnormality located?

• What type of abnormality is present?

• What is the functional status of the kidneys?

Antenatal ultrasound allows visualisation of 90% of fetal kidneys between 17 and 20 weeks of gestation, and 95% by 22 weeks. The urinary tract abnormalities identified involve either the renal parenchyma itself, with dysplastic lesions of the renal cortex, or the urinary collecting system. Renal function is assessed indirectly, particularly through the characteristics of the amniotic fluid, which must be interpreted in relation to gestational age. Severe uropathies are characterised by the development of early renal dysplasia upstream of an obstructive uropathy. Conversely, dilatation of the collecting system may regress without apparent sequelae. Although antenatal ultrasound allows population screening, it does not always provide a precise diagnosis: observation of urinary tract dilatation before birth does not necessarily establish a diagnosis of true uropathy. Antenatal diagnosis nevertheless has limitations. Ultrasound diagnostic errors have included confusion between dilatation of the gastrointestinal tract and pelvicalyceal dilatation, and imprecision regarding the severity, extent and unilateral or bilateral nature of lesions of the urinary collecting system.

Published series report ultrasound diagnostic error rates ranging from 23% to 61%, with sometimes serious consequences. In a series of 38 terminations of pregnancy for major urinary tract abnormalities, Gauderer et al. [1984] reported 3 unjustified terminations. The series of Huston et al. [1990] showed that 39% of prophylactic caesarean deliveries were followed by early infant death due to respiratory or renal failure. These poor outcomes led the authors to seek a more precise assessment of fetal renal function by evaluating the ultrasound appearance of the renal parenchyma, the volume of amniotic fluid and the amount of urine produced by the fetal kidneys. Oligohydramnios or anhydramnios in the context of a uropathy is a definite marker of severity. A marked reduction in amniotic fluid volume indicates impaired renal function and may provide information about disease progression. Renal function can also be assessed through direct evaluation of renal parenchymal thickness. These two criteria seek to reflect the extent of distension of the urinary tract.

In our series, our initial objective was to involve obstetricians in antenatal diagnosis in general and in the diagnosis of congenital urinary tract malformations in particular. This was not easy, and we therefore sought the assistance of the most senior practitioners with the greatest experience in obstetric ultrasound. Our aim was to detect uropathies antenatally and, above all, to ensure early management in the immediate postnatal period.

In our series, 10 uropathies were detected and confirmed postnatally among 500 pregnant women. Urinary tract malformations ranked second after central nervous system malformations, as reported in the literature. The incidence of antenatally detected uropathies is closely related to the criteria used to define a urinary tract abnormality, namely the appearance of dilatation of the urinary collecting system. Approximately 1% of pregnancies are estimated to be affected.

Our series reports an incidence of 2% of live births, whereas the theoretical incidence is 0.9%–1% [100].

In a study of 6,292 pregnancies, Livera et al. [1989] reported that 1.46% of fetal ultrasound examinations performed at 28 weeks of gestation suggested a uropathy. After birth, only 48% of suspected cases, representing 0.71% of the pregnancies studied, had a confirmed uropathy. In 1992, Johnson et al. studied 7,530 pregnancies and identified suspected fetal uropathy in 0.74%. Only 38% of the infants had a uropathy confirmed after birth, corresponding to 0.28% of the pregnancies studied. Reported incidence varies among authors, from 0.18% in the study by Fugelseth [1994] involving 22,310 pregnancies, to 1% in the study by Mouriquant [2004] involving 1,200 pregnancies.

Our prospective study found an incidence of 2%, comparable with other studies. Antenatal diagnosis is still in its early stages in our country, and no similar screening study had previously been performed.

The probability of detecting a urinary tract abnormality depends strongly on the experience of the ultrasonographer, for whom detection of a urinary tract malformation is easier in the second half of pregnancy. In our series, detection was substantially better towards the end of pregnancy, a finding also reported by other centres [Cambell S., Pearce J. M., 1995]. This observation is important because, in an era of budget restrictions and healthcare cost control, it supports provision of more than two fetal ultrasound examinations during pregnancy. The number of false positives could not be assessed accurately. We recorded only one case among the 500 pregnancies; subsequently, however, we received a further 20 confirmed cases of uropathy referred by obstetricians who had not participated in the screening programme.

Hydronephrosis due to ureteropelvic junction abnormalities and megaureters account for most antenatally detected renal dilatations, representing 66% of cases in our series. In recent years, immediate management has become increasingly non-surgical. This specific issue is the focus of much of the current research and debate.

Our antenatal screening survey therefore detected 30 cases of congenital urinary tract malformations confirmed postnatally. Ureteropelvic junction obstruction and megaureters remained the uropathies most frequently detected antenatally.

CONCLUSION

Antenatal and postnatal ultrasound play a fundamental role in the early management of congenital urinary tract malformations. Although the diagnostic and functional assessment of uropathies does not rely exclusively on ultrasound, it remains the first-line investigation in the immediate postnatal period, guiding subsequent assessment.

Accurate perinatal diagnosis of obstructive uropathy nevertheless remains a matter of debate. Although screening has already reduced the number of neonatal urological emergencies through improved postnatal management, its value in unilateral obstructive uropathies has yet to be demonstrated, because not every antenatal dilatation signifies obstruction. The postnatal work-up should not be undertaken in haste. Surgery is rarely required during the neonatal period, and many dilatations observed in utero regress spontaneously during the first months or years of life. Regular surveillance is nevertheless necessary until the ultrasound findings have normalised.

Decisions and the organisation of antenatal and postnatal care should be based on multidisciplinary discussion involving obstetricians, radiologists, laboratory specialists, neonatologists, nephrologists and surgeons. Effective cooperation among the members of the multidisciplinary team provides the best assurance of prompt and efficient management.

REFERENCES

Bonnin F., Lottman H. (1996). Scintigraphie rénale: Un examen majeur pour les uropathies de l'enfant [Renal scintigraphy: a major investigation for childhood uropathies]. La presse medical; 25, No. 12: 571–2.

Brenbridge An, Chevalier Rl, Kaisser DL. (1986). Increased renal cortical echogenicity in pediatric renal disease: histopathology correlations. J Clin Ultrasound; 14: 595–600.

Cambell S., Pearce J. M. (1995). The prenatal diagnosis of fetal structural anomalies by ultrasound. Clin obstet Gynecol; 10: 475–506.

Couture A. (1988). Les malformations congénitales: Diagnostic anté natal et devenir [Congenital malformations: antenatal diagnosis and outcomes]. Couture A., Sauramps médical. Ed. Vigot, France, 1988.

Dodat H., Chatelard Ph., ChamPetier Th., Philibert M., Takvorian Ph., Chappuis JP. (1985). Les thérapeutiques chirurgicales in utéro [In utero surgical treatments]. Pédiatrie – Txxxx, No. 3: 237–245.

Dodat H., Dubois R., Szwarc S. (2001). Conduite à tenir prè et post-natale devant une dilatation des voies urinaires dépistées in utéro [Antenatal and postnatal management of urinary tract dilatation detected in utero]. Urology Congress, Paris.

Dubois R. (1994). Le méga-uretère primitif de l'enfant. Commentaires à propos de 88 observations (106 uretères) [Primary megaureter in children: comments on 88 cases (106 ureters)]. Medical thesis, Lyon, No. 117.

Duckett JW Jr. (1993). When to operate on neonatal hydronephrosis (editorial). Urology; 42: 617–9.

Economu H., Egginlon J. A., Broot Field DSK. (1994). The importance of late pregnancy scans for renal tract abnormalities. Prenatal diagnosis; 14: 177–80.

Fugelseth D., Liudemann R., Sande HA. (1994). Prenatal diagnosis of urinary tract anomalies. The value of two ultrasound examinations. Acta Obstet Gynecol Scand; 73: 290–293.

Garret W. J., Grunwald G., Robinson D. E. (1970). Prenatal diagnosis of fetal polycystic kidney by ultrasound. Aust. M. obstet gynecol; 10: 7–9.

Gasser B., Linder V., Bussier L., Faure C., Galatir L., Wilt M., Vetter J. M., Laborde K. (2001). Le rein foetal – Néphropathie foetale: Le point de vue du pathologiste [The fetal kidney – fetal nephropathy: the pathologist's perspective]. Physiology course. Hôpital Necker Enf-Mal, Paris.

Gauder M. W. L., Jassani M. N., Izant R. J. (1984). Ultrasonic antenatal diagnosis: will it change the spectrum of neonatal surgery? J Pediatr Surg; 19: 407–7.

Grasset D. (1970). La chirurgie conservative des hydronéphroses [Conservative surgery for hydronephrosis]. J Urol (Paris); 76: 252–272.

Greigj D., Raine PAM, Young DG, Azmy AF, Ruth. (1989). Value of antenatal diagnosis of abnormalities of the urinary tract. Br Med J; 298: 1417–19.

Homsy YL, Saad F., Laberge I., Willot P., Pinson C. (1990). Transitional hydronephrosis of the newborn and infant. J Urol; 144: 579–83.

Huston J. M., Mc Nay MB, Mc Kenzie J. R. Antenatal diagnosis of surgical disorders by ultrasonography. Lancet; 1: 621–3.

Johnson CE, Elder JS, Judge NE, Adeeb FN, Grisoni ER, Fattar DC. (1992). The accuracy of antenatal ultrasonography in identifying renal abnormalities. Am J Dis Child; 146: 1181–4.

Johnson JH, Evan JP, Glassberg KL. (1993). Hydronephrosis in children. A review of 219 personal cases. Urol Int; 51: 79–84.

Juskiewenski S., Moscovici J., Boussou F., et al. (1983). Le syndrome de la jonction pyélo urétérale chez l'enfant, à propos de 178 observations [Ureteropelvic junction obstruction in children: a report of 178 cases]. J Urology (Paris); 89: 173–82.

Kass E. J., Fink Benett D. (1990). Contemporary techniques for the radioisotopic evaluation of the dilated urinary tract. Urol Clin North Am; 17: 273–89.

Kerzabi K. (1986). Le diagnostic anté-natal: Apport de l'échographie et conduite à tenir [Antenatal diagnosis: the contribution of ultrasound and management]. DEMS thesis, Oran, 1986.

Livera LN, Brookfield DSK, Eggiuton JA, Hawnaur JM. (1989). Antenatal ultrasonography to detect fetal renal abnormalities: a prospective screening programme. Br Med; 298: 1421–23.

Macher Ma, LoiRat C., Pillion G., Mathieu H. (1986). Chronic renal insufficiency in the child. Arch Fr Pediatr; 43: 401–6.

Mahan J., Gonzales R., Godec C. J. (1982). Intrauterine obstructive uropathy: is early detection and intervention beneficial? Proc North Pediatr Soc, 1982.

Mouriquand P. (2004). Anomalie congénitale à l'écoulement des urines [Congenital abnormality of urinary outflow]. Interuniversity teaching course, Lyon.

N. Engl. J. Med. Report of the international fetal surgery registry: catheter shunt for fetal hydronephrosis and hydrocephalus. 315: 338–40.

Palmer J. M., Disandio M. (1995). Diuretic-enhanced duplex Doppler sonography in 33 children presenting with hydronephrosis: study of test sensitivity, specificity and precision. J Urol; 154: 1885–8.

Ring E., Petritsh P., Vilitis P. (1990). Therapy and prognosis of children with prenatally diagnosed urinary tract abnormalities. Wien klini woclienschr; Any 31: 102–16: 463–6.

Scott J. E. S., Renwinck M. (1988). Antenatal diagnosis of congenital abnormalities in the urinary tract: results from the northern region fetal abnormality survey. B J U; 62: 295–300.

Scott J. E. S., Renwinck M. (1988). Antenatal diagnosis of congenital abnormalities in the urinary tract: results from the northern region fetal abnormality survey. B J U; 62: 295–300.

Tripp Bj, Homsy Y. (1985). Neonatal hydronephrosis: controversy and treatment. J Pediatr Surg; 20: 376–87.

Pediatric Neurosurgery

SEVERE CRANIOCERVICAL JUNCTION STENOSIS IN ACHONDROPLASIA:
Two Pediatric Cases and Their Surgical Indications

BOUDJELOUD Yasmina[1], HABCHI Nawel[1], MAHI Naziha[1] and TLIBA Souhil[1]

1: Department of Neurosurgery, Frantz Fanon University Hospital, Blida, Saad Dahlab University Blida 1, Algeria

***Corresponding Author:** BOUDJELOUD Yasmina, Department of Neurosurgery, Frantz Fanon University Hospital, Blida, Saad Dahlab University Blida 1, Algeria*

***Received:** August 13, 2026 — **Accepted:** September 15, 2026 — **Published:** October 01, 2026*

Citation: BOUDJELOUD Yasmina, HABCHI Nawel, MAHI Naziha and TLIBA Souhil. Severe Craniocervical Junction Stenosis in Achondroplasia: Two Pediatric Cases and Their Surgical Indications.
OLCIAS Vol.3, Issue 2.

ABSTRACT

Introduction: Achondroplasia predisposes patients to craniocervical junction stenosis, which may compress the cervicomedullary junction (hypotonia, central apneas, sudden death). The objective is to present two pediatric cases assessed using the AFMS (Achondroplasia Foramen Magnum Score) and to discuss the surgical indication.

Materials and Methods: Two children with genetically confirmed achondroplasia underwent clinical assessment, MRI with AFMS scoring, and polysomnography.

Results:

Case 1 (girl, 16 months): severe axial hypotonia and inability to maintain head control. MRI: anteroposterior (AP) foramen magnum diameter = 7 mm, obliteration of the posterior CSF spaces, cervicomedullary compression, and no signal abnormality → AFMS 3.

Case 2 (boy, 3 years): falls and central apneas requiring ventilatory support. MRI: AP diameter < 7 mm, obliteration of the anterior and posterior CSF spaces, cervicomedullary compression, no signal abnormality, and moderate ventriculomegaly without intracranial hypertension → AFMS 3.

Both children are symptomatic with AFMS ≥ 3 and are being considered for cervicomedullary decompression at a multidisciplinary conference.

Conclusion: In symptomatic children with achondroplasia, an AFMS ≥ 3 (AP diameter ≤ 7 mm, obliteration of the CSF spaces) supports a surgical indication, even in the absence of spinal cord signal abnormality. Moderate ventriculomegaly is not a contraindication to decompression.

***Keywords:** Achondroplasia – AFMS – Foramen magnum – surgical decompression – child*

INTRODUCTION

Achondroplasia is the most common constitutional skeletal dysplasia, with an incidence of approximately 1 in 25,000 births. It is caused by an activating mutation of the FGFR3 gene, resulting in impaired endochondral ossification [1]. One of the most feared complications is foramen magnum stenosis, secondary to hypoplasia of the skull base. This stenosis may compress the cervicomedullary junction, presenting with axial hypotonia, central apneas, psychomotor delay, and, in severe cases, sudden death, with the risk estimated at up to 7.5% [2].

The AFMS (Achondroplasia Foramen Magnum Score), described by Cheung et al. in 2021, is a validated tool for stratifying the severity of stenosis. It ranges from 0 (normal) to 4 (compression with T2 hyperintensity). Stage 3 – compression without signal abnormality – is considered a surgical threshold [3].

The objective of this study is to present two pediatric cases of achondroplasia with severe foramen magnum stenosis and to discuss the surgical indications in light of recent data from the literature.

MATERIALS & METHODS

We report two cases of children with genetically confirmed achondroplasia who were managed in the Department of Neurosurgery at Blida University Hospital. Clinical data (age, sex, neurological signs, head circumference, polysomnography) and radiological data (brain and spinal MRI with measurement of the anteroposterior diameter of the foramen magnum and calculation of the AFMS) were collected. The presence of ventriculomegaly and possible hydrocephalus was assessed. Surgical indications were discussed at a multidisciplinary meeting involving neurosurgeons, pediatricians, ENT specialists, and rehabilitation physicians.

The AFMS was assessed according to the classification of Cheung et al. [3] Fig. 1: stage 0 (normal), stage 1 (narrowing with preserved CSF), stage 2 (narrowing with loss of CSF without spinal cord deformation), stage 3 (spinal cord compression without T2 hyperintensity), and stage 4 (compression with T2 hyperintensity).

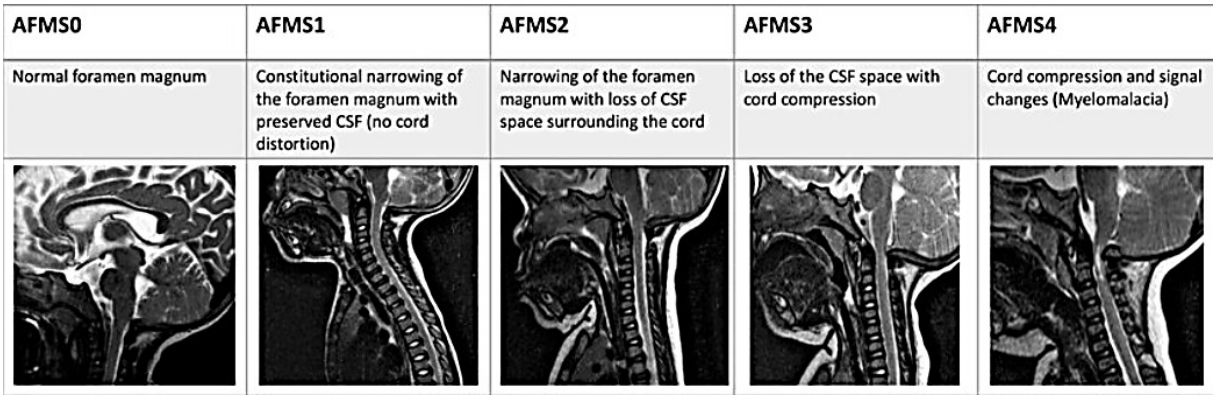


Fig. 1: AFMS according to Cheung MS et al. Arch Dis Child 2021; Guidelines AAP & Best Practice Consensus 2024

At birth 15 to 20 mm; Achondroplasia 9 to 11 mm; Severe stenosis ≤ 7 mm

RESULTS

Case 1: a 16-month-old girl, Fig. 2A, was referred for psychomotor delay. The diagnosis of achondroplasia was confirmed by genetic testing. Clinical examination revealed macrocephaly (head circumference 54 cm) and severe axial hypotonia, with inability to maintain head control or sit unsupported. Nocturnal snoring was present in association with adenoid hypertrophy. Polysomnography was negative. Sagittal T2-weighted MRI showed severe foramen magnum stenosis, with an anteroposterior diameter measured at 7 mm, complete obliteration of the posterior CSF spaces, and clear cervicomedullary compression. There was no intramedullary T2 hyperintensity and no associated hydrocephalus. The AFMS was stage 3.

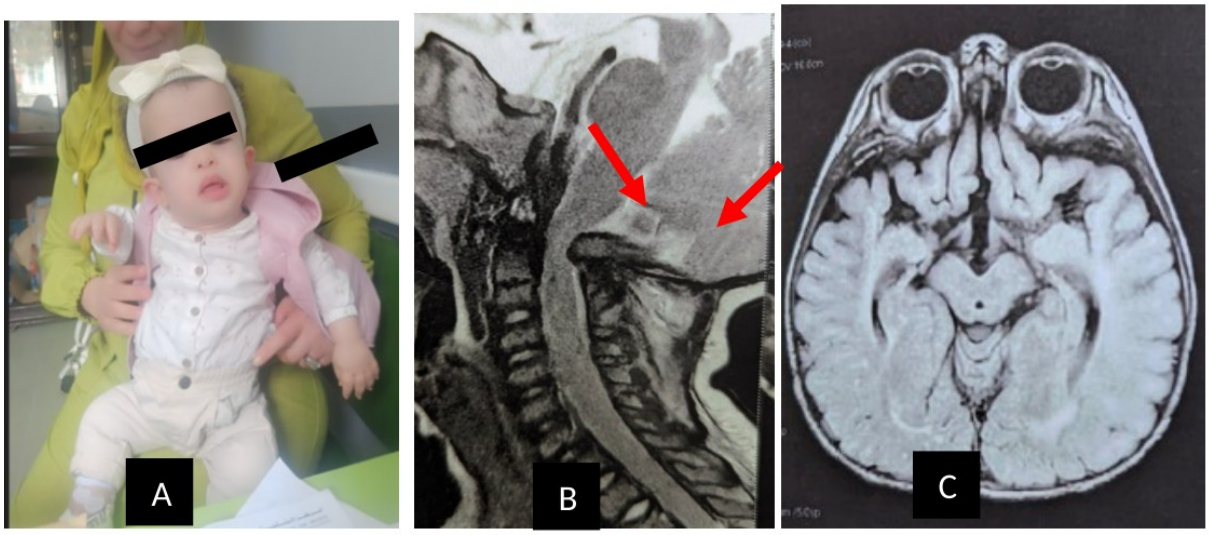


Fig. 2: A, Case 1, a 16-month-old girl; B, sagittal T2-weighted MRI of the cervicomedullary junction showing compression (red arrow) without spinal cord signal abnormality; C, absence of ventricular dilatation.

Case 2: a 3-year-old boy followed for achondroplasia (Fig. 3A) presented with unexplained falls while walking and abnormal motor fatigability at the end of the day. Polysomnography demonstrated severe central sleep apnea syndrome requiring nocturnal assisted ventilation. MRI showed an AP diameter of less than 7 mm, with complete circumferential obliteration (anterior and posterior) of the subarachnoid spaces. The cervicomedullary compression was severe. There was no T2 hyperintensity. Moderate, stable ventriculomegaly was noted, without signs of intracranial hypertension. The AFMS was stage 3, bordering on stage 4.

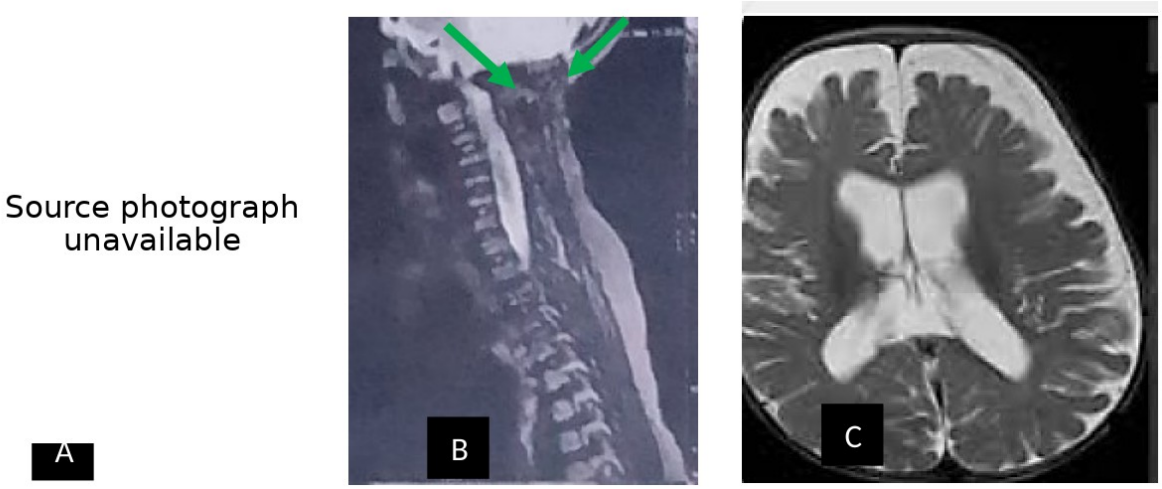


Fig. 3: A, Case 2, a 3-year-old boy; B, sagittal T2-weighted MRI showing an AP diameter of less than 7 mm, with complete circumferential obliteration (anterior and posterior) of the subarachnoid spaces. The cervicomedullary compression is severe without T2 hyperintensity; C, moderate ventriculomegaly. Panel A: source photograph unavailable.

DISCUSSION

Foramen magnum stenosis in achondroplasia is a common and potentially serious complication. Early screening is essential. In the literature, the median age at radiological diagnosis is 9.5 months [4]. Clinical examination alone lacks sensitivity for predicting severe stenosis, hence the recommendation for routine MRI before 6 months of age in every infant with achondroplasia, in accordance with AAP recommendations [5].

The AFMS, validated by Ando et al. in 2026, is a tool that supports surgical decision-making. In their cohort, the mean anteroposterior diameter in operated patients was 5.2 mm, compared with 10.7 mm in non-operated patients. The surgical threshold was set at 7.6 mm [4]. Our two patients, with diameters of 7 mm and less than 7 mm, are below this threshold.

An essential point is the potential pitfall of relying on T2 signal changes. The review by La et al. (2025) emphasizes that the absence of T2 hyperintensity (AFMS stage 3) should not lead to postponement of surgery. Waiting for T2 hyperintensity to appear amounts to accepting irreversible neurological injury [6].

Regarding ventriculomegaly, Kashanian et al. (2020) showed that 70% of children experience improvement or stabilization of ventriculomegaly after bony decompression alone, and that only 14% require secondary ventricular shunting [7]. This finding supports our approach: in the presence of moderate ventriculomegaly without signs of intracranial hypertension, primary CSF diversion should not be performed.

Surgical safety is a major concern. Cracchiolo et al. (2024) showed that 3D neuronavigation allows accurate screw placement without complications, owing to reliable identification of the often dysplastic course of the vertebral arteries [8].

Finally, a systematic review of the literature (2023) including 153 operated patients reported symptomatic improvement in 91% of children, confirming the effectiveness of decompression when appropriately indicated [9].

Limitations of our study: this is a retrospective, single-center series of two cases. Prospective studies with larger numbers of patients are needed to validate our conclusions.

Perspectives: the identification of genetic or molecular biomarkers could enable earlier screening and personalized treatments [10].

CONCLUSION

Foramen magnum stenosis in achondroplasia is a severe complication that warrants early, multidisciplinary management. MRI with calculation of the AFMS is the reference examination. An anteroposterior diameter ≤ 7.6 mm or an AFMS ≥ 3, associated with clinical signs (hypotonia, falls, central apneas), constitutes a surgical indication for cervicomedullary decompression. The absence of T2 hyperintensity should not lead to postponement of surgery. In the presence of moderate ventriculomegaly without intracranial hypertension, decompression alone is the initial procedure, with shunting reserved for failures. Surgery is effective, with a 91% rate of symptomatic improvement in published series.

REFERENCES

1. Pauli RM. Achondroplasia: a comprehensive clinical review. Orphanet J Rare Dis. 2019;14(1):1-18.
2. Cheung MS, et al. Achondroplasia Foramen Magnum Score: screening infants for stenosis. Arch Dis Child. 2021;106(2):180-184.
3. Ando T, et al. Multicentric review of surgical decompression in pediatric bone dysplasias. Pediatr Neurosurg J. 2026.
4. La QD, et al. Pediatric Craniovertebral Junction Anomalies: A Literature Review. Cureus. 2025;17(7):e87164. PMID: 40755617.
5. Guidelines AAP & ESDN. Pediatric Craniovertebral Junction. 2024.
6. Kashanian A, et al. Foramen Magnum Stenosis in Achondroplasia: Imaging-Based Surgical Indications and the Role of Ventriculomegaly. J Imaging. 2020;10(11):291.
7. Cracchiolo G, et al. The impact of intraoperative CT-based navigation in congenital craniovertebral junction anomalies. Brain Sci. 2024;14:1228.
8. Isaacs AM, et al. Surgical treatment of craniovertebral junction instability in children with Down syndrome: a systematic review. J Neurosurg Pediatr. 2023;32:163-172.
9. Patel R, et al. Surgical outcomes of posterior occipitocervical decompression and fusion for basilar invagination. J Clin Orthop Trauma. 2021;13:127-133.
10. Giangiobbe S, et al. Expanding the phenotype of Wiedemann-Steiner syndrome: craniovertebral junction anomalies. Am J Med Genet A. 2020;182:2877-2886.

Neuro-Oncology

HISTOLOGICAL NECROSIS AND IDH STATUS IN GLIOBLASTOMA:
Contribution of a Prospective Study and VEGFR2 Redocking

HASSANI Lynda[1], HABCHI Nawel[1] and TLIBA Souhil[1]

1: Department of Neurosurgery, Frantz-Fanon University Hospital, Blida, Algeria

***Corresponding Author:** HASSANI Lynda, Department of Neurosurgery, Frantz-Fanon University Hospital, Blida, Algeria — Faculty of Medicine, University of Blida 1*

***Received:** August 30, 2026 — **Accepted:** September 15, 2026 — **Published:** October 01, 2026*

Citation: HASSANI Lynda, HABCHI Nawel and TLIBA Souhil. Histological Necrosis and IDH Status in Glioblastoma: Contribution of a Prospective Study and VEGFR2 Redocking. ***OLCIAS Vol.3, Issue 2.***

ABSTRACT

Background. Necrosis is a major histological feature of grade 4 astrocytic tumors and, according to published experimental and tissue-based evidence, occurs within a hypoxic perinecrotic microenvironment associated with activation of the HIF-1α–VEGF-A–VEGFR2 axis. The presence of necrosis alone, however, is not a measurement of hypoxia or VEGFR2 activity.

Objective. The primary objective was to characterize the frequency of histological necrosis in a prospective cohort of 100 tumors initially diagnosed as glioblastoma and to study its association with IDH status when documented. The secondary objectives were to place this phenotype within the published biological rationale of the hypoxia–VEGF/VEGFR2 axis and to validate, by redocking the co-crystallized ligand 42Q, the ability of an AutoDock Vina protocol to reproduce an experimental pose in the VEGFR2 kinase domain.

Methods. The source cohort comprised 100 patients managed prospectively at Frantz-Fanon University Hospital between June 2022 and June 2025 for a tumor initially diagnosed as glioblastoma on pathological examination. All had undergone preoperative CT and MRI. Histological necrosis was recorded as present or absent in pathology reports. IDH status was known in 85 patients (71 wild-type, 14 mutant) and unspecified in 15; these 15 cases were retained in the cohort description but excluded from the inferential IDH–necrosis analysis. The principal comparison used a two-sided Fisher's exact test. Ligand 42Q was redocked into VEGFR2 (PDB 3VHE) using AutoDock Vina v1.2.7 and then evaluated by direct RMSD over the 32 heavy atoms of the ligand.

Results. Histological necrosis was reported in 86/100 patients (86.0%; Wilson 95% CI: 77.9–91.5). Among the 85 patients with known IDH status, necrosis was present in 65/71 tumors recorded as IDH-wildtype (91.5%) and 9/14 IDH-mutant tumors (64.3%), corresponding to an absolute difference of 27.3 percentage points (Newcombe 95% CI: 6.0–53.2). The empirical odds ratio was 6.02, the exact conditional 95% CI was 1.16–28.90, and the two-sided Fisher's exact test yielded $p = 0.0154$. Among the 15 patients with unspecified IDH status, 12 had necrosis and three did not; no distinct biological interpretation was assigned to this group. Redocking generated 20 modes; the highest-scoring mode had a Vina score of −12.832 kcal/mol and a direct RMSD of 0.860 Å relative to the crystallographic pose.

Conclusion. Histological necrosis was frequent in this cohort and was reported more often in tumors whose IDH status was recorded as wild-type. The hypoxia–HIF-1α–VEGF-A–VEGFR2 axis constitutes a mechanistic framework established by the literature, but it was not measured directly in the tumors studied. Redocking 42Q provides a geometric validation restricted to the VEGFR2–3VHE system and establishes a structural basis for subsequent pharmacological investigations, without demonstrating therapeutic efficacy or clinical benefit.

***Keywords:** glioblastoma; grade 4 astrocytoma; necrosis; IDH; hypoxia; VEGF; VEGFR2; molecular docking.*

1. Introduction

Glioblastoma is the most aggressive adult-type diffuse glioma and remains associated with frequent recurrence despite maximal safe resection followed, in eligible patients, by radiotherapy with concomitant and then adjuvant temozolomide [1–3]. The 2021 WHO classification now reserves the term “glioblastoma” for IDH-wildtype diffuse astrocytic gliomas meeting grade 4 criteria. Grade 4 IDH-mutant tumors belong to the entity astrocytoma, IDH-mutant, grade 4 [1]. This nosological evolution is particularly important when analyzing cohorts assembled from historical diagnoses or practices in which molecular characterization was not uniform.

From a neuroradiological perspective, preoperative MRI permits assessment of tumor heterogeneity, extent, and relationships with adjacent structures. In the illustrative case presented in Figure 1, the left temporal lesion appears heterogeneous, while the coronal section and MR spectroscopy complement its morphological and metabolic characterization.

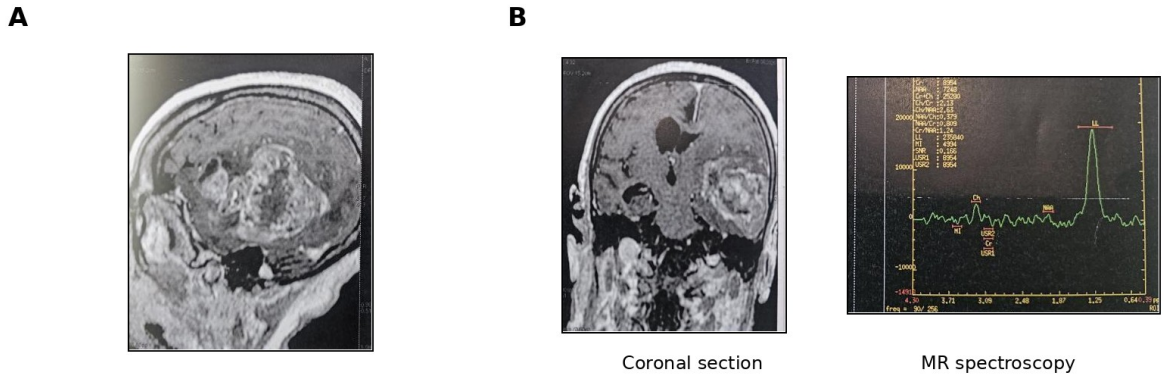


Figure 1. Preoperative imaging of a left temporal glioblastoma. A, sagittal section showing a heterogeneous tumor mass. B, coronal section and associated MR spectroscopy, illustrating the morphological and metabolic heterogeneity of the lesion.

Neurosurgical management is based on maximal safe resection, adapted to tumor location, neurovascular relationships, and functional constraints. Figure 2 illustrates the microsurgical setting under an operating microscope during tumor resection.



Figure 2. Intraoperative view during microsurgical resection under an operating microscope. The procedure aims to achieve maximal cytoreduction while preserving functional and neurovascular structures.

Necrosis and microvascular proliferation are major morphological features of grade 4 astrocytic tumors. Perinecrotic pseudopalisades have been described as biologically active regions containing hypoxic and migratory tumor cells [4]. Hypoxia stabilizes HIF factors and promotes VEGF expression, contributing to pathological angiogenesis [5]. VEGF-A exerts a substantial proportion of its angiogenic effects through VEGFR2/KDR, a receptor tyrosine kinase whose catalytic domain is accessible to small molecules. This mechanistic chain is well established in the literature, but must not be confused with patient-by-patient demonstration of hypoxia, VEGF-A, or VEGFR2 in a cohort in which these markers were not measured.

The human VEGFR2 kinase domain has been crystallized in complex with the pyrrolopyrimidine ligand 42Q in PDB structure 3VHE, resolved at 1.55 Å [6,7]. Redocking a co-crystallized ligand is a conventional methodological control designed to determine whether a docking protocol can reproduce a known experimental pose [8,9]. However, pose recovery validates neither the ability to discriminate active from inactive compounds nor pharmacological or clinical efficacy.

The primary objective of this study was to characterize histological necrosis and its association with documented IDH status in a prospective cohort of 100 tumors initially diagnosed as glioblastoma. The secondary objectives were to place this phenotype within the published mechanistic framework of the hypoxia–HIF-1α–VEGF-A–VEGFR2 axis and to validate the geometric reproducibility of the VEGFR2–42Q complex by molecular redocking. These two analytical levels were interpreted separately to avoid attributing unavailable molecular measurements to the patients. The conceptual framework linking the observed necrotic phenotype to the hypoxia–VEGF/VEGFR2 pathway is summarized in Figure 3.

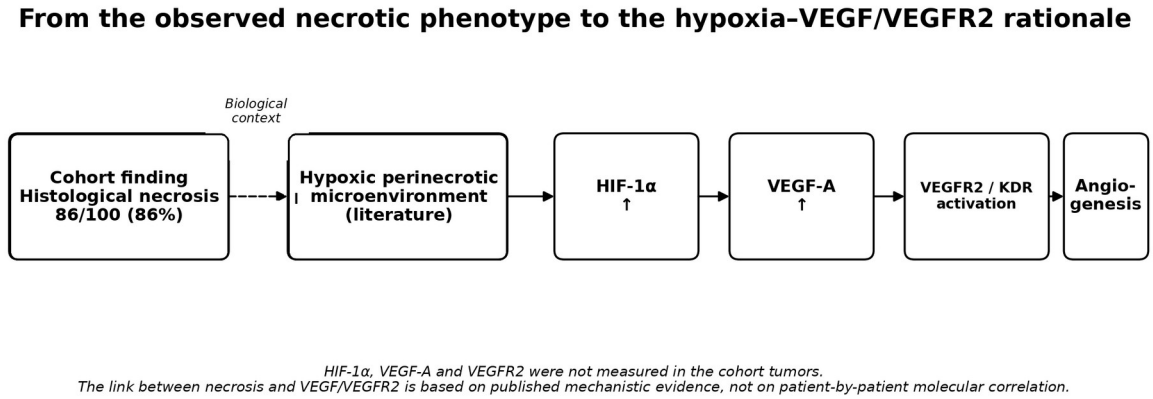


Figure 3. Relationship between the observation in the cohort and the published biological rationale. Histological necrosis is a finding from the series; perinecrotic hypoxia, HIF-1α, VEGF-A, and VEGFR2 represent the literature-based mechanistic framework. These markers were not measured in the cohort tumors.

2. Patients and methods

2.1. Study design and population

This prospective single-center study included 100 patients managed in the Neurosurgery Department of Frantz-Fanon University Hospital, Blida, between June 2022 and June 2025. All included patients had an initial pathological diagnosis of glioblastoma in the department's clinical database. The initial diagnostic designations were retained in the descriptive analysis and interpreted in light of the 2021 WHO nomenclature [1]. Reporting of the observational component follows the applicable STROBE principles [26].

Under the current interpretation, the 14 tumors recorded as IDH-mutant are not equated with IDH-wildtype glioblastomas. In the absence of an integrated review of every specimen with all required markers, they are described as tumors initially diagnosed as glioblastoma with recorded IDH-mutant status.

2.2. Inclusion and exclusion criteria and analytical flow

Patients were retained for analysis if they were included in the source prospective cohort between June 2022 and June 2025; had an initial pathological diagnosis of glioblastoma after resection or biopsy; had preoperative brain imaging with CT and MRI; and had a pathology report from which the presence or absence of necrosis could be extracted. IDH status was not an inclusion criterion and could be absent or unspecified.

This component excluded patients without pathological evidence of the tumor, tumor diagnoses incompatible with the source cohort, absence of preoperative imaging, or inability to extract histological necrosis status. All 100 patients in the cohort were evaluable for the necrosis variable. IDH status was known in 85 patients and unspecified in 15; these 15 patients were retained in the

general description but excluded from the inferential comparison between IDH-wildtype and IDH-mutant tumors. The analytical flow of the cohort is shown in Figure 4.

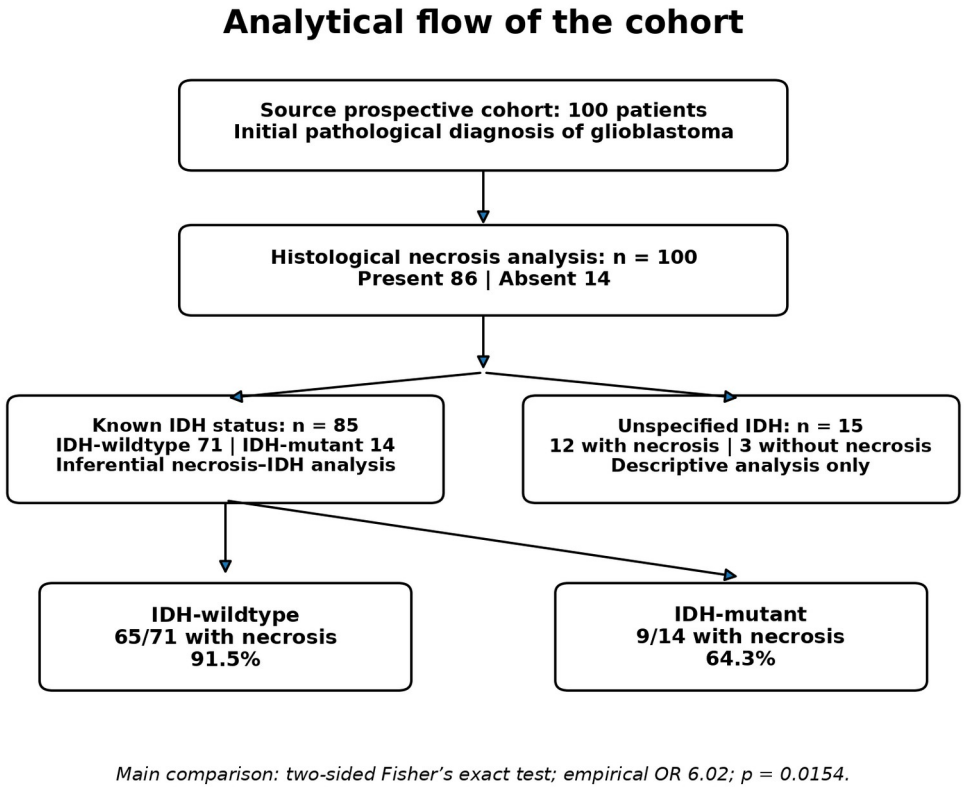


Figure 4. Analytical flow of the cohort. The 15 unspecified IDH results are treated as missing molecular information rather than as a third biological group.

2.3. Neuroradiological and surgical data

All patients had undergone brain CT and MRI; spectroscopy was available when feasible in clinical practice. Imaging was used for localization, assessment of extent, and treatment planning. The source database does not contain standardized quantification of radiological necrotic volume across the 100 patients; no frequency of "radiological necrosis" was therefore assigned to the cohort in this analysis. The illustrative images are descriptive and do not constitute a measurement of tissue hypoxia.

Surgical management consisted of total or partial microsurgical resection where possible, or stereotactic biopsy. The extent of resection used in this manuscript corresponds to categories recorded in the clinical database, rather than centralized postoperative volumetry.

2.4. Pathological and molecular variables

Histological necrosis was extracted from pathology reports as a binary variable, present or absent. It was documented for all 100 patients. Necrotic area, the extent of pseudopalisades, and microvascular proliferation were not centrally quantified in this analysis.

IDH status corresponds to the result recorded in the pathology report. It was recorded as IDH-wildtype in 71 patients, IDH-mutant in 14, and unspecified/NOS in 15. The available documents do not allow uniform patient-by-patient reconstruction of the exact technique used to determine IDH; no additional methodological assumption was introduced. The 15 unspecified results are treated as missing data for the inferential analysis.

2.5. Statistical analysis

Qualitative variables are described as counts and percentages. The proportion of histological necrosis in the complete cohort was accompanied by a 95% confidence interval calculated using the Wilson method. The principal analysis of the necrosis–IDH association was restricted to the 85 patients with known IDH status. Necrosis proportions in tumors recorded as IDH-wildtype and IDH-mutant were compared using a two-sided Fisher's exact test. The empirical odds ratio was calculated as the ratio of cross-products; the 95% confidence interval was obtained using the exact conditional method. The absolute difference in proportions was accompanied by a Newcombe confidence interval. The 15 unspecified IDH cases were described separately, without a three-group biological test. No multivariable adjustment, imputation, or survival analysis by necrosis status was performed in this exploratory component.

2.6. Structural target and verification of ligand chemistry

PDB structure 3VHE corresponds to the human VEGFR2 kinase domain, chain A, in complex with ligand 42Q and resolved by X-ray diffraction at 1.55 Å [6]. The entry contains a construct of 359 residues, of which 303 are modeled in the crystallographic structure, together with 467 water molecules and one 42Q ligand. The 56 unmodeled residues were not reconstructed in the redocking protocol; residues explicitly analyzed in the binding pocket, notably Glu885, Cys919, and Asp1046, are present in the experimental structure [6,10].

The chemical identity of 42Q was checked using the Protein Data Bank Chemical Component Dictionary rather than inferred from PDB coordinates alone. The compound is a nonpolymeric ligand with formula C21H15F4N5O2, zero formal charge, and no chiral center; its connectivity, bond orders, and InChIKey TWOLOZGQZKJZKJ-UHFFFAOYSA-N are defined in the RCSB resource [10]. This verification addresses the need to preserve chemical information during small-molecule preparation, since PDB coordinate files are not designed to exhaustively encode bond orders and ionization states [17].

For redocking, the co-crystallized ligand was separated from the receptor, and crystallographic water molecules were not included in the receptor PDBQT file. Hydrogens and partial charges compatible with AutoDockTools/MGLTools 1.5.6 were assigned during preparation. The neutral form of 42Q defined in the chemical dictionary was retained; no exhaustive ensemble of tautomers or alternative protonation microstates was generated. Cys919 was treated as a standard noncovalent residue; no covalent ligand–cysteine bond model was specified. Alternative histidine microstates were not systematically sampled. These choices describe the reproduced protocol and are considered when interpreting its scope. The crystallographic reference structure is presented in Figure 5.

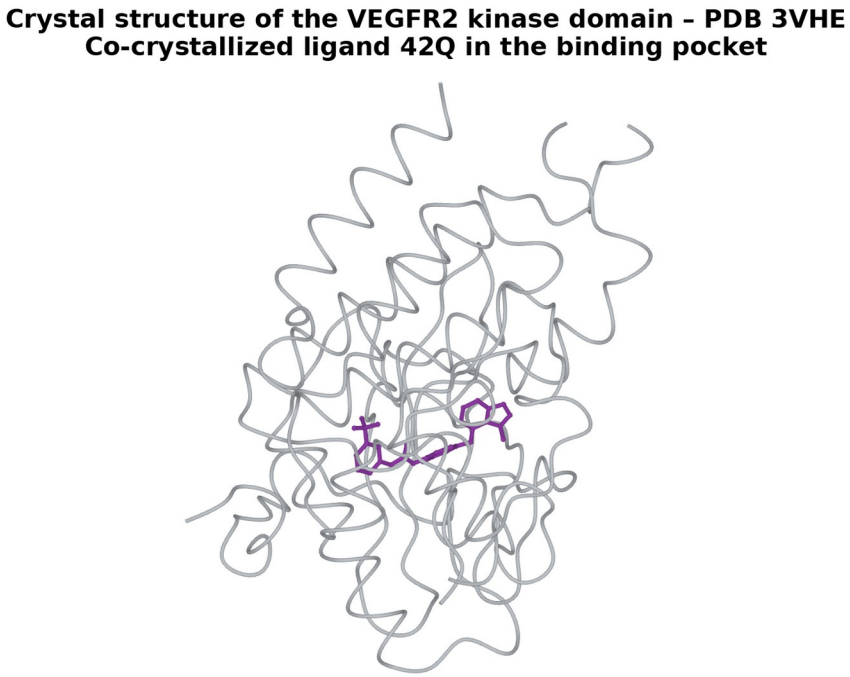


Figure 5. Crystallographic structure of the human VEGFR2 kinase domain (PDB 3VHE), with co-crystallized ligand 42Q in the binding pocket. 42Q is used as the reference ligand for redocking.

2.7. Redocking parameters and geometric validation

Receptor and ligand preparation was performed with AutoDockTools in the MGLTools 1.5.6 environment. The receptor was kept rigid and five ligand torsions were active. Redocking was performed using AutoDock Vina v1.2.7 and the Vina scoring function [8,9]. The search box was centered on the position of the co-crystallized ligand. One calculation with a fixed random seed was analyzed; the generated modes do not constitute independent experimental replicates. The redocking workflow and its geometric assessment are summarized in Figure 6.

Table 1. Parameters for redocking 42Q into VEGFR2.

Parameter	Value
Receptor structure	VEGFR2, PDB 3VHE, chain A
Reference ligand	42Q / compound 20d
Software	AutoDock Vina v1.2.7
Box center (x; y; z)	−24.303; −0.681; −8.955 Å
Dimensions	22 × 20 × 22 Å
Exhaustiveness	32
Maximum number of modes	20
Energy range	5 kcal/mol
Random seed	20260911
Flexibility	Rigid receptor; 5 active ligand torsions

The top-ranked pose was compared with the crystallographic pose by matching the names of the 32 heavy atoms of 42Q. RMSD was calculated in the fixed receptor reference frame, without independent ligand fitting by rotation or translation and without permutation of chemically equivalent atoms. An RMSD below 2 Å was used as a conventional benchmark for pose recovery, without equating it with general validation of the protocol's predictive ability.

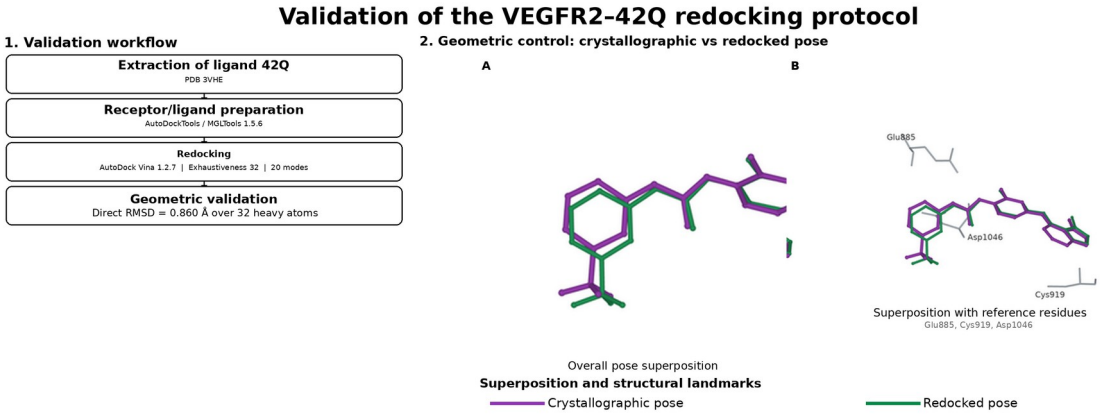


Figure 6. VEGFR2–42Q redocking validation workflow and geometric comparison of the crystallographic and redocked poses.

3. Results

3.1. Cohort characteristics

The cohort included 100 patients, comprising 70 men and 30 women. Mean age was 55 years, with a range of 26–70 years. Macroscopically total resection was reported in 70 cases, partial resection in 25, and biopsy in five. All patients had preoperative CT and MRI. Representative

preoperative and operative illustrations are presented in Figures 1 and 2. General population characteristics are summarized in Table 2.

Table 2. General characteristics of the clinical cohort.

Variable	Count / value
Mean age	55 years (26–70)
Men	70/100
Women	30/100
Macroscopically total resection	70/100
Partial resection	25/100
Biopsy	5/100
Histological necrosis present	86/100
Recorded IDH-wildtype	71/100
Recorded IDH-mutant	14/100
Unspecified IDH	15/100

3.2. Histological necrosis and IDH status

Histological necrosis was explicitly reported in 86 patients and absent in 14, corresponding to a frequency of 86.0% (Wilson 95% CI: 77.9–91.5). Among the 85 patients with known IDH status, 74 had necrosis and 11 did not. Necrosis was present in 65/71 tumors recorded as IDH-wildtype (91.5%) and 9/14 IDH-mutant tumors (64.3%). The overall frequency of necrosis is illustrated in Figure 7, and its distribution by IDH status is detailed in Table 3.

Table 3. Distribution of histological necrosis by recorded IDH status.

Known IDH status	Necrosis present	Necrosis absent	Total	Necrosis (%)
IDH-wildtype	65	6	71	91.5
IDH-mutant	9	5	14	64.3
Total	74	11	85	87.1

The absolute difference in proportions was 27.3 percentage points (Newcombe 95% CI: 6.0–53.2). The empirical odds ratio was 6.02, with an exact conditional 95% CI of 1.16–28.90. The two-sided Fisher’s exact test yielded p = 0.0154. Among the 15 unspecified IDH cases, 12 had histological necrosis and three did not; these cases were not included in the principal test. The graphical comparison of necrosis proportions by known IDH status is presented in Figure 8.

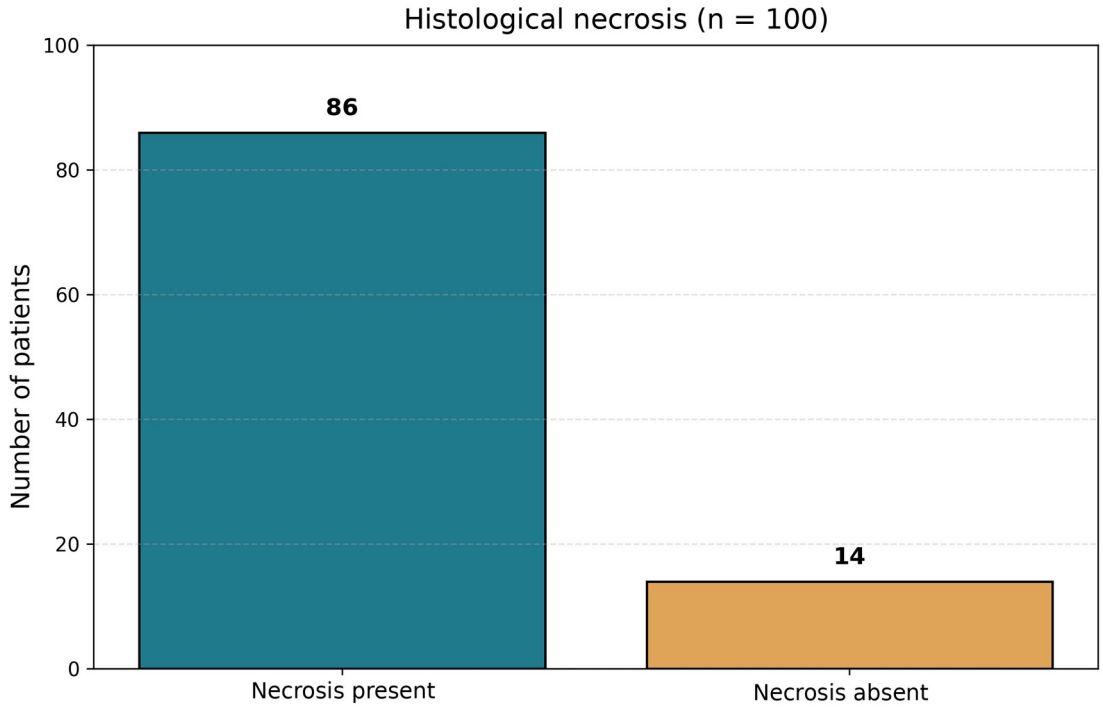


Figure 7. Frequency of histological necrosis in the complete cohort (n = 100).

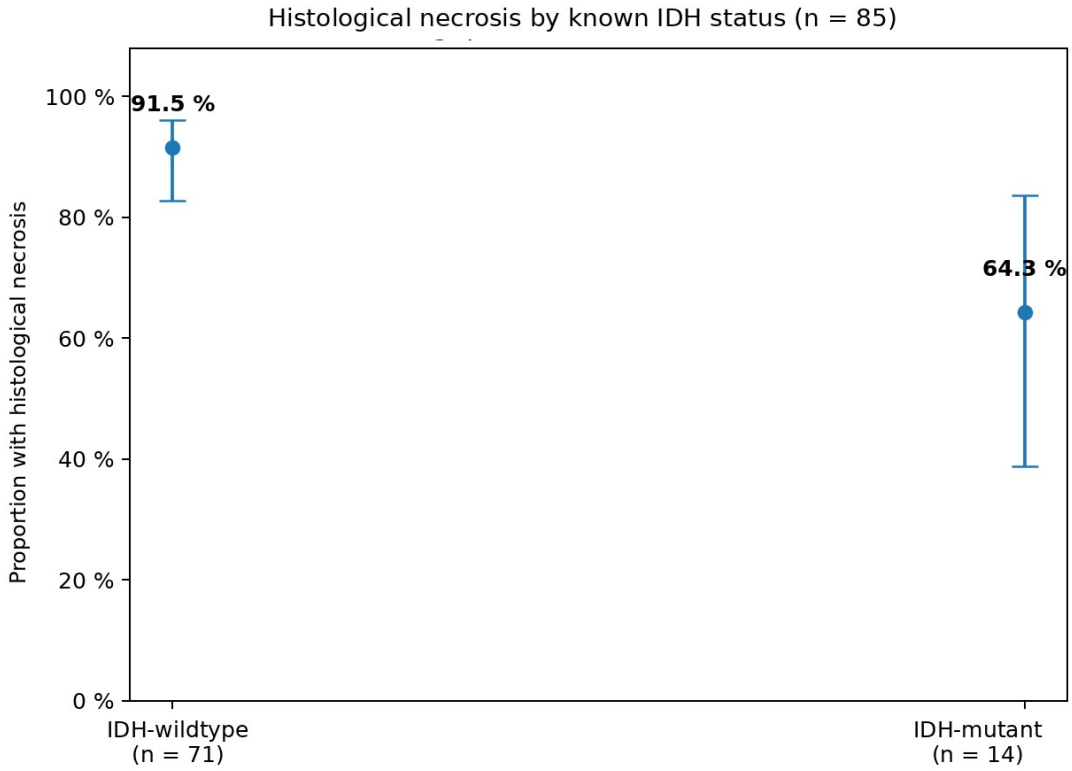


Figure 8. Proportion of histological necrosis by known IDH status (n = 85), with Wilson 95% confidence intervals.

3.3. Redocking of the reference ligand 42Q

The Vina calculation generated 20 modes. The top-ranked pose had a Vina score of −12.832 kcal/mol. Direct comparison of its 32 heavy atoms with the crystallographic pose yielded an RMSD of 0.859944 Å, rounded to 0.860 Å. This value indicates satisfactory geometric recovery of the pose in the complex studied. The highest-scoring redocked pose is presented in Figure 9.

In the redocked pose, several heteroatoms of 42Q lay close to Glu885, Cys919, and Asp1046. Selected interatomic distances ranged from 2.80 to 3.15 Å. These describe geometric proximities consistent with a polar binding environment; they are neither individual binding energies nor evidence of dynamic persistence of the contacts. Three-dimensional superposition with the crystallographic pose and the quantitative summary are presented in Figures 10 and 11; selected interatomic distances are detailed in Table 4.

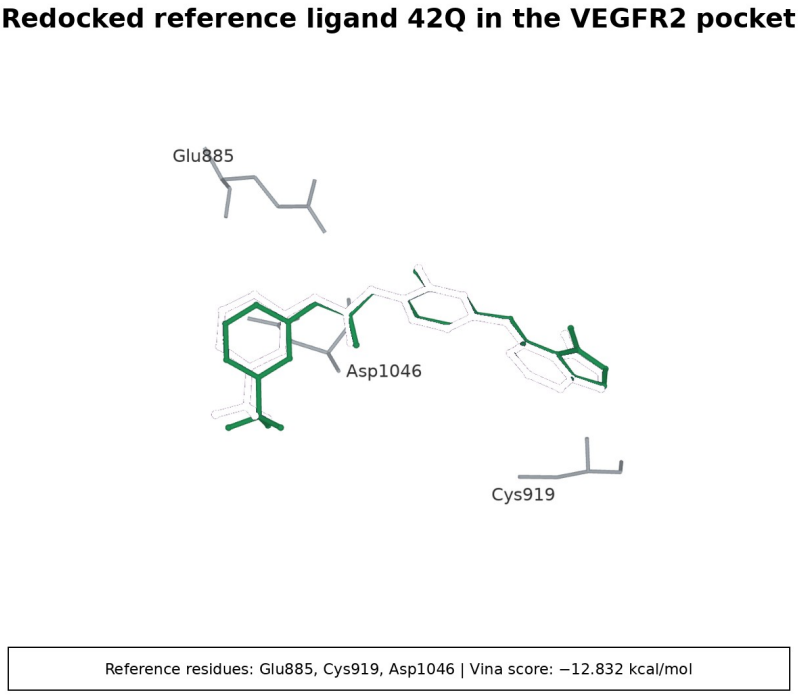


Figure 9. Redocked pose of 42Q in the VEGFR2 pocket. Residues Glu885, Cys919, and Asp1046 are shown as structural landmarks. Vina score for mode 1: −12.832 kcal/mol.

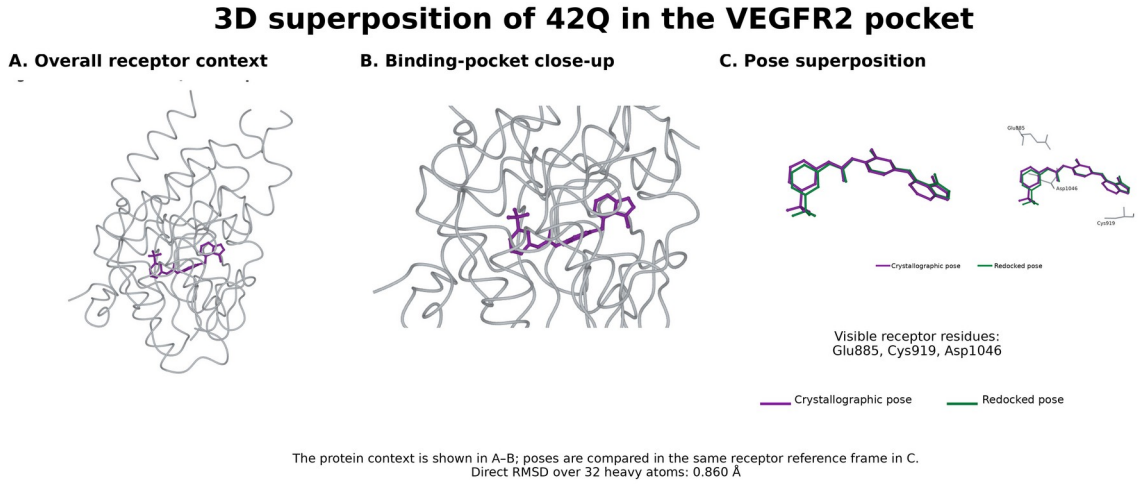


Figure 10. Structural superposition of 42Q with the receptor context visible. A, global view of VEGFR2; B, close-up of the binding pocket; C, comparison of the crystallographic and redocked poses in the same protein reference frame. Direct RMSD over 32 heavy atoms: 0.860 Å.

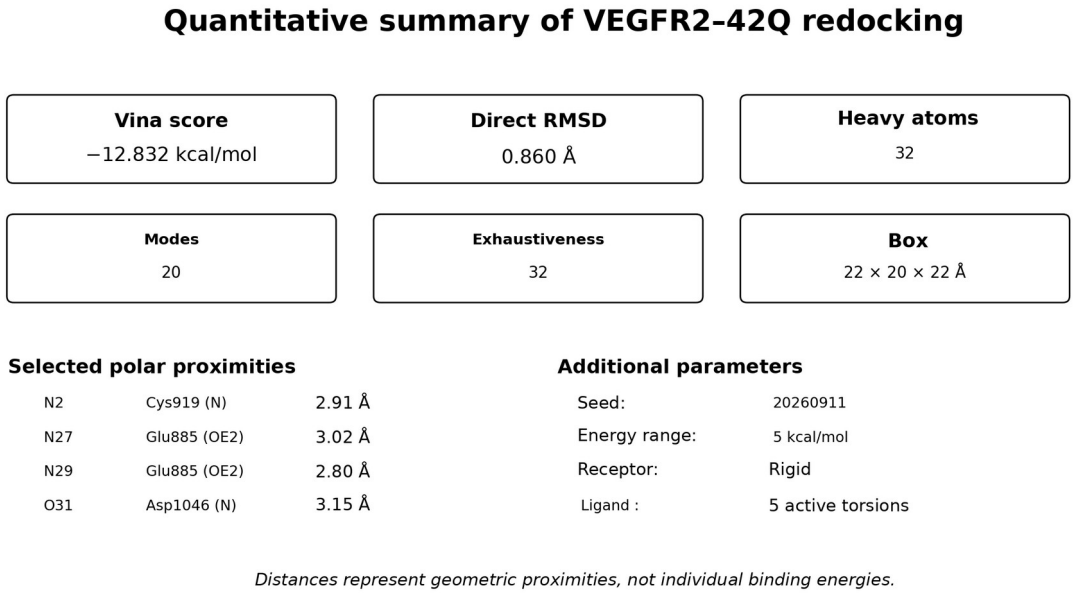


Figure 11. Quantitative summary of VEGFR2–42Q redocking. The indicated distances are interatomic proximities, not binding energies.

Table 4. Selected interatomic proximities in the redocked pose of 42Q.

Ligand atom	VEGFR2 residue	Protein atom	Distance (Å)
N2	Cys919	N	2.91
N27	Glu885	OE2	3.02
N29	Glu885	OE2	2.80
O31	Asp1046	N	3.15

4. Discussion

4.1. Frequency of necrosis and relationship with IDH status

Histological necrosis was reported in 86% of tumors in this cohort. This high frequency is consistent with the initial selection of tumors diagnosed as glioblastoma in clinical practice: necrosis itself contributes to the morphological recognition of grade 4 astrocytic tumors. It should therefore not be interpreted as a frequency applicable to all diffuse gliomas, or as an independent biomarker of aggressiveness in an unselected population.

The principal analysis restricted to the 85 known IDH results showed a higher proportion of necrosis in tumors recorded as IDH-wildtype than in IDH-mutant tumors. The absolute difference was 27.3 percentage points, but the confidence interval for the odds ratio remained wide because of the small IDH-mutant group. The observed association is exploratory and does not establish a causal effect of IDH status on necrosis. The 15 patients with unspecified IDH status were retained in the cohort description but excluded from inference, avoiding the conversion of missing information into a biological category.

The nosological distinction is essential. Under WHO 2021, a grade 4 IDH-mutant diffuse astrocytoma is no longer classified as glioblastoma. The findings in this cohort therefore describe categories as they were recorded in the source database, rather than a uniform retrospective molecular reclassification [1].

4.2. From necrosis to the hypoxic microenvironment: level of evidence

Histological necrosis observed in the cohort and tumor hypoxia are distinct variables. The work of Brat and colleagues established the hypoxic and migratory nature of glioblastoma pseudopalisades [4], while hypoxia-induced VEGF expression has been demonstrated experimentally and in tumor tissues [5]. These data provide a coherent mechanistic framework linking the perinecrotic compartment to an angiogenic response. They do not show that HIF-1α, VEGF-A, or VEGFR2 was activated in every patient in this cohort.

The source database contains no standardized quantitative measurement of radiological necrosis across all 100 patients. All patients had CT and MRI, but the images cannot retrospectively be turned into a quantitative variable without segmentation and standardized reading protocols. Presumed radiological necrosis, histological necrosis, and tissue hypoxia must therefore remain three distinct levels.

4.3. Robustness and scope of VEGFR2–42Q redocking

The direct RMSD of 0.860 Å shows that the protocol reproduced the experimental position of 42Q in complex 3VHE with high geometric agreement. Comparison was performed in the fixed receptor reference frame, assessing the relative positioning of the ligand in the pocket rather than simple conformational similarity after independent superposition. The Vina score of −12.832 kcal/mol describes the value of the scoring function under the calculation conditions; it is not an experimental binding free energy and must not be converted into a clinical affinity constant.

Chemical preparation parameters that may influence docking reproducibility were explicitly documented. Entry 3VHE contains 303 modeled protein residues from a construct of 359 residues and 467 water molecules [6]. Unmodeled residues were not reconstructed. The chemistry of 42Q was checked against the Chemical Component Dictionary, including connectivity, bond orders, zero formal charge, and lack of chirality [10]. Preparation retained a single reference protonation/tautomeric form; it did not sample every possible microstate. This transparency reduces the risk of confusing pose recovery with general pharmacological validation.

Nevertheless, redocking relies on a single complex, a rigid receptor, one seed, and a ligand known to bind the site. It tests neither discrimination between active and inactive compounds, robustness to alternative preparations, receptor flexibility, nor the effect of structural water molecules. The result must therefore be regarded as pose validation restricted to the 3VHE–42Q system.

4.4. Biological relevance of VEGFR2 and antiangiogenic evidence

The biological relevance of VEGFR2 in glioblastoma rests on the importance of pathological angiogenesis and the vascular response to hypoxia. Preclinical models have shown that VEGFR2 blockade can produce a transient phase of vascular normalization accompanied by improved oxygenation and radiation response [11]. Human observations with cediranib have also associated improved perfusion with better oxygenation in some settings [12].

These observations do not justify equating VEGF/VEGFR2 inhibition with assured clinical benefit. In first-line trials, adding bevacizumab to chemoradiotherapy did not improve overall survival, although some progression-free survival and symptom-control measures may have changed [13,14]. In recurrent glioblastoma, cediranib and various antiangiogenic combinations have not demonstrated a uniform overall survival benefit [21,23]. The redocking presented here tests neither bevacizumab nor the efficacy of 42Q and must be interpreted as a structural step preceding any potential pharmacological assessment.

4.5. Neurosurgical implications, recurrence, and the multimodal pathway

Recurrence remains a major component of the course of glioblastoma. Maximal safe resection reduces tumor burden but does not eliminate infiltrating cells beyond radiological boundaries. A strategy targeting the vascular microenvironment could theoretically be studied as an adjunct to postoperative treatments, but no result in this manuscript demonstrates prevention of recurrence or a reduction in the need for reoperation.

At first recurrence, the indication for further surgery depends particularly on functional status, location, potentially resectable extent, and the ability to continue oncological treatments. Data from the RANO resect group associated low residual tumor volume after reoperation with more

favorable survival in selected patients, subject to the limitations inherent in retrospective analyses [22]. The RANO 2.0 criteria also emphasize the need to distinguish tumor progression, pseudoprogression, and treatment effects, particularly during the first weeks after radiotherapy and during antiangiogenic therapy [16].

Trials in the recurrent setting illustrate the possible dissociation between radiological control, progression-free survival, and overall survival. Lomustine–bevacizumab improved progression-free survival without an overall survival benefit in EORTC 26101 [23]. In NRG Oncology/RTOG1205, adding reirradiation to bevacizumab improved six-month progression-free survival without a significant difference in overall survival [24]. These data place structural exploration of VEGFR2 within a multimodal pathway still dominated by clinical patient selection, follow-up imaging, surgery, radiotherapy, and systemic treatments.

4.6. Limitations

This study has several limitations. The clinical component is single-center and concerns a cohort historically assembled from initial glioblastoma diagnoses, with 15 unspecified IDH results and no uniform integrated molecular review. Histological necrosis is binary and was not subject to morphometric quantification or centralized rereview. The database does not permit systematic quantification of radiological necrosis or spatial matching of imaging with specimens. HIF-1α, VEGF-A, and VEGFR2 were not measured in the tumors; no individual relationship between necrosis, hypoxia, VEGFR2 activation, and clinical response can therefore be established.

The structural component is independent of patient samples and relies on a public structure. Only one co-crystallized ligand and one calculation were analyzed; the receptor is rigid, and no exhaustive sampling of tautomers, protonation states, structural waters, or alternative conformations was performed. Redocking validates recovery of a known pose in a specific setting, rather than the performance of a molecular screen or the efficacy of an anti-VEGFR2 strategy in glioblastoma. Figure 12 summarizes the relationship between cohort findings, the biological rationale, and the structural component.

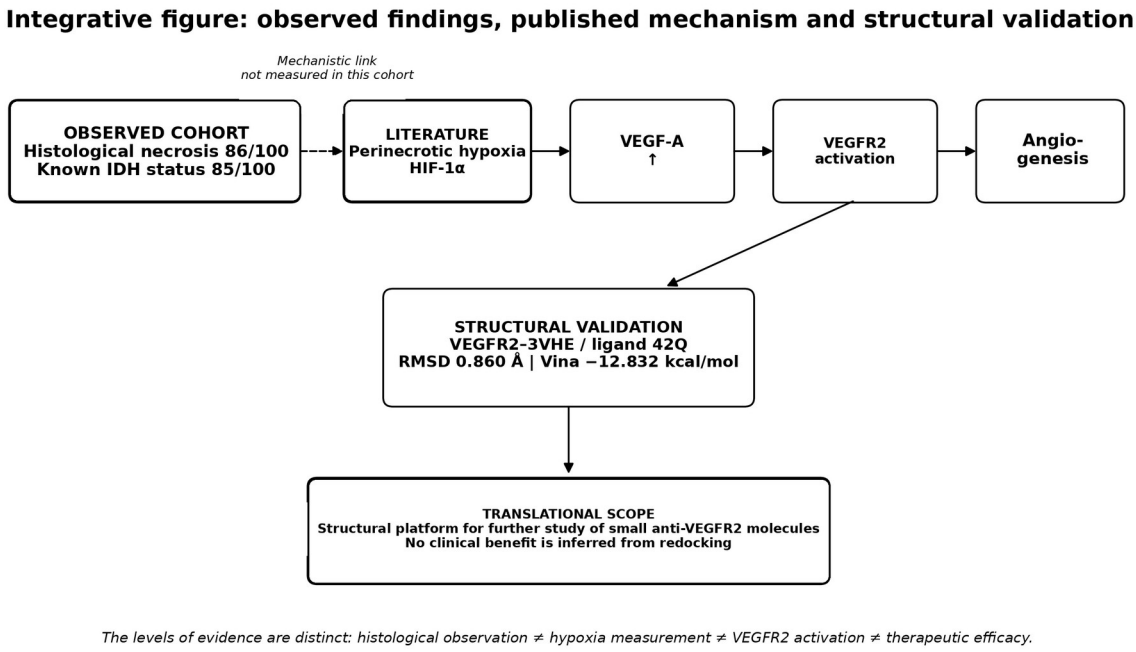


Figure 12. Integration of the levels of evidence. Histological necrosis is observed in the cohort; the hypoxia–HIF-1α–VEGF-A–VEGFR2 link comes from the literature; redocking validates a reference binding geometry in VEGFR2. These levels are not interchangeable and do not demonstrate clinical benefit.

5. Conclusion

In this prospective cohort of 100 tumors initially diagnosed as glioblastoma, histological necrosis was reported in 86% of cases. Among the 85 patients with documented IDH status, necrosis was more frequent in tumors recorded as IDH-wildtype than in IDH-mutant tumors. The 15 unspecified IDH results were retained in the cohort description but excluded from the inferential analysis, consistent with their nature as missing molecular data.

The relationship between necrosis, hypoxia, and activation of the VEGF/VEGFR2 axis rests on published mechanistic evidence and was not measured directly in this cohort. Redocking 42Q into VEGFR2–3VHE reproduced the crystallographic pose with a direct RMSD of 0.860 Å. With ligand chemistry, receptor preparation, and structural limitations explicitly described, this result constitutes methodological pose validation rather than evidence of therapeutic efficacy. The scientific value of this work lies in explicitly connecting three distinct levels: an observed histological phenotype, a documented biological mechanism, and in silico structural validation.

DECLARATIONS

Ethics approval and consent to participate

The study was conducted in accordance with the ethical principles of the Declaration of Helsinki.

Consent for publication

Written informed consent was obtained from the patient's legal guardian for publication of this case report and any accompanying images.

Availability of data and materials

The data supporting the findings of this case report are available from the corresponding author upon reasonable request.

Competing interests

The authors declare that they have no competing interests.

Funding

This research received no specific grant from any funding agency in the public, commercial, or not-for-profit sectors.

REFERENCES

1. Louis DN, Perry A, Wesseling P, et al. The 2021 WHO Classification of Tumors of the Central Nervous System: a summary. Neuro Oncol. 2021;23(8):1231–1251. doi:10.1093/neuonc/noab106.
2. Stupp R, Mason WP, van den Bent MJ, et al. Radiotherapy plus concomitant and adjuvant temozolomide for glioblastoma. N Engl J Med. 2005;352(10):987–996. doi:10.1056/NEJMoa043330.
3. Wen PY, Weller M, Lee EQ, et al. Glioblastoma in adults: A Society for Neuro-Oncology and European Association of Neuro-Oncology consensus review on current management and future directions. Neuro Oncol. 2025;27(11):2751–2788. doi:10.1093/neuonc/noaf177.
4. Brat DJ, Castellano-Sanchez AA, Hunter SB, et al. Pseudopalisades in glioblastoma are hypoxic, express extracellular matrix proteases, and are formed by an actively migrating cell population. Cancer Res. 2004;64(3):920–927. doi:10.1158/0008-5472.CAN-03-2073.
5. Shweiki D, Itin A, Soffer D, Keshet E. Vascular endothelial growth factor induced by hypoxia may mediate hypoxia-initiated angiogenesis. Nature. 1992;359(6398):843–845. doi:10.1038/359843a0.
6. RCSB Protein Data Bank. 3VHE: Crystal structure of human VEGFR2 kinase domain with a novel pyrrolopyrimidine inhibitor. doi:10.2210/pdb3VHE/pdb. Accessed 12 September 2026.
7. Oguro Y, Miyamoto N, Okada K, et al. Design, synthesis, and evaluation of 5-methyl-4-phenoxy-5H-pyrrolo[3,2-d]pyrimidine derivatives: novel VEGFR2 kinase inhibitors binding to inactive kinase conformation. Bioorg Med Chem. 2010;18(20):7260–7273. doi:10.1016/j.bmc.2010.08.017.
8. Trott O, Olson AJ. AutoDock Vina: improving the speed and accuracy of docking with a new scoring function, efficient optimization, and multithreading. J Comput Chem. 2010;31(2):455–461. doi:10.1002/jcc.21334.
9. Eberhardt J, Santos-Martins D, Tillack AF, Forli S. AutoDock Vina 1.2.0: new docking methods, expanded force field, and Python bindings. J Chem Inf Model. 2021;61(8):3891–3898. doi:10.1021/acs.jcim.1c00203.
10. RCSB Protein Data Bank. Chemical Component 42Q: 1-{2-fluoro-4-[(5-methyl-5H-pyrrolo[3,2-d]pyrimidin-4-yl)oxy]phenyl}-3-[3-(trifluoromethyl)phenyl]urea. Chemical Component Dictionary. Accessed 12 September 2026.
11. Winkler F, Kozin SV, Tong RT, et al. Kinetics of vascular normalization by VEGFR2 blockade governs brain tumor response to radiation: role of oxygenation, angiopoietin-1, and matrix metalloproteinases. Cancer Cell. 2004;6(6):553–563. doi:10.1016/j.ccr.2004.10.011.

12. Batchelor TT, Gerstner ER, Emblem KE, et al. Improved tumor oxygenation and survival in glioblastoma patients who show increased blood perfusion after cediranib and chemoradiation. Proc Natl Acad Sci U S A. 2013;110(47):19059–19064. doi:10.1073/pnas.1318022110.

13. Gilbert MR, Dignam JJ, Armstrong TS, et al. A randomized trial of bevacizumab for newly diagnosed glioblastoma. N Engl J Med. 2014;370(8):699–708. doi:10.1056/NEJMoa1308573.

14. Chinot OL, Wick W, Mason W, et al. Bevacizumab plus radiotherapy-temozolomide for newly diagnosed glioblastoma. N Engl J Med. 2014;370(8):709–722. doi:10.1056/NEJMoa1308345.

15. Morris GM, Huey R, Lindstrom W, et al. AutoDock4 and AutoDockTools4: automated docking with selective receptor flexibility. J Comput Chem. 2009;30(16):2785–2791. doi:10.1002/jcc.21256.

16. Wen PY, van den Bent M, Youssef G, et al. RANO 2.0: update to the Response Assessment in Neuro-Oncology criteria for high- and low-grade gliomas in adults. J Clin Oncol. 2023;41(33):5187–5199. doi:10.1200/JCO.23.01059.

17. AutoDock Vina Documentation. Ligand and receptor preparation guidance, release 1.2.x. https://autodock-vina.readthedocs.io/. Accessed 12 September 2026.

18. Tong RT, Boucher Y, Kozin SV, Winkler F, Hicklin DJ, Jain RK. Vascular normalization by vascular endothelial growth factor receptor 2 blockade induces a pressure gradient across the vasculature and improves drug penetration in tumors. Cancer Res. 2004;64(11):3731–3736. doi:10.1158/0008-5472.CAN-04-0074.

19. Gerstner ER, Emblem KE, Chang K, et al. Bevacizumab reduces permeability and concurrent temozolomide delivery in a subset of patients with recurrent glioblastoma. Clin Cancer Res. 2020;26(1):206–212. doi:10.1158/1078-0432.CCR-19-1739.

20. Hegi ME, Diserens AC, Gorlia T, et al. MGMT gene silencing and benefit from temozolomide in glioblastoma. N Engl J Med. 2005;352(10):997–1003. doi:10.1056/NEJMoa043331.

21. Batchelor TT, Mulholland P, Neyns B, et al. Phase III randomized trial comparing cediranib as monotherapy, cediranib plus lomustine, and lomustine alone in recurrent glioblastoma. J Clin Oncol. 2013;31(26):3212–3218. doi:10.1200/JCO.2012.47.2464.

22. Karschnia P, Dono A, Young JS, et al. Prognostic evaluation of re-resection for recurrent glioblastoma using the novel RANO classification for extent of resection: a report of the RANO resect group. Neuro Oncol. 2023;25(9):1672–1685. doi:10.1093/neuonc/noad074.

23. Wick W, Gorlia T, Bendszus M, et al. Lomustine and bevacizumab in progressive glioblastoma. N Engl J Med. 2017;377(20):1954–1963. doi:10.1056/NEJMoa1707358.

24. Tsien CI, Pugh SL, Dicker AP, et al. NRG Oncology/RTOG1205: a randomized phase II trial of concurrent bevacizumab and reirradiation versus bevacizumab alone for recurrent glioblastoma. J Clin Oncol. 2023;41(6):1285–1295. doi:10.1200/JCO.22.00164.

25. Clark AJ, Butowski NA, Chang SM, et al. Impact of bevacizumab chemotherapy on craniotomy wound healing. J Neurosurg. 2011;114(6):1609–1616. doi:10.3171/2010.10.JNS101042.

26. von Elm E, Altman DG, Egger M, Pocock SJ, Gøtzsche PC, Vandenbroucke JP; STROBE Initiative. The Strengthening the Reporting of Observational Studies in Epidemiology (STROBE) statement: guidelines for reporting observational studies. Lancet. 2007;370(9596):1453–1457. doi:10.1016/S0140-6736(07)61602-X.

Neuro-Oncology

INTRAVENTRICULAR WHO GRADE 1 GLIONEURONAL TUMOR IN A PEDIATRIC PATIENT: A Rare Third Ventricular Presentation

OUADI Hayet[1], HARCHAOUI Nabila[1], ATROUNE Lynda[1] and YOUSFI Yamina[2]

1: Department of Neurosurgery, Ali Ait Idir Hospital, University of Algiers, Algiers, Algeria

2: Department of Pathology, UHC Nefisa Hammoud, University of Algiers, Algiers, Algeria

***Corresponding Author:** OUADI Hayet, Department of Neurosurgery, Ali Ait Idir Hospital, University of Algiers, Algiers, Algeria*

***Received:** August 10, 2026 — **Accepted:** September 15, 2026 — **Published:** October 01, 2026*

***Citation:** OUADI Hayet, HARCHAOUI Nabila, ATROUNE Lynda and YOUSFI Yamina. Intraventricular WHO Grade 1 Glioneuronal Tumor in a Pediatric Patient: A Rare Third Ventricular Presentation.*
OLCIAS Vol.3, Issue 2.

ABSTRACT

Background: Glioneuronal tumors are rare central nervous system (CNS) neoplasms exhibiting both glial and neuronal differentiation. The 2021 WHO classification recognizes multiple entities within this group, most of which are low-grade tumors with a favorable prognosis. Intraventricular locations are particularly uncommon.

Case Presentation: We report the case of a 14-year-old child presenting with intracranial hypertension secondary to a third ventricular mass causing obstructive hydrocephalus. Initial management consisted of ventriculoperitoneal shunting. One year later, the patient developed shunt dysfunction with recurrence of symptoms, requiring external ventricular drainage. Brain MRI confirmed a third ventricular lesion, and the patient subsequently underwent endoscopic subtotal resection combined with endoscopic third ventriculostomy. The postoperative course was favorable, with complete resolution of transient complications, and no adjuvant therapy was administered. Histopathology revealed a low-cellularity glioneuronal tumor composed of oligodendroglial-like cells within a myxoid background, with associated calcifications. Immunohistochemistry showed OLIG2 and GFAP positivity, focal chromogranin A expression, a low Ki-67 index, and negative p53 staining, consistent with a WHO grade 1 glioneuronal tumor.

Conclusion: Intraventricular glioneuronal tumors are rare and diagnostically challenging. Accurate diagnosis relies on the integration of histological and immunohistochemical findings. Endoscopic surgery is a safe and effective approach for deep ventricular locations, with favorable outcomes.

***Keywords:** glioneuronal tumor; third ventricle; pediatric; hydrocephalus; endoscopic neurosurgery; WHO grade 1*

INTRODUCTION

Glioneuronal tumors constitute a distinct group of rare central nervous system neoplasms composed of neoplastic cells with both glial and neuronal differentiation, distinguishing them from purely glial or purely neuronal tumors [1]. In the 2021 WHO Classification of Tumors of the Central Nervous System (CNS WHO, 5th edition), glioneuronal tumors are grouped together with neuronal tumors and now encompass a broader spectrum of entities defined by integrated histopathological, immunohistochemical, and molecular features [2].

This updated classification recognizes multiple subtypes of glioneuronal tumors, including ganglioglioma, dysembryoplastic neuroepithelial tumor (DNET), papillary glioneuronal tumor (PGNT), rosette-forming glioneuronal tumor (RGNT), myxoid glioneuronal tumor (MGT), and diffuse glioneuronal tumor with oligodendroglioma-like features and nuclear clusters (DGONC), among others, reflecting a growing understanding of their biology and clinical behavior [2]. Many glioneuronal tumors are considered WHO grade 1 neoplasms owing to their generally indolent course and favorable prognosis, particularly when gross total resection is achievable [1].

The intraventricular location of glioneuronal tumors is particularly uncommon; most reported cases involve the lateral or third ventricles and often present with hydrocephalus and symptoms of cerebrospinal fluid obstruction [3]. Magnetic resonance imaging plays a crucial role in preoperative tumor characterization, but definitive diagnosis always relies on histopathological and immunohistochemical analysis demonstrating both glial and neuronal elements [4].

Herein, we report the case of a 14-year-old child with an intraventricular WHO grade 1 glioneuronal tumor, with emphasis on the clinical presentation, imaging findings, surgical approach, and histopathological confirmation, in the context of the current WHO 2021 classification.

CASE PRESENTATION

Clinical presentation and initial management

A 14-year-old child presented with a syndrome of intracranial hypertension characterized by persistent headaches, vomiting, and blurred vision. Emergency brain CT revealed biventricular hydrocephalus associated with an intraventricular lesion occupying the third ventricle, hyperdense on non-contrast images (Figure 1). The patient underwent urgent placement of a ventriculoperitoneal shunt, with effective control of intracranial hypertension (Figure 2).

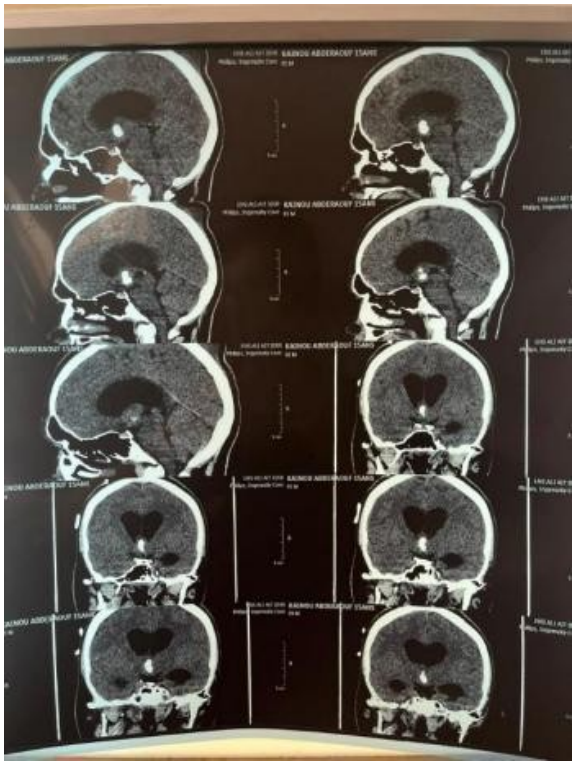


Figure 1. Preoperative brain CT scan in coronal and sagittal sections showing dilation of the lateral ventricles, with the third ventricle occupied by a hyperdense lesion.

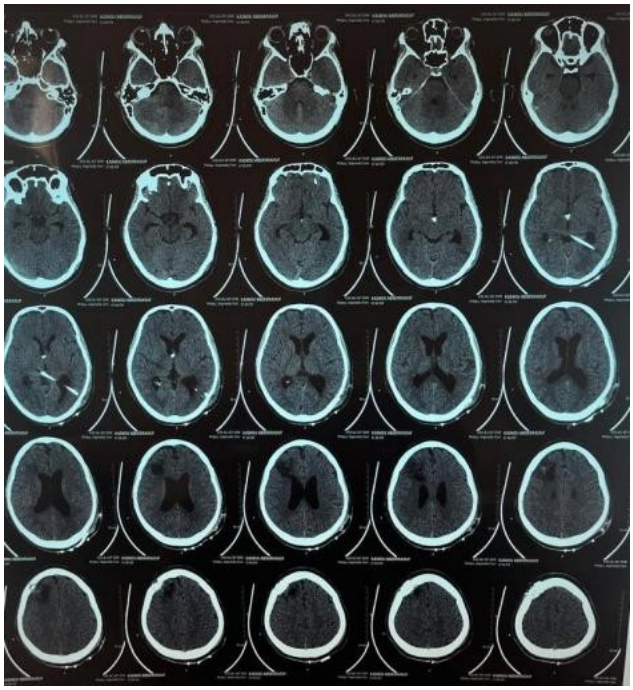


Figure 2. Postoperative brain CT scan in axial sections after placement of a ventriculoperitoneal shunt (VP shunt).

One year after shunt placement, the patient presented again with the same clinical symptoms, secondary to ventriculoperitoneal shunt dysfunction. An external ventricular drain was temporarily placed to relieve intracranial hypertension, and definitive endoscopic management was subsequently decided upon.

Imaging findings

Brain MRI was then performed, confirming an intraventricular lesion within the third ventricle. The lesion was isointense on T1-weighted sequences and predominantly isointense on T2-weighted images, with a peripheral hyperintense rim and a central hypointense component. No contrast enhancement was observed after gadolinium administration (Figure 3).

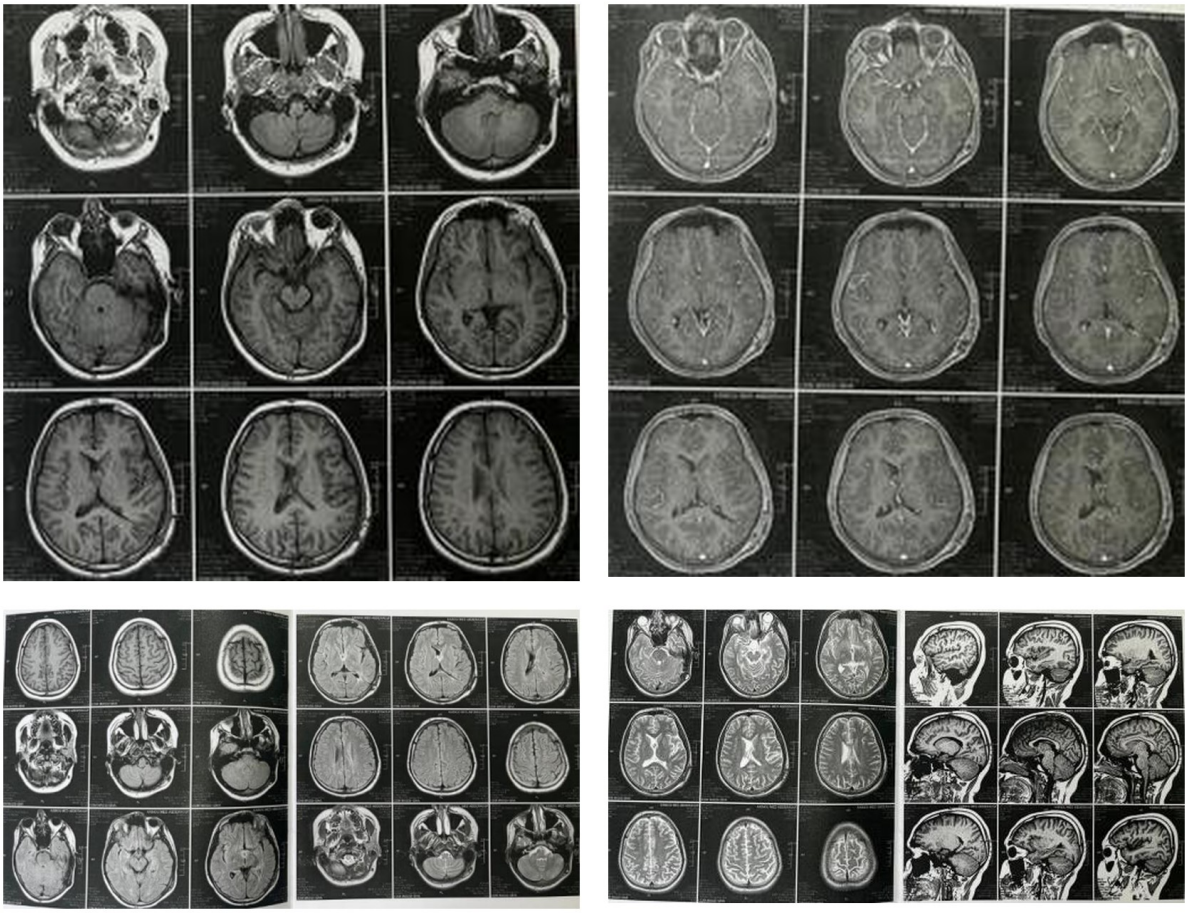


Figure 3. Brain MRI in axial and sagittal sections, including T1-weighted, non-contrast T1, T2-weighted, and FLAIR sequences.

Surgical management

The patient underwent endoscopic subtotal resection of the intraventricular lesion combined with endoscopic third ventriculostomy.

Intraoperatively, the tumor showed heterogeneous consistency, firm in some areas and friable in others, with a whitish appearance and numerous intratumoral calcifications (Figure 4).

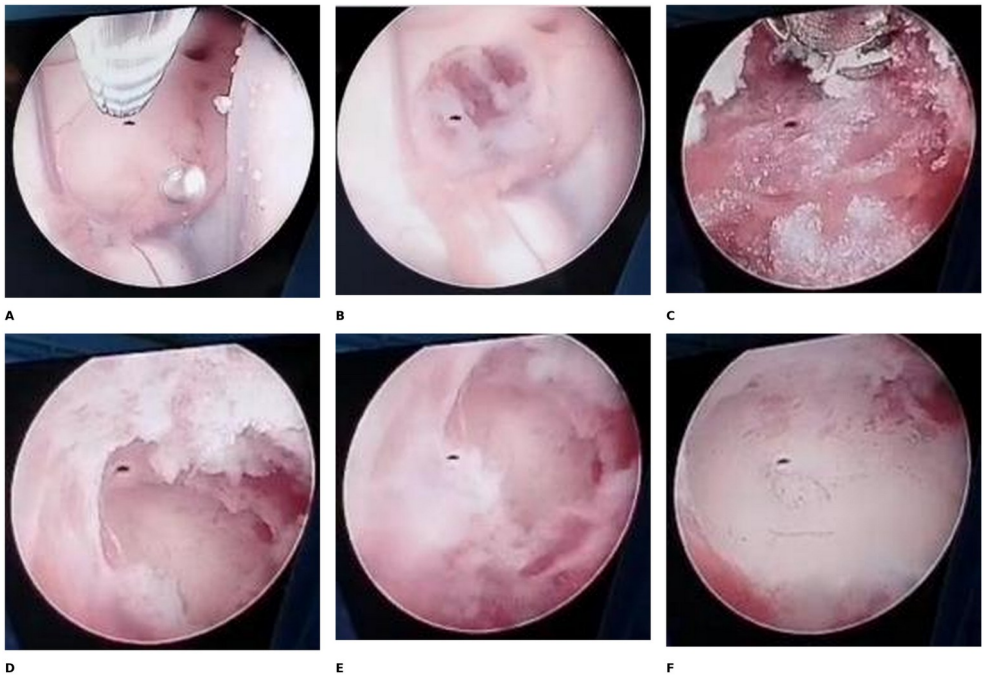


Figure 4. Intraoperative endoscopic images. (A) Lesion visualized through the foramen of Monro. (B) Beginning of debulking. (C) Appearance of the center of the lesion. (D–E–F) Visualization of the floor of the third ventricle after major debulking of the lesion.

Postoperative course

The postoperative course was marked by seizures, which were successfully controlled with antiepileptic medication. The patient also developed transient diabetes insipidus and memory disturbances, both of which resolved during follow-up. Postoperative flow-sensitive brain MRI confirmed patency of the third ventriculostomy (Figure 5).

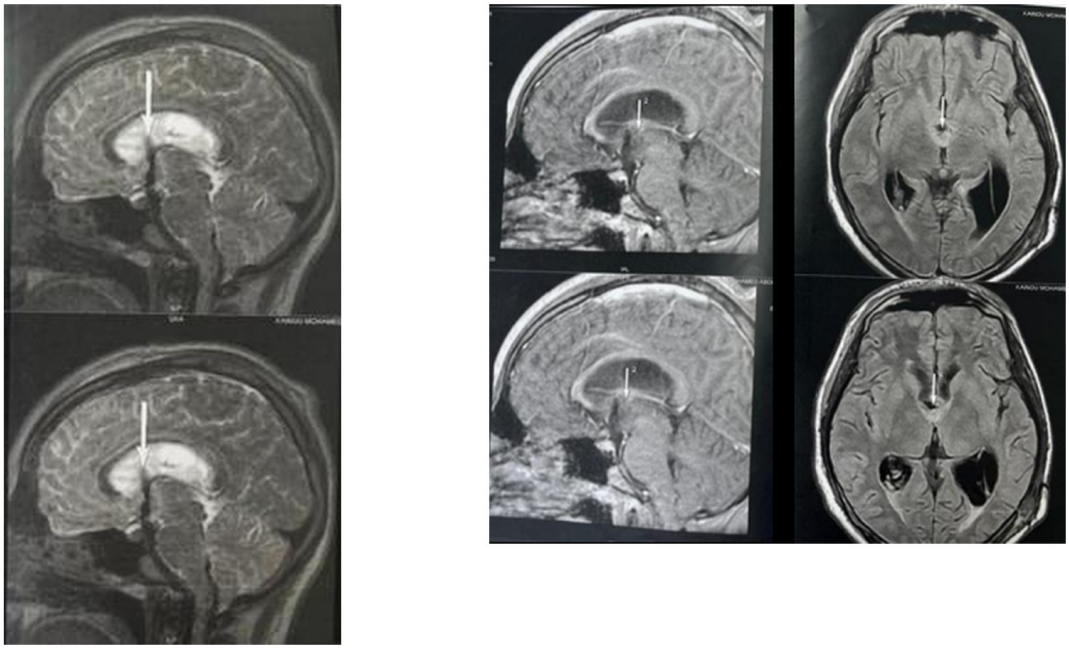


Figure 5. Brain MRI with flow-sensitive (phase-contrast) sequences, showing partial resection of the lesion and good patency of the ventriculocisternostomy.

Histopathological and immunohistochemical findings

Microscopic examination revealed a moderately cellular glioneuronal proliferation composed of oligodendroglial-like cells arranged in clusters, associated with numerous calcifications. The tumor background was myxoid. A perivascular lymphocytic infiltrate was observed, and fragments of choroid plexus tissue were identified in the specimen.

Immunohistochemical analysis demonstrated:

- Positivity for OLIG2 and GFAP.
- No extravascular CD34 staining.
- Negative NeuN.
- Focal chromogranin A positivity in a small subset of tumor cells.
- Negative p53 expression.
- A low Ki-67 labeling index, indicating low proliferative activity.

Based on the morphological features, immunohistochemical profile, and anatomical location, these findings were consistent with a low-grade glioneuronal tumor, classified as WHO grade 1 according to the 2021 WHO Classification of Tumors of the Central Nervous System. The patient did not receive any adjuvant treatment.

DISCUSSION

Glioneuronal tumors constitute a heterogeneous group of rare central nervous system neoplasms characterized by the coexistence of neoplastic glial and neuronal components, generally associated with low-grade biological behavior and a favorable long-term prognosis [1]. The 5th edition of the WHO Classification of Tumors of the Central Nervous System (2021) has substantially reshaped the conceptual framework of these tumors by integrating histological features, immunophenotypic profiles, and molecular alterations into a unified diagnostic approach [1,5]. Recent updates have further expanded the spectrum of glioneuronal tumors to include newly recognized entities such as DGONC, MGT, and multinodular and vacuolating neuronal tumor (MVNT), underscoring the increasing heterogeneity of this tumor group and emphasizing that they should no longer be regarded as a single clinicopathological entity but rather as a family of tumors with distinct anatomical predilections, molecular signatures, and clinical behaviors [6].

Clinically, glioneuronal tumors in pediatric patients often present with symptoms of intracranial hypertension, including headaches, vomiting, and visual disturbances, particularly when cerebrospinal fluid pathways are obstructed [7,8]. This clinical pattern was observed in our 14-year-old patient, whose intraventricular tumor caused obstructive hydrocephalus. While seizures are a common presenting symptom in cortically based glioneuronal tumors, intraventricular lesions are more frequently associated with hydrocephalus-related manifestations than with epilepsy [7, 13].

Radiologically, glioneuronal tumors are typically well-circumscribed lesions with variable cystic components and minimal peritumoral edema, reflecting their indolent nature [10, 12]. On computed tomography, these tumors may appear isodense or hyperdense and frequently contain intralesional calcifications, a feature clearly identified in our patient and consistently reported in the literature [8, 10, 11]. Magnetic resonance imaging usually shows heterogeneous signal characteristics, with hypointense to isointense areas on T1-weighted sequences and hyperintense regions on T2-weighted and FLAIR images, often corresponding to myxoid or cystic components [10– 12]. Contrast enhancement is generally mild or patchy, and diffusion-weighted imaging typically shows no restricted diffusion, supporting the low-grade nature of these tumors [12]. However, when arising in intraventricular locations, glioneuronal tumors may closely mimic other ventricular neoplasms such as central neurocytoma, ependymoma, or colloid cyst, making preoperative radiological diagnosis challenging and histopathological confirmation mandatory [8, 13].

Intraventricular glioneuronal tumors are exceptionally rare, with only isolated case reports and small series described in the literature [8, 13]. The third ventricular location observed in our case further broadens the anatomical spectrum of these tumors and underscores the diagnostic difficulty associated with non-cortical presentations [8].

Histopathological examination remains the cornerstone of diagnosis, particularly in atypical intraventricular locations [1]. According to the WHO 2021 classification, glioneuronal tumors are defined by the coexistence of neoplastic glial and neuronal components at the microscopic level, distinguishing them from purely glial or purely neuronal tumors [1,5]. In our case, microscopic examination revealed a low-cellularity proliferation composed of oligodendroglial-like cells embedded within a prominent myxoid background, associated with abundant calcifications. This

histomorphological pattern closely corresponds to that described in myxoid glioneuronal tumors, a recently recognized WHO entity characterized by circumscribed oligodendrocyte-like cells within a myxoid stroma [6, 14].

Immunohistochemistry plays a critical role in confirming the mixed lineage differentiation of glioneuronal tumors. GFAP expression supports glial differentiation, while neuronal markers such as synaptophysin, chromogranin, MAP2, or NeuN may variably label the neuronal component [1,6, 14]. In our patient, positivity for OLIG2 and GFAP confirmed glial differentiation, while focal chromogranin positivity supported a neuronal lineage despite negative NeuN staining, a pattern frequently reported in immature or poorly differentiated neuronal components of glioneuronal tumors [6, 14]. The absence of extravascular CD34 staining helped exclude alternative diagnoses such as ganglioglioma, while negative p53 expression and a low Ki-67 proliferation index were consistent with a WHO grade 1 tumor and a favorable prognosis [1,7]. Additionally, the perivascular lymphocytic infiltrates observed in our specimen have been described in several low-grade glioneuronal tumors and are thought to reflect their indolent, non-infiltrative biological behavior [7].

Molecular profiling has become an essential adjunct to the modern classification of glioneuronal tumors. Myxoid glioneuronal tumors, in particular, frequently harbor recurrent PDGFRA mutations, which help distinguish them from other low-grade neuroepithelial tumors such as DNET [14, 15]. Although comprehensive molecular testing was not available in all reported intraventricular cases, the integrated histopathological and immunophenotypic profile in our patient was sufficient to establish a definitive diagnosis according to WHO 2021 criteria [1,5].

From a neurosurgical perspective, surgical resection remains the treatment of choice for glioneuronal tumors. Gross total resection is associated with excellent long-term disease control, although subtotal resection may be acceptable in deep or intraventricular locations given the benign biological behavior of these tumors [1, 13]. In our case, an endoscopic approach allowed subtotal tumor resection combined with ventriculocisternostomy, achieving effective tumor debulking and cerebrospinal fluid diversion while minimizing surgical morbidity [9, 16]. Endoscopic approaches to third ventricular tumors have been increasingly adopted in pediatric neurosurgery, offering minimally invasive access, reduced brain retraction, and the possibility of simultaneous CSF pathway restoration compared with transcallosal or transcortical approaches [9, 16]. The risk of recurrence after subtotal resection remains low, and malignant transformation is exceedingly rare, supporting a conservative postoperative strategy with close radiological surveillance [1,6].

CONCLUSION

This case illustrates an uncommon intraventricular presentation of a WHO grade 1 glioneuronal tumor in a pediatric patient, expanding the anatomical and clinicopathological spectrum of these rare neoplasms [1,8, 13]. It highlights the importance of integrating clinical presentation, advanced imaging, detailed histopathological and immunohistochemical analysis, and a tailored neurosurgical strategy to achieve accurate diagnosis and optimal management [1,5,9].

DECLARATIONS

Ethics approval and consent to participate

The study was conducted in accordance with the ethical principles of the Declaration of Helsinki.

Consent for publication

Written informed consent was obtained from the patient's legal guardian for publication of this case report and any accompanying images.

Availability of data and materials

The data supporting the findings of this case report are available from the corresponding author upon reasonable request.

Competing interests

The authors declare that they have no competing interests.

Funding

This research received no specific grant from any funding agency in the public, commercial, or not-for- profit sectors.

Authors' contributions

HO, NH and LA were involved in the surgical management of the patient and drafted the manuscript. YY performed the histopathological and immunohistochemical analysis. NH performed the surgical procedure. All authors read and approved the final manuscript.

Acknowledgements

Not applicable.

REFERENCES

1. Louis DN, Perry A, Wesseling P, et al. The 2021 WHO Classification of Tumors of the Central Nervous System: a summary. Neuro Oncol. 2021;23(8):1231–1251. doi:10.1093/neuonc/noab106.
2. Bale TA, et al. An update on pediatric low-grade gliomas and glioneuronal tumors (WHO 2021 classification). Brain Pathol. 2022.
3. Yano H, Nakayama N, Hirose Y, et al. Intraventricular glioneuronal tumor with disseminated lesions at diagnosis – a case report. Diagn Pathol. 2011;6:119. doi:10.1186/1746-1596-6-119.
4. Park YW, et al. The 2021 WHO Classification of Tumors of the Central Nervous System: imaging and molecular updates. J Magn Reson Imaging. 2023.
5. WHO Classification of Tumours Editorial Board. Central Nervous System Tumours. 5th ed. Lyon: IARC; 2021.
6. Barresi V, Gianno F, Marucci G. Newly recognised tumour types in glioneuronal tumours according to the 5th edition of the CNS WHO Classification. Pathologica. 2022;114:447–454.
7. Blumcke I, Aronica E, Urbach H, et al. A neuropathology-based approach to epilepsy-associated tumors. Acta Neuropathol. 2016;131:1–20.

8. Yano H, et al. Intraventricular glioneuronal tumor: case report. Diagn Pathol. 2011;6:119. doi:10.1186/1746 - 1596-6-119.

9. Rangel-Castilla L, et al. Endoscopic approaches to third ventricular tumors. Neurosurg Focus. 2016;41(3):E6.

10. Koeller KK, Henry JM. Superficial glioneuronal tumors: radiologic-pathologic correlation. Radiographics. 2001;21:1533–1556.

11. Osborn AG. Diagnostic Imaging: Brain. 3rd ed. Elsevier; 2016.

12. Blasel S, et al. Imaging characteristics of glioneuronal tumors. AJNR Am J Neuroradiol. 2010;31:176–184.

13. Hasselblatt M, et al. Intraventricular low-grade neuroepithelial tumors. Acta Neuropathol. 2018;136:273– 285.

14. Chiang JCH, et al. Myxoid glioneuronal tumor: clinicopathologic and molecular characterization. Acta Neuropathol. 2022;144:1–15. doi:10.1007/s00401-022-02492-7.

15. Korshunov A, et al. Molecular genetics of pediatric low-grade glioneuronal tumors. Brain Pathol. 2022.

16. Schroeder HWS. Intraventricular neuroendoscopy. Neurosurg Rev. 2015;38:1–14.

Spinal Neurosurgery

SPINAL METASTASES:
Clinical Features, Imaging and Prognosis in 52 Patients

ABDELMALEK Adel[1], HABCHI Nawel[1] , KARA Samira[1] and TLIBA Souhil[1]

1: Department of Neurosurgery, Blida University Hospital, Algeria

***Corresponding Author:** ABDELMALEK Adel, Department of Neurosurgery, Blida University Hospital, Algeria*

***Received:** August 31, 2026 — **Accepted:** September 15, 2026 — **Published:** October 01, 2026*

*Citation: ABDELMALEK Adel, HABCHI Nawel, KARA Samiraand TLIBA Souhil. Spinal Metastases: Clinical Features, Imaging and Prognosis in 52 Patients. **OLCIAS Vol.3, Issue 2.***

ABSTRACT

Background and objective. To describe the clinical, imaging, pathological and prognostic features of spinal metastases managed at Blida University Hospital and examine the relevance of legacy survival scores.

Methods. This prospective, single-center descriptive study included 52 patients with a confirmed secondary vertebral tumor. Assessment comprised pain, Karnofsky Performance Status, Frankel/ASIA grades, computed tomography, magnetic resonance imaging, and revised Tokuhashi and Tomita scores. Analyses used aggregate data.

Results. Mean age was 54.7 ± 13.25 years (range, 16-82), with equal sex distribution. Breast cancer predominated among women (57.7%) and lung cancer among men (34%). Carcinomas, adenocarcinomas and multiple myeloma accounted for 42.3%, 25% and 15.4% of diagnoses. Pain, motor deficit and Frankel A/B grades were reported in 90%, 96% and 30.8%, respectively. Karnofsky status was favorable in 76.9%. Lesions were predominantly lytic (67.3%), with epidural extension in 67%. Tokuhashi groups 0-8, 9-11 and 12-15 comprised 42.3%, 38.5% and 19.2%. Six-month mortality was 45.5% for lung primaries and 20% for breast primaries. Six-month survival of 63% was reported in the Tokuhashi 0-8 group.

Conclusion. This series highlights severe neurological presentation and heterogeneous prognosis across primary tumors. Reported survival in the Tokuhashi 0-8 group suggests possible prognostic underestimation but does not constitute formal validation. Scores should inform multidisciplinary assessment; patient-level survival analysis and assessment of discrimination and calibration remain necessary.

Keywords: spinal metastases; metastatic spinal cord compression; spine surgery; Tokuhashi; Tomita; NESMS; survival; prognosis.

1. Introduction

Spinal metastases are a major cause of oncological morbidity, involving pain, bone destruction, pathological fracture, instability, and neurological compression. A systematic review highlights their clinical frequency and complications, particularly epidural compression and vertebral fractures [1].

The treatment strategy is based on neurological status, spinal stability, radiosensitivity, systemic disease extent, and general condition. In selected patients, decompression combined with radiotherapy may preserve or restore ambulation and improve pain [2-5]. Stabilization and reconstruction techniques are tailored to the spinal level and the goals of local and mechanical control.

Survival estimates should avoid both undertreatment resulting from pessimistic predictions and disproportionate intervention. The Tokuhashi and Tomita scores have provided a framework for this decision [6,7], but predate targeted therapies, immunotherapy, and stereotactic radiotherapy. More recent models, including the New England Spinal Metastasis Score (NESMS), place greater emphasis on functional status and biological parameters [13-15].

In a North African setting that is underrepresented in the literature, local data can characterize patterns of presentation and help examine the transportability of prognostic tools.

This study describes the epidemiological, clinical, radiological, histopathological, and prognostic characteristics of 52 patients managed at Blida University Hospital. It also explores the concordance between Tokuhashi categories and short-term survival, together with the potential contribution of contemporary prognostic factors.

2. Materials and methods

2.1. Study design and population

This prospective, single-center, descriptive study was conducted in the Department of Neurosurgery at Blida University Hospital. The reported period of clinical activity extended from 2022 to 2025; exact calendar dates of inclusion were not provided.

The reported inclusion criteria were age older than 16 years and a confirmed secondary vertebral tumor. The aggregate data did not specify the exclusion criteria, whether inclusion was consecutive, the methods used to confirm the primary tumor, or the number of patients initially assessed.

2.2. Clinical, radiological, and histopathological assessment

Variables included age, sex, time to consultation, pain assessed using a visual analog scale from 0 to 10, Karnofsky Performance Status, and Frankel/ASIA grades. The thresholds defining “good” or “intermediate” Karnofsky status were not specified.

Computed tomography (CT) distinguished lytic, mixed, and osteoblastic lesions. Magnetic resonance imaging (MRI) assessed vertebral involvement, deformities, dislocations, and epidural extension. Spinal level, Bilsky compression grade, and the Spinal Instability Neoplastic Score (SINS) were not available as aggregate data.

Histopathology was described by histological type and primary tumor site. The categories “carcinoma” and “adenocarcinoma” were presented separately in the analyzed data.

2.3. Surgical strategy

Surgical approaches depended on the spinal level, compression, and instability. In the cervical spine, the options described were anterior corpectomy with an expandable cage and screw fixation plate, or posterior cervical/occipitocervical fixation. At the thoracic and lumbar levels, options included decompressive laminectomy, pedicle screw fixation, and, in selected situations, posterior retropleural or retroperitoneal approaches with vertebral body reconstruction.

The number of patients who underwent surgery, the distribution of techniques, perioperative data, complications, and adjuvant treatments were not specified. The figures therefore illustrate technical examples rather than the frequency of these procedures in the cohort.

2.4. Prognosis and statistical analysis

Revised Tokuhashi and Tomita scores were reported for the cohort. The available outcomes were cumulative mortality at 3 and 6 months according to primary tumor site and 6-month survival in the Tokuhashi 0-8 group. In the absence of individual serum albumin levels and ambulatory status, the NESMS was neither calculated nor validated in this series.

The analysis was descriptive: quantitative variables were expressed as mean ± standard deviation and range, and categorical variables as counts and percentages. Counts reconstructed from N = 52 and the reported percentages, rounded to the nearest compatible integer, are marked with †. No patient-level survival analysis, confidence intervals, or hypothesis tests were available.

2.5. Ethical considerations

Annotations that could identify an examination had been masked in the illustrations. Information on ethics approval, consent, and permission to publish the images was not provided in the available data.

3. Results

3.1. General characteristics and clinical presentation

The series included 52 patients, with a mean age of 54.7 ± 13.25 years (range, 16-82 years) and a male-to-female ratio of 1. Mean age was 57.7 years in men and 51.7 years in women (Table 1).

Time to consultation was ≤1 month in 23% of patients, 2-4 months in 46%, and >4 months in 30%. For lumbar lesions, 34% of patients presented after 6 months; 88% of cervical and thoracic lesions were assessed before 4 months.

Pain was reported in 90% of patients, motor deficit in 96%, and sensory deficit in 60%. Frankel grades A/B, C, and D accounted for 30.8%, 26.9%, and 42.3%, respectively.

Karnofsky status was favorable in 76.9% of patients and intermediate in 23.1%. Favorable status was reported in 84.6% of women and 69.2% of men, as well as in 80% of patients with breast primaries, 77.8% with hematological malignancies, and 63.6% with lung primaries.

Table 1. Demographic and clinical characteristics of the cohort (N = 52)

Variable	Result
Age, mean ± SD (range)	54.7 ± 13.25 years (16-82)
Men / women	26 / 26 (50% / 50%)†
Consultation within the first month	≈ 12 (23%)†
Consultation at 2-4 months	≈ 24 (46%)†
Consultation after 4 months	≈ 16 (30%)†
Pain	≈ 47 (90%)†
Motor deficit	≈ 50 (96%)†
Sensory deficit	≈ 31 (60%)†
Frankel A/B	16 (30.8%)†
Frankel C	14 (26.9%)†
Frankel D	22 (42.3%)†
Favorable Karnofsky status	40 (76.9%)†
Intermediate Karnofsky status	12 (23.1%)†

† Counts estimated from the percentages and N = 52. SD: standard deviation.

3.2. Primary tumor site and histopathology

Among women, primary tumors were predominantly breast cancer (57.7%), followed by hematological malignancies (15%), lung cancer, and thyroid cancer (7.6% each). Among men, lung cancer predominated (34%), followed by hematological malignancies (23%), prostate cancer (11.5%), gastrointestinal tumors, and thyroid cancer (7.6% each).

Carcinomas (42.3%), adenocarcinomas (25%), and multiple myeloma (15.4%) predominated in the histological distribution. The other categories and unknown diagnoses are detailed in Table 2; Figure 1 presents two histopathological examples.

Table 2. Reported histopathological distribution

Histological type	Estimated n†	%
Carcinomas	22	42.3
Adenocarcinomas	13	25.0
Multiple myeloma	8	15.4
Lymphomas	3	5.8
Liposarcomas	2	3.8
Neuroendocrine tumors	1	1.9
Unknown	3	5.8

† Counts reconstructed from the percentages.

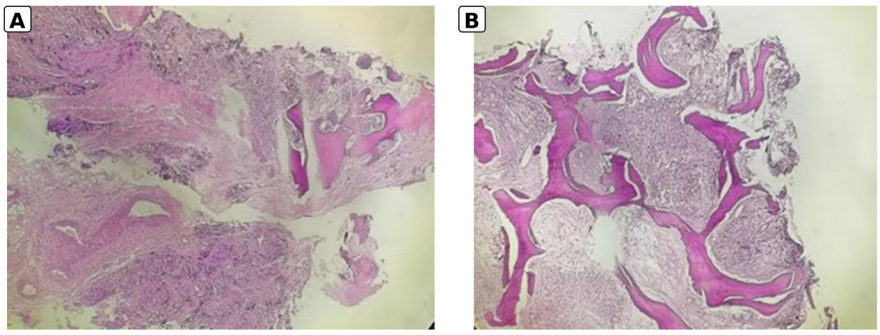


Figure 1. Histopathological examples of secondary vertebral lesions in the series. (A) Spinal involvement by breast carcinoma. (B) Diffuse large B-cell lymphoma involving the L3 vertebra.

3.3. Radiological characteristics

Lesions were predominantly lytic on CT (67.3%), with epidural extension on MRI in 67% of cases (Table 3; Figure 2). Deformities were reported in 93.3% of patients with breast primaries, 75% with lung primaries, and 33% with prostate primaries. The reported dislocations involved the cervical spine (75%) and lower thoracic spine (25%). Denominators for these subgroups were unavailable.

Table 3. Radiological phenotype of vertebral lesions

Characteristic	Estimated n†	%
Lytic lesion on CT	35	67.3
Mixed lesion on CT	14	26.9
Osteoblastic lesion on CT	3	5.8
Epidural tumor extension on MRI	≈ 35	67.0

† Counts estimated from the percentages and N = 52.

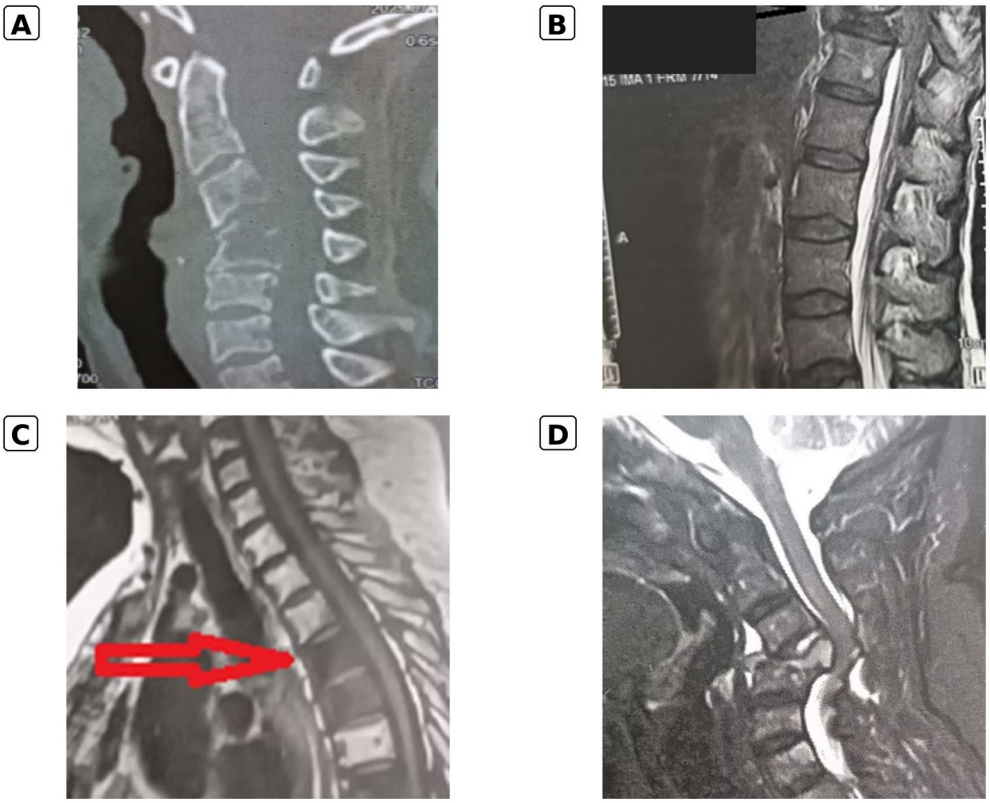


Figure 2. Radiological illustrations of spinal metastases in the series. (A) Sagittal CT showing cervical bone destruction. (B-D) Sagittal MR images illustrating different patterns of vertebral involvement, deformity, and epidural extension.

3.4. Decompression and stabilization: illustrations

Figures 3 and 4 illustrate anterior cervical reconstruction with a cage and plate, posterior cervical stabilization, and thoracolumbar pedicle screw fixation. The frequency of these techniques was not provided.

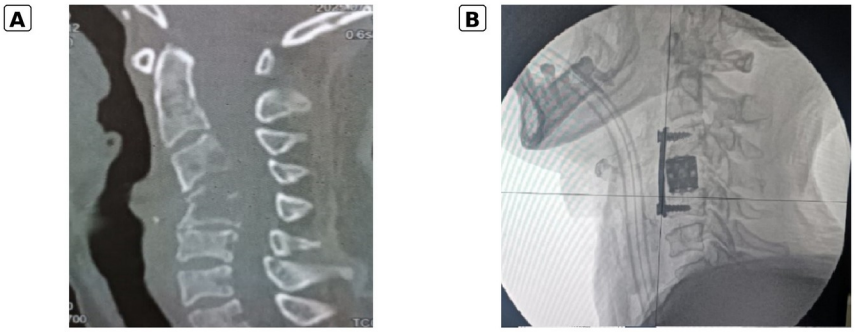


Figure 3. Example of anterior cervical management. (A) Sagittal CT showing a destructive cervical vertebral lesion. (B) Lateral fluoroscopic image following corpectomy and anterior reconstruction with a vertebral body implant and screw fixation plate.

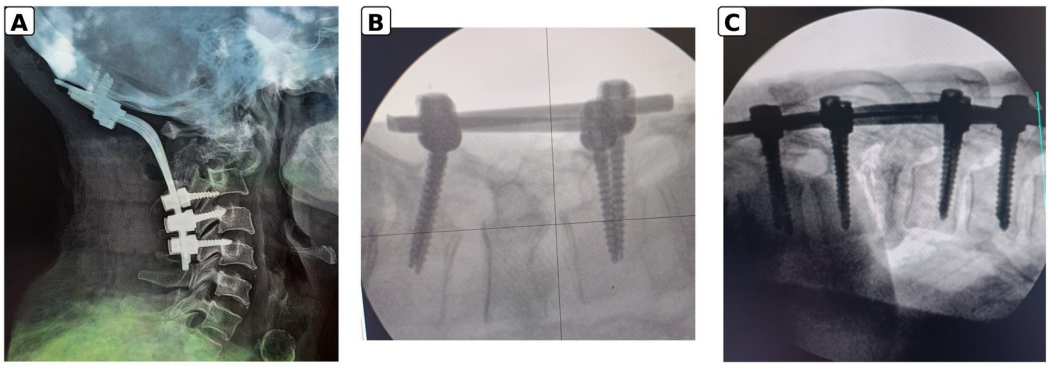


Figure 4. Examples of posterior stabilization in the series. (A) Postoperative radiograph of cervical/occipitocervical instrumentation. (B-C) Intraoperative fluoroscopic images of posterior thoracolumbar fixation with pedicle screws and rods.

3.5. Prognostic scores and short-term survival

The Tokuhashi 0-8, 9-11, and 12-15 groups accounted for 42.3%, 38.5%, and 19.2% of the cohort, respectively. The 0-8 group historically corresponds to an expected survival of less than 6 months. According to the Tomita score, 73.1% of patients belonged to the unfavorable group (Table 4).

Cumulative mortality at 3 and 6 months was 18.2% and 45.5% for lung primaries, compared with 6.7% and 20% for breast primaries. Six-month survival of 100% was reported for prostate, thyroid, muscle, and bladder primaries, although these subgroups were probably small.

Six-month survival of 63% was reported in the Tokuhashi 0-8 group. In the absence of numbers at risk, individual events, dates of death, censoring information, and a confidence interval, this discrepancy with historical expectations remains descriptive and does not constitute formal validation.

Table 4. Distribution of prognostic scores and survival data

Indicator	Result
Tokuhashi 0-8	22 patients (42.3%)†
Tokuhashi 9-11	20 patients (38.5%)†
Tokuhashi 12-15	10 patients (19.2%)†
Unfavorable Tomita	38 patients (73.1%)†
Intermediate Tomita (4-5)	11 patients (21.2%)†
Favorable Tomita (2-3)	3 patients (5.8%)†
Lung - mortality at 3 / 6 months	18.2% / 45.5%
Breast - mortality at 3 / 6 months	6.7% / 20.0%
Tokuhashi 0-8 - survival at 6 months	63%; denominator and CI not provided

† Count derived from the percentage and N = 52. CI: confidence interval.

4. Discussion

4.1. Main findings

This series describes a relatively young population with a substantial neurological burden at presentation and a predominance of lytic lesions and epidural extension. Breast cancer predominated among women and lung cancer among men. Survival varied according to the primary tumor; survival reported in the least favorable Tokuhashi group appeared better than historical expectations.

4.2. Tumor profile and relevance of the local setting

The distribution of primary tumors is consistent with that of cancers responsible for spinal metastases. However, Van den Brande et al. highlight the heterogeneity of estimates according to screening, oncological survival, and imaging practices [1]. The proportions in this series remain hospital-based and cannot be used to estimate incidence or prevalence in the general population.

Differences in Karnofsky status and survival according to the primary tumor should be interpreted in light of histological and molecular subtypes, visceral disease burden, lines of therapy, and response to systemic treatment. The absence of these data limits interpretation of oncological trajectories, particularly for breast, thyroid, prostate, and lung primaries.

The distinction between “carcinoma” and “adenocarcinoma” supports the use of a hierarchical nomenclature incorporating primary site, histological type, relevant molecular subtype, and confirmation status of the primary tumor.

4.3. Diagnostic delay and neurological severity

Nearly one-third of patients presented after four months, particularly those with lumbar lesions. The frequency of Frankel grades A/B and C suggests an already advanced presentation. Because pain may precede neurological deficit, a rapid referral pathway involving primary care, oncology, emergency medicine, radiology, and spine surgery is essential.

A study of surgical timing associated intervention within 48 hours with better neurological outcomes, without demonstrating an independent effect on survival [3]. The prospective AOSpine cohort also reported improvements in pain, function, and quality of life after surgery in selected patients [4]. These observations highlight the importance of the intervals between neurological deficit, MRI, corticosteroid therapy, multidisciplinary consultation, and surgery.

4.4. Imaging, epidural extension, and mechanical instability

Bone destruction, mechanical instability, and epidural compression should be distinguished. The SINS standardizes the assessment of neoplastic instability [8], whereas the NOMS framework integrates neurological, oncological/radiosensitivity, mechanical, and systemic considerations to guide irradiation, stabilization, decompression, and systemic treatments [9]. These dimensions complement the description of the lytic lesions and epidural extension observed here.

Location, mechanical pain, lesion type, alignment, vertebral collapse, and posterolateral involvement are required to calculate the SINS. The absence of these data and of the Bilsky grade limits standardized assessment of instability and epidural compression in this series.

4.5. Role and objectives of surgery

The illustrated reconstructions address the goals of decompression, stability, and reduction of mechanical pain while allowing oncological treatment to continue. However, they do not allow the surgical benefit specific to this cohort to be measured, because detailed postoperative outcomes are unavailable.

In selected patients, the trial by Patchell et al. demonstrated an improvement in ambulation with decompression followed by radiotherapy compared with radiotherapy alone [2]. Subsequent cohorts reported improvements in pain, Karnofsky status, and quality of life, with persistent vulnerability to systemic complications [4,5]. Surgery is therefore a component of a multimodal strategy rather than an exclusive treatment option.

Separation surgery aims to create a margin between the epidural tumor and the spinal cord to permit ablative irradiation, rather than extensive resection. The SC.24 trial reported a higher complete pain response with stereotactic radiotherapy in selected patients [17]; guidelines address postoperative contouring [18]. The absence of data on irradiation type, dose, and timing, as well as systemic treatments, limits analysis of the multimodal strategy in this series.

4.6. Historical scores and prognostic discrepancy

Tokuhashi combines general condition, bone and visceral metastatic burden, primary tumor, and neurological deficit; the 0-8 category originally corresponded to an expected survival of less than 6 months [6]. Tomita emphasizes primary tumor growth and visceral and skeletal dissemination [7]. Their simplicity remains useful, but their calibration may change as oncological treatments evolve.

The reported 6-month survival of 63% in the Tokuhashi 0-8 group suggests possible underestimation, consistent with some discrepancies described in external validations [10-12]. It does not demonstrate that the score is invalid in Blida. Confirmation requires Kaplan-Meier curves, confidence intervals, analysis of censoring, and assessment of discrimination and calibration.

Six-month mortality was higher for lung than for breast primaries (45.5% versus 20%), but the small subgroups require caution. An observed survival of 100% for a rare primary tumor does not provide prognostic certainty: it may reflect the absence of an event in only a few cases.

4.7. Contemporary factors and the role of the NESMS

The NESMS combines the dichotomized modified Bauer score, serum albumin at a threshold of 3.5 g/dL, and independent ambulation [13].

Its prospective validation included both surgically and nonsurgically treated patients [14]. A prospective comparison reported 1-year c-statistics of 0.79 for NESMS, 0.69 for Tomita, 0.67 for Tokuhashi, and 0.54 for SINS [15]. A multicenter external validation in 2026 described increasing mortality with worsening NESMS [21]. These findings do not replace local validation.

In this cohort, the absence of serum albumin, independent ambulation, and the components of the modified Bauer score prevents calculation of the NESMS. Nutritional and inflammatory parameters, renal function, frailty, functional status, metastatic burden, and tumor and treatment characteristics offer avenues for a prospective extension. The importance of nutritional status is also supported by prospective data [19].

SORG-type tools and machine learning provide individualized estimates [16,20,22], without guaranteeing transportability. With 52 patients, the priority remains validation of existing models, using few predictors, penalization, and bootstrapping, rather than development of a complex model.

4.8. Limitations

The main limitations are the single-center design, small sample size, and use of aggregate data, without multivariable analysis or patient-level verification. Recruitment dates, inclusion flow, exclusions, Karnofsky thresholds, and histological nomenclature remain incomplete. Operative data, complications, changes in pain, ambulation, and neurological status, oncological treatments, follow-up duration, losses to follow-up, and censoring are not reported. The NESMS and SINS cannot be fully calculated.

These limitations restrict the prognostic scope without negating the descriptive value of the study. The discrepancy between the distribution of Frankel grades and the reported rate of motor deficit also limits the precision of the neurological description. A more complete assessment depends on the availability of standardized patient-level data, in accordance with the STROBE principles for reporting observational studies [23].

4.9. Practical implications

The proposed local algorithm sequentially assesses neurological urgency, instability, degree of compression and radiosensitivity, systemic and functional status, and then plausible survival according to the primary tumor, metastatic burden, serum albumin, and independence. Multidisciplinary consultation should involve neurosurgery, oncology, radiotherapy, radiology, pathology, anesthesiology and intensive care, and rehabilitation.

Tokuhashi may remain a common language, but should not be an automatic exclusion criterion. An unfavorable score despite preserved function, a controllable primary tumor, or a relevant therapeutic option warrants multidisciplinary reassessment.

5. Conclusion

This series of 52 patients from Blida University Hospital describes frequently advanced spinal metastases, dominated by pain, motor deficit, osteolysis, and epidural extension. The reported 6-month survival of 63% in the Tokuhashi 0-8 group raises, but does not establish, the possibility of prognostic underestimation.

Decompression and stabilization should be integrated into a multimodal oncological strategy. Assessment combines scores, functional and nutritional status, metastatic burden, and treatment options. A verified patient-level database and a complete survival analysis remain essential to confirm the findings and validate the models.

Ethics approval and consent to participate

The study was conducted in accordance with the ethical principles of the Declaration of Helsinki.

Consent for publication

Written informed consent was obtained from the patient's legal guardian for publication of this case report and any accompanying images.

Availability of data and materials

The data supporting the findings of this case report are available from the corresponding author upon reasonable request.

Competing interests

The authors declare that they have no competing interests.

Funding

This research received no specific grant from any funding agency in the public, commercial, or not-for-profit sectors.

References

1. Van den Brande R, Cornips EMJ, Peeters M, Ost P, Billiet C, Van de Kelft E. Epidemiology of spinal metastases, metastatic epidural spinal cord compression and pathologic vertebral compression fractures in patients with solid tumors: a systematic review. J Bone Oncol. 2022;35:100446. doi:10.1016/j.jbo.2022.100446.

2. Patchell RA, Tibbs PA, Regine WF, Payne R, Saris S, Kryscio RJ, et al. Direct decompressive surgical resection in the treatment of spinal cord compression caused by metastatic cancer: a randomised trial. Lancet. 2005;366(9486):643-648. doi:10.1016/S0140-6736(05)66954-1.

3. Quraishi NA, Rajagopal TS, Manoharan SR, Elsayed S, Edwards KL, Boszczyk BM. Effect of timing of surgery on neurological outcome and survival in metastatic spinal cord compression. Eur Spine J. 2013;22(6):1383-1388. doi:10.1007/s00586-012-2635-y.

4. Fehlings MG, Nater A, Tetreault L, Kopjar B, Arnold P, Dekutoski M, et al. Survival and clinical outcomes in surgically treated patients with metastatic epidural spinal cord compression: results of the prospective multicenter AOSpine study. J Clin Oncol. 2016;34(3):268-276. doi:10.1200/JCO.2015.61.9338.

5. Choi D, Fox Z, Albert T, Arts M, Balabaud L, Bunger C, et al. Prediction of quality of life and survival after surgery for symptomatic spinal metastases: a multicenter cohort study to determine suitability for surgical treatment. Neurosurgery. 2015;77(5):698-708. doi:10.1227/NEU.0000000000000907.

6. Tokuhashi Y, Matsuzaki H, Oda H, Oshima M, Ryu J. A revised scoring system for preoperative evaluation of metastatic spine tumor prognosis. Spine. 2005;30(19):2186-2191. doi:10.1097/01.brs.0000180401.06919.a5.

7. Tomita K, Kawahara N, Kobayashi T, Yoshida A, Murakami H, Akamaru T. Surgical strategy for spinal metastases. Spine. 2001;26(3):298-306. doi:10.1097/00007632-200102010-00016.

8. Fourney DR, Frangou EM, Ryken TC, DiPaola CP, Shaffrey CI, Berven SH, et al. Spinal Instability Neoplastic Score: an analysis of reliability and validity from the Spine Oncology Study Group. J Clin Oncol. 2011;29(22):3072-3077. doi:10.1200/JCO.2010.34.3897.

9. Laufer I, Rubin DG, Lis E, Cox BW, Stubblefield MD, Yamada Y, Bilsky MH. The NOMS framework: approach to the treatment of spinal metastatic tumors. Oncologist. 2013;18(6):744-751. doi:10.1634/theoncologist.2012-0293.

10. Bollen L, van der Linden YM, Pondaag W, Fiocco M, Pattynama BPM, Marijnen CAM, et al. Prognostic factors associated with survival in patients with symptomatic spinal bone metastases: a retrospective cohort study of 1,043 patients. Neuro Oncol. 2014;16(7):991-998. doi:10.1093/neuonc/not318.

11. Choi D, Pavlou M, Omar R, Arts M, Balabaud L, Buchowski JM, et al. A novel risk calculator to predict outcome after surgery for symptomatic spinal metastases: use of a large prospective patient database to personalise surgical management. Eur J Cancer. 2019;107:28-36. doi:10.1016/j.ejca.2018.11.011.

12. Morgen SS, Fruergaard S, Gehrchen M, Bjørck S, Engelholm SA, Dahl B. A revision of the Tokuhashi revised score improves the prognostic ability in patients with metastatic spinal cord compression. J Cancer Res Clin Oncol. 2018;144(1):33-38. doi:10.1007/s00432-017-2519-y.

13. Schoenfeld AJ, Le HV, Marjoua Y, Leonard DA, Belmont PJ Jr, Bono CM, et al. Assessing the utility of a clinical prediction score regarding 30-day morbidity and mortality following metastatic spinal surgery: the New England Spinal Metastasis Score. Spine J. 2016;16(4):482-490. doi:10.1016/j.spinee.2015.09.043.

14. Schoenfeld AJ, Ferrone ML, Schwab JH, et al. Prospective validation of a clinical prediction score for survival in patients with spinal metastases: the New England Spinal Metastasis Score. Spine J. 2021;21(1):28-36. doi:10.1016/j.spinee.2020.02.009.

15. Schoenfeld AJ, et al. Prospective comparison of the accuracy of the New England Spinal Metastasis Score to legacy scoring systems in prognosticating outcomes following treatment of spinal metastases. Spine J. 2022;22(1):39-48. doi:10.1016/j.spinee.2021.03.007.

16. Pereira NRP, Janssen SJ, van Dijk E, Harris MB, Hornicek FJ, Ferrone ML, Schwab JH. Development of a prognostic survival algorithm for patients with metastatic spine disease. J Bone Joint Surg Am. 2016;98(21):1767-1776. doi:10.2106/JBJS.15.00975.

17. Sahgal A, Myrehaug SD, Siva S, Masucci GL, Maralani PJ, Brundage M, et al. Stereotactic body radiotherapy versus conventional external beam radiotherapy in patients with painful spinal metastases: an open-label, multicentre, randomised, controlled, phase 2/3 trial. Lancet Oncol. 2021;22(7):1023-1033. doi:10.1016/S1470-2045(21)00196-0.

18. Redmond KJ, Robertson S, Lo SS, Soltys SG, Ryu S, McNutt T, et al. Consensus contouring guidelines for postoperative stereotactic body radiation therapy for metastatic solid tumor malignancies to the spine. Int J Radiat Oncol Biol Phys. 2017;97(1):64-74. doi:10.1016/j.ijrobp.2016.09.014.

19. Japan Association of Spine Surgeons With Ambition Study Group. Effect of preoperative nutritional status on postoperative clinical outcomes of patients with metastatic spinal tumors: a multicenter study. Spine. 2025;50(22):1571-1580. doi:10.1097/BRS.0000000000005487.

20. Kitagawa K, Maki S, Shiratani Y, et al. Machine learning-based prediction of quality of life improvement after surgery for spinal metastases: a prospective multicenter study. Spine. 2025;50(20):1410-1419. doi:10.1097/BRS.0000000000005367.

21. Giles W, Low L, Watts AL, et al. Multicentre external validation of the New England Spinal Metastasis Score in operative and nonoperative patients with metastatic spinal cord compression. Spine J. 2026;26(2):354-360. doi:10.1016/j.spinee.2025.08.333.

22. Maki S, Shiratani Y, Orita S, et al. Predicting postoperative neurological outcomes in metastatic spinal tumor surgery using machine learning. Spine. 2026;51(2):100-106. doi:10.1097/BRS.0000000000005322.

23. von Elm E, Altman DG, Egger M, Pocock SJ, Gøtzsche PC, Vandenbroucke JP; STROBE Initiative. The Strengthening the Reporting of Observational Studies in Epidemiology (STROBE) statement: guidelines for reporting observational studies. Lancet. 2007;370(9596):1453-1457. doi:10.1016/S0140-6736(07)61602-X.

Spinal Neurosurgery

INTRADURAL TERATOMA OF THE CAUDA EQUINA IN AN ADOLESCENT GIRL:
A Rare Case Report and Review of the Literature

BELGACEM Ibrahim, DJOUADI Yasmina, ABOUDJABEL Mohamed, IZIROUEL Karim and AIT BACHIR Mustapha

Neurosurgery Department, University Hospital Nadir Mohamed, TiziOuzou, Algeria

***Corresponding Author:** BELGACEM Ibrahim, Neurosurgery Department, University Hospital Nadir Mohamed, TiziOuzou, Algeria*

***Received:** June 19, 2026 — **Accepted:** September 15, 2026 — **Published:** October 01, 2026*

Citation:** BELGACEM Ibrahim, DJOUADI Yasmina, ABOUDJABEL Mohamed, IZIROUEL Karim and AIT BACHIR Mustapha. Intradural Teratoma of the Cauda Equina in an Adolescent Girl: A Rare Case Report and Review of the Literature. **OLCIAS Vol.3, Issue 2.

ABSTRACT

Introduction: Intradural teratomas of the cauda equina are exceptionally rare, particularly in adolescents. Case report: We report the case of a 17-year-old female high school student with a one-year history of poorly localized lumbosciatic pain refractory to appropriate medical treatment. Lumbosacral MRI revealed an intradural mass at the L3-L4 level, displacing the cauda equina roots. Complete excision was performed through a posterior approach. Histopathological examination confirmed a mature teratoma. The postoperative course was favorable, with complete resolution of symptoms. Conclusion: This case highlights the importance of considering a neoplastic etiology in the presence of atypical chronic low back pain in an adolescent girl and demonstrates the effectiveness of neurosurgical management.

***Keywords:** Spinal teratoma, Cauda equina, Adolescent girl, Intradural tumor, Chronic lumbosciatica*

INTRODUCTION

Teratomas are rare germ cell tumors derived from pluripotent cells capable of forming tissues originating from the three embryonic germ layers (ectoderm, mesoderm, and endoderm). Their location within the spinal canal is exceptional, accounting for less than 0.5% of all spinal tumors [1]. When they arise in the cauda equina or conus medullaris region, they are even rarer, particularly in adolescent girls. The literature reports only 11 cases to date, 9 of which were mature teratomas [2]. This tumor was first described in 1863 by Virchow and later, in 1888, by Horsley and Gowers [3].

The pathogenesis of spinal teratoma remains controversial. Several embryogenic hypotheses have been proposed, particularly involving abnormal migration of germ cells during neural tube development. The extreme rarity of these tumors makes them difficult to study, and the available clinical data are derived mainly from isolated case reports.

The objective of our study is to report a new case of a teratoma of the conus medullaris (or cauda equina), presenting with atypical low back pain refractory to treatment, and to discuss its diagnostic, therapeutic, and prognostic aspects in light of the available literature.

CASE PRESENTATION

We report the case of a 17-year-old female high school student with no significant medical history who presented with right-sided lumbosciatic pain that had been evolving for approximately one year. The pain was poorly localized and fluctuating, without typical radicular radiation or a clear neurological deficit, and had failed to respond to medical treatment comprising analgesics, nonsteroidal anti-inflammatory drugs, and physiotherapy sessions. Because the symptoms persisted, an imaging workup was performed. Lumbosacral CT revealed an intraspinal mass at the L3-L4 level (Fig. 01).

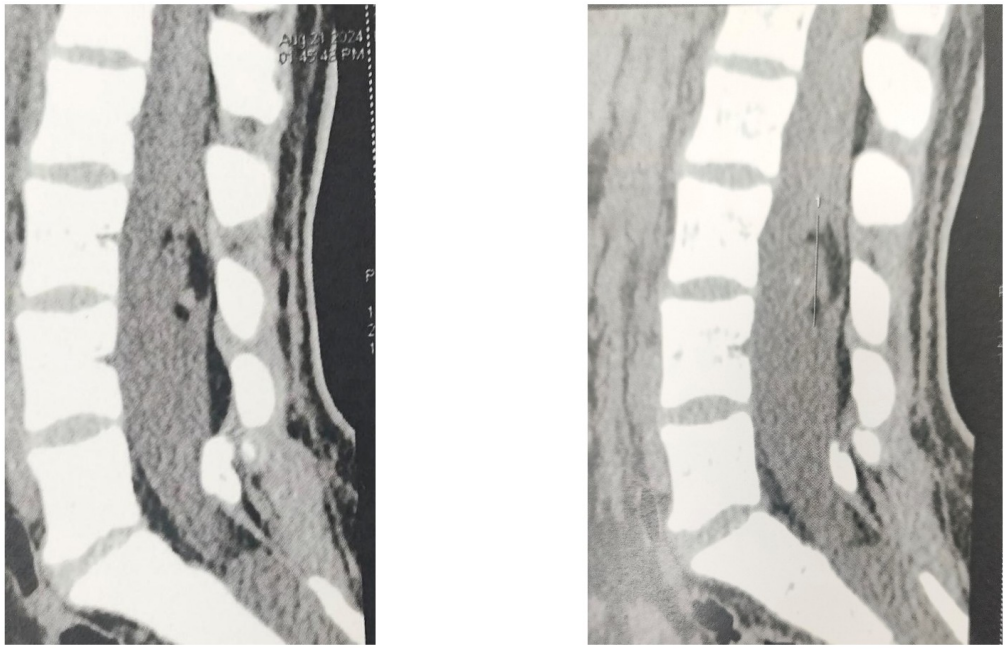
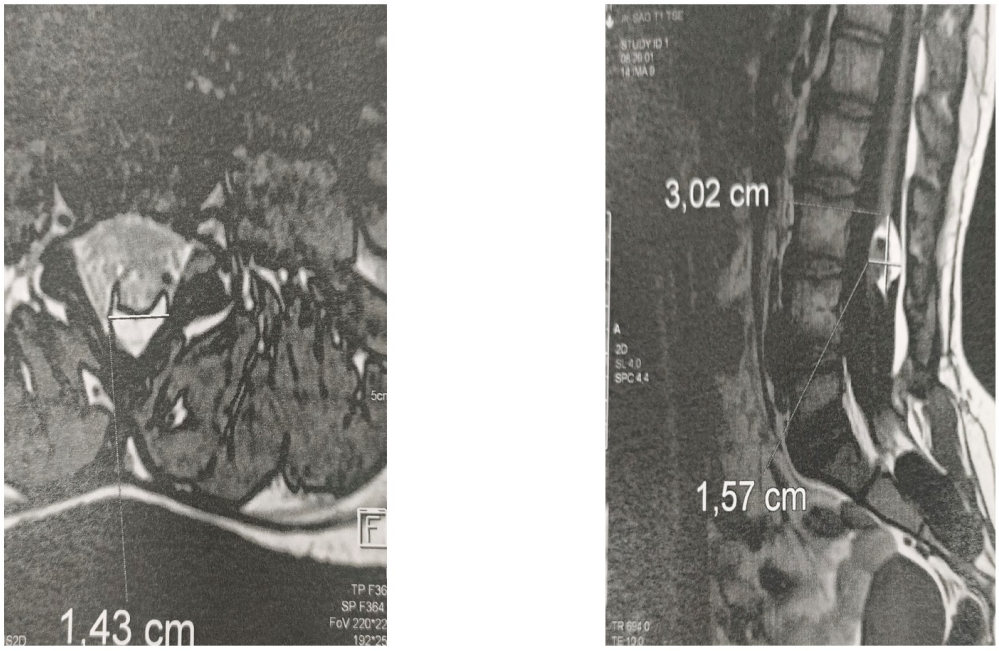


Fig. 01: Lumbosacral CT scan with and without contrast administration, demonstrating a lesion at the D3-D4 level.

Lumbosacral MRI further characterized an intradural lesion that was iso-hypointense on T1-weighted images and heterogeneous on T2-weighted images, displacing the cauda equina roots, without marked contrast enhancement or extradural extension (Fig. 02).



a b

Fig. 02 : a - Axial T2-weighted MRI and b - sagittal contrast-enhanced T1-weighted MRI, showing an intradural lesion at the D3-D4 level, heterogeneous on T2-weighted images and showing slight contrast enhancement. It measures 3 cm in height and 1.6 cm in width and displaces the cauda equina roots.

The patient was admitted to the neurosurgery department and underwent surgery in the prone position, with the lower limbs flexed in a Z-shaped position. A laminectomy centered on L3-L4 was performed, followed by opening of the dura mater. Intraoperative exploration revealed a yellowish, fibrous-appearing mass that was highly adherent to the nerve roots of the cauda equina (Fig. 03). Meticulous excision was performed, allowing complete removal of the tumor without injury to the neural structures (Fig. 04).

Figure 3. Operative photograph not reproduced in this version.

Fig. 03: Intraoperative image. A - Before opening the dura mater, showing a lesion visible through it. B - After opening the dura mater, revealing a yellowish lesion surrounded by the cauda equina roots

Figure 4. Operative photograph not reproduced in this version.

Fig. 04: Image at the end of the procedure showing complete excision of the lesion with release of the cauda equina roots

The histopathological examination confirmed a mature teratoma. The postoperative course was uncomplicated, with complete resolution of the painful symptoms and no new neurological deficit. At the three-month follow-up, the patient was asymptomatic and had resumed her school activities normally.

DISCUSSION

Spinal intradural teratomas are extremely rare tumors, accounting for less than 0.5% of spinal cord tumors [1]. Their occurrence in the cauda equina region is even more exceptional, particularly in adolescent girls. Their origin is thought to be related to the abnormal persistence of migrating germ cells within the neural tube during embryogenesis [2].

Clinically, the symptoms are often nonspecific: low back pain, atypical radicular pain, and sensory or motor disturbances that may mimic sciatica, as in our case. The absence of initial neurological deficits complicates the diagnosis and frequently delays management.

MRI is the diagnostic imaging modality of choice. It allows localization of the tumor, assessment of its intradural nature, and evaluation of its relationship with the nerve roots [3]. A mature teratoma often appears as a heterogeneous mass that may contain fatty, cystic, or even calcified components.

Treatment is based on complete surgical excision, which is curative for mature teratomas. However, surgery may be challenging because of the frequent adherence of the tumor to the nerve roots. Histopathological examination remains essential to confirm the nature of the teratoma and guide follow-up. Unlike immature forms, mature teratomas generally do not require additional treatment [4].

The prognosis is generally excellent after complete excision. Recurrence is rare, but prolonged clinical and radiological follow-up is recommended.

CONCLUSION

This rare case of an intradural cauda equina teratoma in an adolescent girl emphasizes that, despite their rarity, neoplastic etiologies should be considered in the presence of atypical chronic low back pain refractory to medical treatment. MRI is a key diagnostic tool. Complete surgical excision remains the treatment of choice and allows optimal clinical recovery in benign forms. This case also highlights the need for increased clinical vigilance when evaluating prolonged low back pain in adolescents.

REFERENCES

1. Solero CL, Fornari M, Giombini S, et al. Spinal neurinomas: review of 174 cases. Neurosurgery. 1989;25(6):792–798.
2. Park SH, Won JH, Youm JY, et al. Mature spinal teratoma in an adolescent: case report and literature review. J Korean Neurosurg Soc. 2008;44(1):45–48.
3. Virchow R. Krankhafte Geschwülste. Pathologische Anatomie und Physiologie für Praktische Ärzte. Berlin: August Hirschwald; 1863.
4. Horsley V, Gowers WR. A case of spinal tumour successfully removed by laminectomy. Medico-Chirurgical Transactions. 1888;71:377–422.
5. Kanev PM, Mason L, Park TS. Spinal teratomas in children. Neurosurgery. 1990;26(2):269–272.
6. Lee M, Rezai AR, Abbott R, et al. Intramedullary spinal teratoma: case report. Neurosurgery. 1995;36(6):1181–1186.

Pediatric Spinal Trauma

POST-TRAUMATIC CERVICOTHORACIC SPINAL EPIDURAL HEMATOMA IN AN 18-MONTH-OLD INFANT: A Case Report and Literature Review

HASNAOUI Amina[1,*], SIDI MAAMAR Mohamed Amokrane[1] and ABDELMALEK Adel[1]

1: Department of Neurosurgery, Frantz-Fanon University Hospital Center, Blida, Algeria

***Corresponding Author:** HASNAOUI Amina, Department of Neurosurgery, Frantz-Fanon University Hospital Center, Blida, Algeria.*

***Received:** August 15, 2026 — **Accepted:** September 01, 2026 — **Published:** October 01, 2026*

Citation:** HASNAOUI Amina, SIDI MAAMAR Mohamed Amokrane and ABDELMALEK Adel. Post-Traumatic Cervicothoracic Spinal Epidural Hematoma in an 18-Month-Old Infant: A Case Report and Literature Review. **OLCIAS Vol.3, Issue 2.

ABSTRACT

Post-traumatic spinal epidural hematoma (SEH) is an extremely rare entity in the pediatric population [1]. We report the case of an 18-month-old infant who presented with a cervicothoracic SEH extending from C5 to T4 following a minor domestic fall from a bed. The initial presentation consisted of torticollis and progressive tetraparesis, diagnosed more than one week after the trauma. Spinal magnetic resonance imaging (MRI) confirmed a compressive posterior epidural hematoma. Emergency surgical decompression enabled the evacuation of a dense, highly adherent, and organized epidural clot, leading to complete neurological recovery. This case highlights the importance of considering SEH in young pediatric patients presenting with delayed post-traumatic motor deficits, even in the absence of underlying bone fractures [1].

***Keywords:** Spinal epidural hematoma, Pediatric neurosurgery, Cervicothoracic spine, Spinal cord compression.*

INTRODUCTION

Spinal epidural hematoma (SEH) is a rare neurosurgical emergency [1]. Unlike spontaneous forms—which typically occur in elderly patients or in the presence of predisposing risk factors such as anticoagulant therapy, coagulopathies, or hypertension [1, 2]—its post-traumatic occurrence in infants, particularly without associated osseous lesions, remains exceptional [1, 3]. Early diagnosis in very young children is frequently challenged by subtle or delayed clinical manifestations. We report an original observation managed at the Neurosurgery Department of Frantz Fanon University Hospital in Blida.

CASE PRESENTATION

An 18-month-old male infant with no prior medical history or known bleeding diathesis suffered a domestic trauma (fall from a bed) resulting in a cervicothoracic injury. Following the fall, progressive muscle weakness in all four limbs accompanied by torticollis developed gradually. These symptoms were initially overlooked by the family.

Due to the persistence and progression of the motor deficit over a week after the event, the patient was brought for neurosurgical consultation. Physical examination upon admission revealed a severe cervical spinal syndrome along with tetraparesis.

Emergency spinal MRI demonstrated a compressive, biconvex posterior epidural mass extending from the C5 to T4 vertebral levels. The signal characteristics were consistent with a subacute hematoma, without associated bone or disc injury (Figure 2).

The patient was taken to the operating room urgently following neuroradiological confirmation via a posterior approach. Intraoperatively, a dense, organized, and strongly adherent epidural clot was identified. Clot evacuation was technically delicate but achieved satisfactory spinal cord decompression. No active bleeding source or macroscopic vascular malformation was identified.

The postoperative course was marked by significant clinical improvement, culminating in the complete resolution of tetraparesis and full functional recovery (Figure 3).

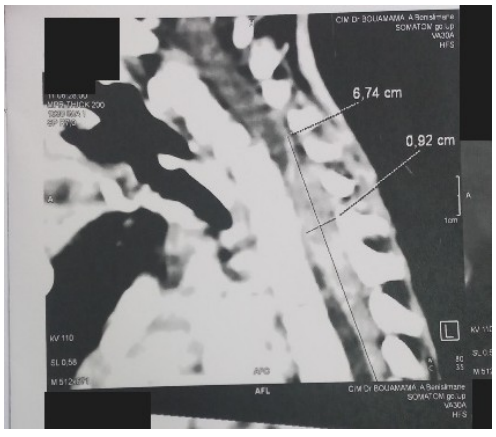


Figure 1. Sagittal reconstruction CT scan demonstrating the craniocaudal extent (6.74 cm) and maximum thickness (0.92 cm) of the posterior epidural hematoma compressing the cervicothoracic spinal cord.

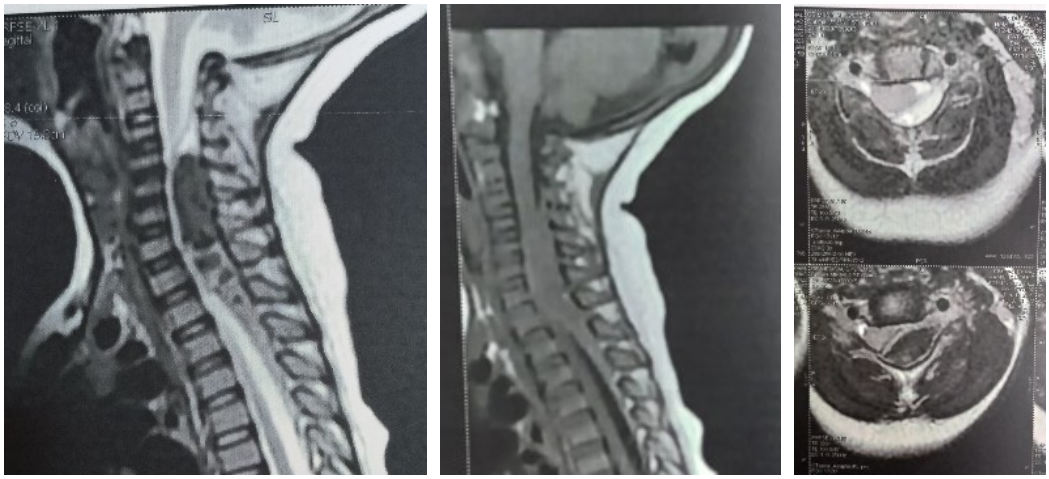


Figure 2. Detailed MRI evaluation reveals a biconvex, posterior epidural collection extending 48 mm in height from C5 to T4, with an average thickness of 13 mm. The signal characteristics (hypointense on T2-weighted images, heterogeneous hyperintense on T1-weighted images, with no enhancement after gadolinium injection) are pathognomonic for an early subacute stage epidural hematoma (intracellular methemoglobin).

Intraoperative photographs are not reproduced in this version.

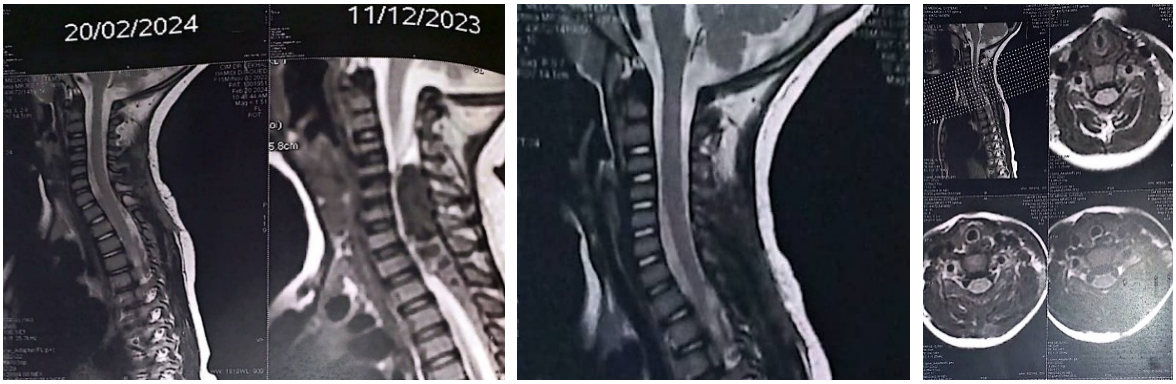


Figure 3. Comparative sagittal T2-weighted MRI (December 11, 2023 vs. February 20, 2024). This figure illustrates the definitive surgical outcome. The initial scan (December 11) shows severe posterior spinal cord compression by the hematoma (labeled). The follow-up MRI (February 20) demonstrates complete resorption of the cervicothoracic epidural hematoma. The spinal canal diameter is fully restored, showing optimal re-expansion of the spinal cord and restoration of the perimedullary cerebrospinal fluid spaces. No signs of residual compression, spinal cord edema, or suffering are present. The only persisting findings are expected post-surgical fibrous changes in the posterior soft tissues along the approach route.

DISCUSSION

Post-traumatic spinal epidural hematoma accounts for less than 10% of all spinal epidural hematomas according to the classic series by Bruyn and Bosna [1, 4]. Most cases reported in the literature are associated with spinal fractures or fracture-dislocations [1, 3]. The occurrence of a post-traumatic SEH in the absence of bone injury or predisposing bleeding factors is exceptional [1].

Pathophysiology and Delayed Onset

In infants, the high plasticity and ligamentous laxity of the spine allow significant flexion-extension or shearing forces without causing radiologically visible fractures [1]. This shearing mechanism can tear the veins of the posterior epidural plexus [1]. The low pressure within the epidural venous network leads to slow, low-pressure bleeding, gradual clot organization, and progressive meningeal dural stripping [1, 5]. This pathophysiological mechanism accounts for the delayed symptom onset and the diagnostic lag of over one week observed in our patient [1]. Intraoperative findings of a highly organized and condensed clot confirmed the subacute nature of the hemorrhage.

Location and Imaging

According to series by Foo and Rossier, cervical and cervicothoracic locations represent 25% to 43% of all epidural hematomas, developing preferentially within the posterior compartment where the epidural space is anatomically wider [1, 3]. Spinal MRI remains the diagnostic modality of choice [1]. It confirms the epidural location, delineates the craniocaudal extent (C5 to T4 in our patient), and evaluates the severity of spinal cord compression [1]. Hyperintensity on both T1- and T2-weighted images corresponds to extracellular methemoglobin, characteristic of a hematoma older than 7 days [1]. CT scanning may supplement the workup to rule out sagittal fractures not visualized on MRI or plain radiographs [1].

Etiologies to Exclude

In cases of minor trauma, a comprehensive coagulation profile must be systematically performed to rule out an underlying or undiagnosed coagulopathy (e.g., hemophilia) [1, 2]. Occasionally, minor trauma merely unmasks an occult vascular malformation (such as a fistula or angioma), leading several authors to advocate for histopathological examination of the evacuated clot and postoperative spinal angiography [1]. In our patient, coagulation studies were strictly normal.

Prognosis and Pediatric Specificity

Neurological outcome depends on the severity of the preoperative neurological deficit and the promptness of surgical decompression [1, 6]. Foo and Rossier emphasized superior clinical outcomes when surgical decompression is performed early, ideally within the first 36 hours [1, 6]. In the series by Nuti et al., motor recovery reached 95.3% for patients with initial partial deficits, compared to 45.3% when the deficit was complete [1, 7].

However, whereas delayed diagnosis in adults often leads to incomplete functional recovery (as reported by Bencherif et al., where motor recovery remained limited to 3/5 after a 20-day delay) [1], our case demonstrates complete motor recovery in an infant despite a delayed presentation. This highlights the remarkable capacity for neuroplasticity and spinal cord tolerance to subacute compression in infants [1].

CONCLUSION

Post-traumatic spinal epidural hematoma in infants is a rare condition [1]. Diagnosis is frequently delayed owing to progressive clinical presentation and examination difficulties in young pediatric patients [1]. Emergency MRI is the pivotal diagnostic examination [1]. Surgical decompression via hematoma evacuation yields excellent neurological outcomes due to the high recovery potential of the developing pediatric nervous system.

REFERENCES

[1] Bencherif L, Mahfouf L, Abdennebi B. Hématome extradural dorsal post traumatique : à propos d'un cas et revue de la littérature. Journal de Neurochirurgie (Alger). 2008; (7): 20-22.

[2] Bouderka M, Bouaggad A, Ait Benali S, Barrou H, Abassi O. Hématome extradural cervical révélateur d'une hémophilie. Neurochirurgie. 1999; 45(3): 247-249.

[3] Foo D, Rossier AB. Post-traumatic spinal epidural hematoma. Journal of Neurosurgery. 1982; 11: 25-32.

[4] Bruyn GW, Bosma SK. Spinal extradural hematoma. In: Vinken PJ, Bruyn GW, eds. Handbook of Clinical Neurology. Amsterdam: North-Holland; 1976; 26: 1-30.

[5] Clark DB, Bertrand G, Tampieri D. Spontaneous spinal epidural hematoma causing paraplegia: resolution and recovery without surgical decompression. Neurosurgery. 1992; 30(1): 108-111.

[6] Foo D, Rossier AB. Preoperative neurological status in predicting surgical outcome of spinal epidural hematoma. Surgical Neurology. 1981; 15(5): 389-401.

[7] Nuti C, Fotso R, Duthel R, Hatem B, Dumas JP, Brunon J. Revue des hématomes épiduraux non traumatiques du rachis : présentation de 20 cas. Neurochirurgie. 2003; 49(6): 563-570.

Spinal Infections

TUBERCULOUS SPONDYLODISCITIS AT THE NEUROSURGERY DEPARTMENT OF DONKA TEACHING HOSPITAL IN CONAKRY:

Epidemiological, Clinical, Radiological and Therapeutic Aspects — A 27-Case Series

KOMARA CA[1], MANSARÉ L[1], DIALLO B[1], DIALLO AR[1], BAH D[1] and BEAVOGUI LK[1]

1: Department of Neurosurgery, CHU Hôpital National Donka, Conakry, Republic of Guinea

***Corresponding Author:** Dr. KOMARA Cheick Ahmed*
Email: kcheikahmed@yahoo.fr | Tel: +224 622 94 99 22

***Received:** September 02, 2026 — **Accepted:** September 20, 2026 — **Published:** October 01, 2026*

***Citation:** KOMARA CA, MANSARÉ L, DIALLO B, DIALLO AR, BAH D and BEAVOGUI LK. Tuberculous Spondylodiscitis at the Neurosurgery Department of Donka Teaching Hospital in Conakry: Epidemiological, Clinical, Radiological and Therapeutic Aspects — A 27-Case Series.*
OLCIAS Vol.3, Issue 2.

ABSTRACT

Introduction: Tuberculous spondylodiscitis (TS), or Pott's disease, is a severe form of extrapulmonary tuberculosis particularly common in sub-Saharan Africa. Responsible for disabling neurological complications, it represents a major diagnostic and therapeutic challenge in resource-limited countries such as Guinea. We report a series of 27 cases managed at the neurosurgery department of Donka Teaching Hospital in Conakry.

Methods: Retrospective descriptive study of 27 patients hospitalized for tuberculous spondylodiscitis at the neurosurgery department of Donka Teaching Hospital. Diagnosis was based on clinical, biological (tuberculin skin test), radiological (standard X-ray ± CT scan) and histological criteria.

Results: Mean age was 40 years (range: 10–68) with slight male predominance (sex-ratio 1.1). Workers were the most affected occupational group (33.3%). Spinal pain was present in 100% of cases. Neurological deficit was found in 74.1% of patients, dominated by paraplegia (40.7%) and paraparesis (29.6%). Tuberculin skin test was positive in 100% of patients. Lumbar (40.8%) and dorsolumbar (33.3%) levels predominated. Vertebral body lysis was the most common radiological finding (51.8%). Treatment was medico-surgical in 33.3% (decompressive laminectomy or foraminotomy), medico-orthopedic in 44.5% and medical alone in 22.2%. Outcome was favorable in 81.5% of cases. No in-hospital deaths were observed.

Conclusion: Tuberculous spondylodiscitis is a frequent and serious condition in our context. Early diagnosis based on clinical findings and tuberculin skin testing—in the absence of MRI—allows rapid initiation of antituberculous quadritherapy. Decompressive surgery remains essential in cases of significant neurological deficit or unstable vertebral destruction, with good results in our series.

***Keywords:** Tuberculous spondylodiscitis; Pott's disease; Spinal cord compression; Paraplegia; Antituberculous quadritherapy; Laminectomy; Guinea; Sub-Saharan Africa*

1. INTRODUCTION

Tuberculosis (TB) remains one of the world's major infectious diseases, responsible for nearly 10 million new cases and 1.5 million deaths annually according to the 2023 WHO report [1]. In sub-Saharan Africa, its prevalence remains particularly high, exacerbated by the HIV/AIDS co-epidemic and poor socioeconomic conditions. In Guinea, the incidence of tuberculosis is estimated at 175 per 100,000 inhabitants, making this disease a major public health priority [1].

Tuberculous spondylodiscitis (TS), commonly known as Pott's disease, represents spinal involvement by tuberculosis and constitutes the most frequent extrapulmonary form, accounting for 50–60% of osteoarticular localizations [2, 3]. Its pathophysiology is based on hematogenous dissemination of Mycobacterium tuberculosis from a primary, often silent, pulmonary focus to the most vascularized part of the vertebral body (anterior portion), followed by secondary extension to the adjacent intervertebral disc through the subligamentous route. The necrotizing granulomatous process progressively causes disco-vertebral destruction, angular kyphotic deformity and, in advanced forms, spinal cord compression due to epidural extension or a so-called “cold” abscess [4, 5].

The severity of TS is related to its neurological complications—paraparesis and paraplegia due to spinal cord compression—which occur in 10–47% of cases according to African series [6, 7] and constitute the main indication for surgery. In sub-Saharan Africa, frequent diagnostic delay—related to lack of awareness of the disease, limited access to advanced imaging (MRI is unavailable in many centers), and initial recourse to traditional healers—considerably worsens the neurological prognosis [6].

In Guinea, no published series has specifically addressed tuberculous spondylodiscitis managed in a neurosurgical setting. This study, involving 27 consecutive patients admitted to the neurosurgery department of Donka Teaching Hospital in Conakry, aimed to describe the epidemiological, clinical, radiological and therapeutic profile of this condition in our setting and to discuss our findings in light of recent African and international data.

2. MATERIALS AND METHODS

2.1 Study setting and design

This was a retrospective descriptive study conducted in the neurosurgery department of CHU Hôpital National Donka in Conakry, the main national neurosurgical referral center in Guinea, which receives patients from across the country.

2.2 Inclusion and exclusion criteria

All patients hospitalized for tuberculous spondylodiscitis diagnosed according to clinical criteria (spinal pain, fever, weight loss, neurological deficit), biological criteria (positive tuberculin skin test, biological inflammatory syndrome), radiological criteria (vertebral lysis, disc-space narrowing, paravertebral abscess on radiography and/or CT scan) and/or histological criteria (epithelioid and giant-cell granulomas with caseous necrosis) were included. Spondylodiscitis of non-tuberculous etiology (pyogenic, brucellar, neoplastic) was excluded.

2.3 Variables studied

Collected data included sociodemographic characteristics (age, sex, occupation), clinical symptoms, paraclinical findings (tuberculin skin test, laboratory data, imaging), treatment type (medical alone, medico-orthopedic, medico-surgical) and outcome at discharge.

3. RESULTS

3.1 Sociodemographic data

Twenty-seven patients were included in this series. The population was predominantly of working age, with a mean age of 40 years (range: 10–68). A slight male predominance was observed, with 14 men (51.9%) and 13 women (48.1%), giving a sex ratio of 1.1. Workers represented the most affected occupational category (33.3%), followed by farmers and unemployed individuals.

Table I. Sociodemographic characteristics (n=27)

Parameter	Number	Percentage (%)
Cohort size	27	100
Male sex	14	51.9
Female sex	13	48.1
Mean age (years)	40 (10–68)	
Occupation: Workers	9	33.3

3.2 Clinical presentation

Spinal pain was the main symptom and was present in 100% of patients. Lower-limb neurological deficit was observed in 74.1% of patients. General symptoms suggestive of tuberculosis included asthenia (37%), weight loss (33.3%) and fever (25.9%).

Table II. Functional and general symptoms (n=27)

Clinical sign	Number	Percentage (%)
Spinal pain	27	100.0
Lower-limb weakness	20	74.1
Asthenia	10	37.0
Weight loss	9	33.3
Fever	7	25.9

Table III. Neurological complications (n=27)

Neurological complication	Number	Percentage (%)
Sensory disturbances	12	44.4
Paraplegia	11	40.7
Genitourinary/sphincter dysfunction	9	33.3
Paraparesis	8	29.6

3.3 Paraclinical findings

The tuberculin skin test was positive in all 27 patients (100%). Standard spinal radiography was performed in all patients. CT was available for only 3 patients (11.1%). Spinal MRI could not be performed in any patient because of financial and availability constraints—a major limitation of our management.

Table IV. Paraclinical examinations performed (n=27)

Paraclinical examination	Number	Percentage (%)
Tuberculin skin test (positive)	27	100.0
Standard spinal radiography	27	100.0
Spinal CT	3	11.1
Spinal MRI	0	0.0

3.4 Lesion locations and radiological findings

Lumbar involvement predominated (40.8%), followed by dorsolumbar involvement (33.3%). Vertebral body lysis was the most frequent lesion (51.8%), followed by intervertebral space narrowing (18.5%).

Table V. Location of spinal lesions (n=27)

Lesion location	Number	Percentage (%)
Lumbar	11	40.8
Dorsolumbar	9	33.3
Thoracic	5	18.5
Cervical	2	7.4

Table VI. Radiological lesions (n=27)

Radiological lesion	Number	Percentage (%)
Vertebral body lysis	14	51.8
Intervertebral space narrowing	5	18.5
Vertebral collapse	5	18.5
Paravertebral abscess (X-ray/CT)	3	11.1

3.5 Treatment

All patients received standardized antituberculous treatment: four-drug therapy (rifampicin + isoniazid + pyrazinamide + ethambutol) for 2 months, followed by two-drug therapy (rifampicin + isoniazid) for a minimum of 4 months, for a total duration of at least 6 months.

Surgical treatment was performed in 9 patients (33.3%): decompressive laminectomy or foraminotomy for spinal cord decompression in response to severe neurological deficits or critical bone destruction. Twelve patients (44.5%) received medico-orthopedic treatment (antituberculous therapy + brace or cervical collar), while 6 patients (22.2%) received medical treatment alone.

Table VII. Treatment modalities (n=27)

Type of management	Number	Percentage (%)
Medico-orthopedic	12	44.5
Medico-surgical	9	33.3
Medical alone	6	22.2
Total	27	100.0

3.6 Outcome

Outcome was favorable (clinical and functional improvement) in 22 patients (81.5%). Persistent sequelae—stable residual neurological deficit—were observed in 2 patients (7.4%). No in-hospital deaths were recorded in our series (0%).

Table VIII. Patient outcomes (n=27)

Clinical outcome	Number	Percentage (%)
Improvement	22	81.5
Persistent sequelae	2	7.4
In-hospital death	0	0.0
Lost to follow-up / not specified	3	11.1

4. DISCUSSION

4.1 Epidemiology

Our series of 27 cases of tuberculous spondylodiscitis managed at Donka Teaching Hospital in Conakry represents, to our knowledge, the first published Guinean series on this topic. The mean age of 40 years and slight male predominance (sex ratio 1.1) are consistent with recent African data. The Ivorian series of 46 patients operated on for Pott's disease (Cocody Teaching Hospital, Abidjan, 2019–2023) reported a mean age of 41.3 ± 15.6 years with 52% women [7]. In Cameroon, Ndoumbe et al. (2022) found a similar profile in their series of 86 cases, with a moderate male predominance [6]. The predominance of workers (33.3%) in our series reflects their greater exposure to tuberculosis risk factors: precarious living conditions, overcrowding and occupational exposure.

Although the diagnostic delay was not precisely quantified in our retrospective series, it appeared prolonged in view of the high frequency of neurological complications at admission (74.1% with deficits). This finding is common throughout sub-Saharan Africa: in Cameroon, the mean time before diagnosis was more than 6 months in the majority of cases [6], while a Tunisian series of 15 cases also highlighted diagnostic difficulties in atypical presentations [8].

4.2 Clinical presentation and neurological complications

Spinal pain, present in 100% of our patients, is the cardinal sign of TS in all published series [2, 3, 6, 7, 8]. Its persistence, progressive worsening and association with general symptoms suggestive of tuberculosis (fever, weight loss, asthenia)—found in 25.9%, 33.3% and 37% of our cases, respectively—should systematically raise suspicion of a tuberculous etiology in an endemic setting.

The high rate of neurological complications in our series (74.1% with lower-limb deficits, including 40.7% complete paraplegia and 29.6% paraparesis) reflects the severity of the admitted cases and

diagnostic delay. These figures are higher than those reported in the Ivorian series (46 operated patients/512 hospitalized cases, or 8.9% surgery) [7], but this can be explained by the specifically neurosurgical recruitment profile of our cohort, which selects the most severe forms. The Cameroonian series reported 19.6% spinal cord compression in its general cohort [6], and the meta-analysis by Rajasekaran et al. (2016) [17] estimated the prevalence of neurological deficits at 40–60% in African neurosurgical series.

The frequency of genitourinary and sphincter disturbances (33.3%) in our series indicates significant spinal cord involvement affecting sacral centers. These symptoms, which are often underestimated and not spontaneously reported by patients, should be systematically assessed during clinical examination because they represent an additional severity criterion and influence long-term functional prognosis.

4.3 Paraclinical findings and diagnostic limitations

The universal positivity of the tuberculin skin test (100%) in our series confirms its practical diagnostic value in a setting of high tuberculosis endemicity. However, the test has important limitations: it may be falsely negative in cases of severe immunosuppression (advanced HIV infection, malnutrition) and cannot distinguish active infection from previous infection or BCG vaccination [3].

The absence of MRI in our series constitutes the main diagnostic limitation and represents a major weakness in our management. Spinal MRI is recognized as the reference examination for diagnosing TS, allowing early visualization of disco-vertebral lesions, epidural extension and spinal cord compression, and helping differentiate TS from other causes of spondylodiscitis or neoplastic disease [9, 13]. Its economic unavailability in our setting requires therapeutic decisions to be based on clinical and radiographic criteria—an approach that remains acceptable in resource-limited countries but exposes patients to diagnostic errors and underestimation of lesion extent. Access to spinal MRI should be a priority for improving neurosurgical management in Guinea.

The limited availability of CT (11.1% of patients) is also concerning. GeneXpert MTB/RIF, whose availability is progressively increasing in Guinea, represents a valuable tool for rapid microbiological confirmation and detection of rifampicin resistance [12].

4.4 Lesion location

The predominance of lumbar (40.8%) and dorsolumbar (33.3%) involvement in our series is consistent with international literature, which reports a predominance of thoracic and thoracolumbar involvement in Asian series, but a more marked lumbar predominance in African series [2, 3, 6, 7]. This difference in anatomical distribution between populations could be related to differences in the portal of entry of the organism and patterns of hematogenous dissemination. Cervical involvement (7.4% in our series) is rare and potentially more serious because of the risk of cervical spinal cord compression with tetraplegia [4].

Vertebral body lysis (51.8%) and intervertebral space narrowing (18.5%) were the predominant radiological lesions. These two classic features of Pott's disease reflect the centrifugal progression of infection—from the more vascularized vertebral body to the adjacent disc—which is characteristic of spinal tuberculosis in contrast to pyogenic spondylodiscitis, which preferentially begins at the disc level [3].

4.5 Treatment

Standardized antituberculous four-drug therapy constituted the foundation of management for all our patients. The 6-month duration used in our series is consistent with WHO recommendations [1]. Some authors nevertheless recommend a longer duration (9–12 months) in severe forms with extensive vertebral destruction or immunosuppression [2, 3]. In our setting, the optimal duration remains difficult to assess because of the lack of systematic long-term follow-up.

Surgical treatment (33.3% of our patients)—decompressive laminectomy or foraminotomy—was indicated in cases of severe neurological deficits and critical bone destruction. This rate is comparable to data from the African neurosurgical literature: 33% in the Cameroonian series [6] and 8.9% in the Ivorian series, which included all hospitalized cases rather than only neurosurgical cases [7]. Surgery in TS aims to decompress neurological structures compressed by an epidural abscess or bone fragments, debride necrotic tissue, stabilize the spine, and obtain a specimen for histological and microbiological confirmation [4, 15, 16].

Antituberculous four-drug therapy should be initiated before surgery when the diagnosis has been established and continued postoperatively for a minimum of 6 months. Adjunctive corticosteroid therapy, used by some teams to reduce perioperative spinal cord edema in cases of severe compression, was not systematically used in our series.

4.6 Outcome and prognosis

Favorable outcome in 81.5% of our patients—with clinical and functional improvement—is encouraging, particularly given the neurological severity at admission. This rate is comparable to African literature: the Cameroonian series reported neurological improvement in 75% of operated cases [6], while Rajasekaran et al. (2016) found neurological recovery in 75–85% of surgically treated incomplete forms [17].

The absence of in-hospital deaths (0%) in our series is notable and reflects the relative safety of decompressive surgical management in an experienced team despite resource limitations. However, this finding should be interpreted cautiously because long-term mortality and neurological sequelae could not be assessed—both are crucial for a complete prognostic evaluation.

Persistent neurological sequelae in 7.4% of patients underscore the importance of early intervention before the establishment of irreversible complete paraplegia. The main prognostic factor for neurological recovery remains the duration and severity of the preoperative deficit: complete paraplegia lasting more than 6 months has a very limited probability of recovery, even after adequate surgical decompression [4, 17].

5. CONCLUSION

Tuberculous spondylodiscitis is a frequent and serious condition in the neurosurgery department of Donka Teaching Hospital in Conakry, predominantly affecting active adults of middle age, with a slight male predominance. Constant spinal pain, associated with severe neurological complications in 74% of patients—a reflection of prolonged diagnostic delay—warrants increased clinical vigilance in a tuberculosis-endemic setting.

The universal positivity of the tuberculin skin test confirms its practical diagnostic value in the absence of MRI. Treatment is based on standardized four-drug antituberculous therapy, associated with spinal cord decompressive surgery in one third of cases. The good outcomes observed (81.5% improvement and no in-hospital deaths) support this therapeutic strategy in our setting.

Improving the prognosis of TS in Guinea requires strengthening access to spinal MRI for early diagnosis, developing rapid microbiological confirmation techniques (GeneXpert), and raising awareness among first-line physicians to systematically consider Pott's disease in any patient with chronic spinal pain in our endemic setting. Prospective multicenter studies at the national level are needed to establish epidemiological data representative of the Guinean population.

DECLARATIONS

Conflicts of interest: None.

Funding: No external funding.

Ethical considerations: Retrospective study based on anonymized records, conducted in accordance with the Declaration of Helsinki.

Authors' contributions: Komara CA — study conception, principal surgeon, manuscript drafting; Mansaré L, Diallo B, Diallo AR, Bah D — data collection, clinical management; Beavogui LK — supervision, critical revision.

REFERENCES

1. World Health Organization. Global Tuberculosis Report 2023. Geneva: WHO; 2023.

2. Kalita J, Misra UK, Kumar S, Gupta RK. Antitubercular therapy in tuberculous spondylodiscitis: duration and outcome. J Neurosurg Spine. 2017;26(4):479-87. doi:10.3171/2016.8.SPINE16438

3. Badr F, Khalid C, Mohamed El Faiz Chaoui. Le mal de Pott: à propos de 82 cas. Pan African Medical Journal. 2011;8:1-7.

4. Rakotoson JL, Rakotoarisoa AH, Rajaoarifetra J, et al. Volumineux abcès froid péripottique dorsolombaire. Rev Pneumol Clin. 2010;66(6):359-62. doi:10.1016/j.pneumo.2009.10.007

5. Pieri S, Agresti P, Morucci M, et al. Percutaneous management of complications of tuberculous spondylodiscitis. Radiol Med. 2009;114(6):984-95. doi:10.1007/s11547-009-0425-3

6. Ndoumbe A, Takoutsing BD, Amvene JM, Simeu C. Profil clinique et résultats du traitement chirurgical du mal de Pott à Yaoundé. Interdiscip Neurosurg. 2022. doi:10.1016/j.inat.2022.101525

7. Baguy-Camara O, Adjoumani DJL, Tro DH, et al. Epidemiological, Clinical and Paraclinical Features of Patients Undergoing Surgery for Spinal Tuberculosis in Ivory Coast: A 5-Year Retrospective Single-Centre Study. Health Research in Africa. 2026.

8. Kameleddine G, Lahouimel K, Bouzid N, et al. Spondylodiscite tuberculeuse : à propos de 15 cas. Rev Med Interne. 2020;41(S5):A199.

9. Salaffi F, Ceccarelli L, Carotti M, et al. Differentiation between infectious spondylodiscitis versus inflammatory or degenerative spinal changes. Radiol Med. 2021;126:843-59. doi:10.1007/s11547-021-01347-7

10. Kamoun C, Frikha F, Kaddour N, et al. Volumineuse masse abdominale révélant une spondylodiscite tuberculeuse avec un abcès du psoas bilatéral. Rev Rhum. 2023;90(4):450-1.

11. Ernandes H, et al. Diagnostic étiologique des spondylodiscites infectieuses communautaires. Med Mal Infect Form. 2022;1(2):S90.

12. Ibrahim FM, Abd EL-rady ARM. Transverse process osteotomy for surgical drainage of primary iliopsoas abscess and secondary cases combined with spondylodiscitis. Int Orthop. 2021;45(1):1657-71.

13. Abreu PGP, Lourenço JA, Romero C, et al. Endoscopic treatment of spondylodiscitis: systematic review. Eur Spine J. 2022;31:1765-74. doi:10.1007/s00586-022-07142-w

14. Diallo Moussa, Tokpa André, Sogoba Youssouf, et al. Traitement chirurgical du mal de pott de l'enfant: à propos d'une série de 11 cas. Journal de Neurochirurgie. 2023;35:10-15.

15. Toba Y, Dialo S, Maiga Y, et al. Tuberculose vertébrale: aspects épidémio-cliniques, radiologiques et évolutifs au CHU du Point G. Mali Medical. 2011;26:8-11.

16. Coïc L, Picard B, Hamou HA, Dufour V, Wolff M. Spondylodiscite à pyogènes : revue de la littérature. Rev Med Interne. 2022;43(6):366-74. doi:10.1016/j.revmed.2022.01.003

17. Rajasekaran S, Soundararajan DCR, Shetty AP, Kanna RM. Spinal tuberculosis: current concepts. Global Spine J. 2018;8(4 Suppl):96S-108S. doi:10.1177/2192568218769053

18. Checko Hamala Koné. Étude des aspects épidémio-cliniques de la spondylodiscite tuberculeuse (ou mal de Pott): à propos de 33 cas au CHU du Point G. Thèse de médecine. Bamako; 2007.

19. Beavogui K, Koïvogui A, Souare IS, et al. Profil des traumatismes crânio-encéphaliques et vertébro-médullaires liés aux accidents de la voie publique en Guinée. Neurochirurgie. 2012;58(5):287-92.

20. Lekoubou A, Nkouonlack C, Njamnshi AK, et al. Mal de Pott: aspects épidémiologiques, cliniques, et thérapeutiques dans un hôpital tertiaire au Cameroun. Rev Neurol (Paris). 2010;166:59-63.

Neuro-Ophthalmology

TOLOSA-HUNT SYNDROME: Report of Two Cases

BEKRALAS Houria[1]

1: Department of Neurosurgery, Béjaïa University Hospital

***Corresponding Author:** BEKRALAS Houria, Department of Neurosurgery, Béjaïa University Hospital*

***Received:** May 17, 2026 — **Accepted:** September 15, 2026 — **Published:** October 01, 2026*

Citation:** BEKRALAS H. Tolosa-Hunt Syndrome: Report of Two Cases. **OLCIAS Vol.3, Issue 2.

ABSTRACT

Tolosa-Hunt syndrome (THS) is a diagnosis of exclusion; it is retained only after ruling out tumoral, infectious, and inflammatory conditions. Our study concerns two patients hospitalized for the management of unilateral retro-orbital pain with impairment of ocular motility. Brain MRI, which is a reference examination for the diagnosis of Tolosa-Hunt syndrome, shows a tissue formation of the cavernous sinus, isointense on T1 and isointense on T2, enhancing after Gadolinium injection. The treatment of our patients is based on corticosteroid therapy, which led to a dramatic regression of symptoms. It should be noted that few cases of painful ophthalmoplegia, including Tolosa-Hunt syndrome, have been reported in the literature. The etiology remains unknown in more than 25% of cases despite an extensive etiological investigation. The use of cortisone (corticosteroid therapy) gives excellent results; however, clinical follow-up is mandatory in order to detect possible recurrences.

***Keywords:** Tolosa-Hunt, Cavernous sinus, corticosteroid therapy, MRI.*

INTRODUCTION

Tolosa-Hunt syndrome is a more or less complete, painful, granulomatous ophthalmoplegia, most often unilateral, caused by nonspecific inflammation of the cavernous sinus region and the sphenoidal fissure of unknown origin.

The diagnosis meets precise clinical and radiological criteria. Its course is spontaneously regressive within a few weeks, this period being dramatically shortened under corticosteroid therapy. Its ipsilateral or contralateral recurrence is frequent. Two observations illustrate this discussion.

CLINICAL CASE No. 1

This is a 52-year-old hypertensive female patient who presented with subacute-onset ophthalmoplegia.

Examination reveals incomplete involvement of the third (III) cranial nerve, sparing the pupil, with involvement of the fourth (IV) and sixth (VI) cranial nerves.

The optic nerve is preserved and there is no involvement of the ophthalmic and maxillary divisions of the trigeminal nerve.

The remainder of the clinical examination is normal. Furthermore, the complementary investigations are unremarkable, except for an elevated erythrocyte sedimentation rate.

Biological examination of the cerebrospinal fluid (CSF) shows no abnormalities.

Brain MRI demonstrates a tissue formation within the cavernous sinus, isointense on T1 (Fig. 1, Fig. 2), but also isointense on T2 and enhanced after intravenous Gadolinium injection.



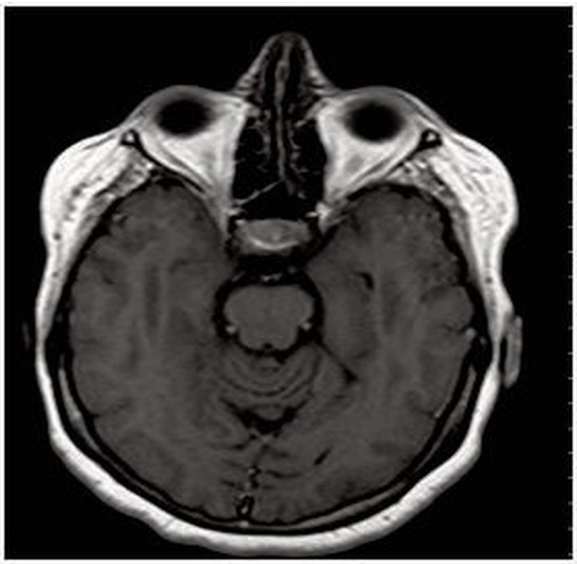


Fig. 1 - Fig. 2: Tissue formation at the level of the cavernous sinus, isointense on T1

CLINICAL CASE No. 2

A 29-year-old patient, with no particular pathological history, was admitted to the emergency department for right fronto-orbital headaches with decreased visual acuity in the right eye.

Clinical examination reveals complete involvement of the third (III) cranial nerve, with involvement of the optic nerve and the ophthalmic division of the trigeminal nerve. Decreased visual acuity is found as well as right exophthalmos. The remainder of the neurological and general examinations is unremarkable. The biological work-up as well as the examination of the cerebrospinal fluid (CSF) reveals no abnormality.

Brain MRI demonstrates a tissue lesion of the cavernous sinus extending toward the right subtemporal fossa, isointense on T1 and isointense on T2, with homogeneous enhancement after Gadolinium injection. Both patients were placed on medical treatment based on corticosteroids: Solumedrol 1 mg/kg/day (i.e., 40 mg twice daily) and a high-protein diet.

A regression of the symptoms is noted by the 5th day for the first case and by the 7th day for the second case. Maintenance treatment is instituted: corticosteroid therapy 0.5 mg/kg/day for 3 months.

After 04 months, MRI demonstrates complete disappearance of the lesion in both patients (Fig. 3 and Fig. 4).





Fig. 3 - Fig. 4

As part of the follow-up of the 1st case, the female patient has been asymptomatic for 4 years, whereas the 2nd case remained asymptomatic until his last consultation, i.e., 2 years after hospitalization.

DISCUSSION

Tolosa-Hunt syndrome was first described in 1954 by Tolosa, then in 1961 by Hunt [2, 3]. It is a nonspecific granulomatous inflammatory condition of the cavernous sinus and the sphenoidal fissure.

It is a diagnosis of exclusion, rare in children, and is seen in adults without sex predominance [4].

Clinically, Tolosa-Hunt syndrome manifests as continuous, lancinating, unilateral retro-orbital pain, rarely bilateral, and total ipsilateral ophthalmoplegia (paralysis of III, IV, and VI) or partial ophthalmoplegia (paralysis of III alone or VI alone) [2, 3, 4, 5].

In our two cases, involvement of III and VI is present. In contrast, involvement of IV and II, associated with mild exophthalmos, is present in only one case.

These symptoms are not specific to Tolosa-Hunt syndrome and can be seen in all disorders of the cavernous sinus compartment and orbital apex [4, 5].

Brain MRI demonstrates enlargement of the cavernous sinus, containing a tissue mass isointense on T1, enhanced after Gadolinium injection [4, 5, 7].

The biological work-up as well as CSF examination are normal in both of our patients, except for an elevated ESR in one case.

Treatment was first proposed by Smith and Taxdal in 1966, based on systemic corticosteroids at a dose of 60 to 80 mg/day [1].

This treatment led to a dramatic improvement in symptoms in both of our patients. Some authors indeed consider corticosteroid therapy as a diagnostic test, but the latter has no absolute value; it may be negative [5, 6].

Tolosa-Hunt syndrome is corticosteroid-resistant in this case. When it is positive, it may correspond to other inflammatory conditions (Wegener syndrome, vasculitis), tumoral conditions (lymphomas, ...), or even ophthalmoplegic migraines.

The natural course is toward remission with or without sequelae, but ipsilateral or contralateral recurrences may occur. In contrast, the course under corticosteroids is classically dramatic without necessarily producing immediate radiological clearance [5, 6, 7]. The differential diagnosis may include lymphoma, meningioma, a specific inflammatory process (localized sarcoidosis of the cavernous sinus), an infectious cause (ophthalmic herpes zoster, sphenoidal sinusitis), or ophthalmoplegic migraine [6].

CONCLUSION

Tolosa-Hunt syndrome is a distinct anatomoclinical entity, despite the lack of knowledge of its etiopathogenic basis. It is a recurrent painful ophthalmoplegia that is generally corticosteroid-sensitive. Its diagnosis is clinical, radiological, and therapeutic, but remains a diagnosis of exclusion.

MRI is a valuable examination because of its better sensitivity for detecting cavernous sinus lesions and its reproducibility. However, it remains nonspecific because several conditions can

mimic Tolosa-Hunt syndrome. Therefore, a neuroradiological and systemic investigation is mandatory in order to rule out other tumoral, inflammatory, or vascular causes.

REFERENCES

1. SMITH JL, TAXDAL DSR. Painful ophthalmoplegia. The Tolosa-Hunt syndrome. Am J Ophthalmol 1966 ; 61 : 1466–72.
2. TOLOSA E. Periarteritic lesions of the carotid siphon with the clinical features of a carotid infraclinoid aneurysm. J Neurol Neurosurg Psychiatry 1954;17:300–2.
3. HUNT WE, MEAGHER JN, LE FEVER HE, ET AL. Painful ophthalmoplegia. Its relation to indolent inflammation of the cavernous sinus. Neurology 1961 ; 11 : 56–62.
4. LAKKE JPWF. Superior orbital fissure syndrome. Report of a case caused by local pachymeningitis. Arch Neurol 1962;7:289–300.
5. C.MASSON, J.M. COLOMBANI, Syndrome de Tolosa-Hunt. Presse Med 2003; 32: 1458-9
6. L B KLINE,W F HOYT : TheTolosa- Hunt syndrome. J NeurolNeurosurg Psychiatry 2001;71:577–582.
7. I MARZOUK. Journées Françaises de Radiologie 2005.

Internal Medicine

EVALUATION OF TOLERANCE TO LONG-TERM CORTICOSTEROID THERAPY IN PATIENTS WITH SYSTEMIC DISEASES:

A Monocentric Observational Study

BOUNZIRA Tewfik[1], BELARBI Nadia[1] and GOUAICH Nesrine Lamia[1]

1: Department of Internal Medicine, University Hospital Center (UHC) of Mostaganem, Faculty of Medicine, University Abdelhamid Ibn Badis, Mostaganem, Algeria

***Corresponding Author:** BOUNZIRA Tewfik, Department of Internal Medicine, University Hospital Center (UHC) of Mostaganem, Faculty of Medicine, University Abdelhamid Ibn Badis, Mostaganem, Algeria. E-mail: bounziratewfik80@gmail.com*

***Received:** August 25, 2026 — **Accepted:** September 15, 2026 — **Published:** October 01, 2026*

Citation:** BOUNZIRA Tewfik, BELARBI Nadia and GOUAICH Nesrine Lamia. Evaluation of Tolerance to Long-Term Corticosteroid Therapy in Patients with Systemic Diseases: A Monocentric Observational Study.* ***OLCIAS Vol.3, Issue 2.

ABSTRACT

Introduction: Although glucocorticoids play an undisputed role in systemic, inflammatory and autoimmune pathology, their prolonged administration is often associated with dose- and time-dependent adverse effects. The purpose of this study was to assess tolerance to long-term glucocorticoid therapy, describe risk factors and protective measures in the context of clinical practice in the Internal Medicine Department of the CHU of Mostaganem.

Materials and Methods: A prospective longitudinal cohort study was conducted among 30 patients followed for more than three months (on average 23.11) receiving a glucocorticoid treatment (average dose: 7.5 mg/day of prednisone). Data were collected using structured questionnaires and analyzed using SPSS software with appropriate parametric and non-parametric tests.

Results: In this cohort, the female population prevailed over the male one. The most common adverse events reported were Cushing's signs (75%), insomnia (70%), fungal (53.3%), and bacterial (43.3%) infections, osteoporosis (16.7%). Of particular interest was the occurrence of glucocorticoid-induced diabetes, which was positively associated ($p = 0.006$) with sarcoidosis. Participants reported weight gain as the most bothersome side effect (40%), while females experienced more sex-related side effects compared to males ($p = 0.008$).

Discussion: The present findings are consistent with the existing literature on this topic, which highlights the impact of prolonged glucocorticoid use on various organs. Furthermore, the association between glucocorticoid-induced diabetes and sarcoidosis identified in our study provides new evidence for the need for targeted metabolic monitoring in this category of patients. Additionally, a prospective design allowed us to document the difficulties of glucocorticoid dose tapering, as well as the significant psychological burden resulting from morphological changes due to glucocorticoid use. These findings emphasize the fact that the issue of prolonged glucocorticoid administration cannot be resolved within the framework of pharmacological intervention only.

Conclusion: Prolonged corticosteroid therapy is associated with significant iatrogenic morbidity, which may not be adequately monitored and controlled in real-world clinical practice. In order to optimize the benefit-risk ratio, it is necessary to implement a strategy that goes beyond the framework of pharmacological treatment and includes rational preventive measures and therapeutic patient education (TPE) in order to combat corticophobia and harmonize professional practices.

***Keywords:** Glucocorticoids; Systemic diseases; Iatrogenic morbidity; Long-term therapy; Therapeutic patient education; Risk factors.*

INTRODUCTION

Since their clinical introduction by Philip Hench and his colleagues at the Mayo Clinic in 1948, glucocorticoids have dramatically transformed the prognosis of numerous previously intractable diseases [1]. Their remarkable anti-inflammatory, immunosuppressive, and anti-tumor properties have made them an invaluable foundation in the management of a wide variety of immune-mediated and inflammatory conditions across both in a medical and a surgical setting [2-6].

The optimal use of these drugs is, However, often challenged by a plethora of dose- and time-dependent adverse effects [7,8]. To address these challenges, a prospective longitudinal cohort study was conducted within the Internal Medicine Department of the CHU of Mostaganem. The study aimed to evaluate the tolerance of these drugs amongst patients receiving a long-term glucocorticoid therapy, identify associated risk factors, and analyze implemented protective measures. Ultimately, this research provides the medical field with the necessary data to improve patient safety and everyday quality of life.

OBJECTIVES

Primary Objective

Assess the prevalence and clinical, biological and behavioral risk factors for adverse effects related to prolonged corticosteroid therapy in an internal medicine ward.

Secondary Objectives

Evaluate the impact of adherence to the treatment, the compliance to a lifestyle and diet adjustment and the understanding of the treatment by the patient on the occurrence of side effects.

Analyze the correlation between the duration of the treatment and the occurrence of adverse effects.

Assess the relevance of the additional measures prescribed and elaborate a specific educational program for patient’s monitoring related to treatment with long term glucocorticoids.

Raise awareness among professionals about the importance of psychological support and monitoring of these patients.

MATERIALS AND METHODS

The purpose of this study is to determine the effects of long-term systemic glucocorticoid treatment in patients with autoimmunity or inflammatory diseases. The prospective longitudinal cohort study was conducted in the Internal Medicine Department of the CHU of Mostaganem in an 11-month period between August 4, 2024, and July 4, 2025, including patients under prolonged glucocorticoid treatment for more than 3 months with a daily dose of prednisone higher than or equal to 7.5 mg/day. Non-inclusion criteria comprised short-term glucocorticoid treatment (less than 3 months) and non-systemic diseases, whereas exclusion criteria involved patients who declined to participate, were lost to follow-up, or developed severe intervening comorbidities. The data were collected using a structured questionnaire and analyzed using SPSS (v29.0.1.1), with qualitative variables described as frequencies and percentages and quantitative variables as means

and standard deviations. Group comparisons were performed using the Chi-square test, Fisher's exact test, Mann-Whitney, and Kruskal-Wallis tests, whereas bivariate associations were evaluated using Pearson or Spearman correlation coefficients based on the Shapiro-Wilk test results (). The study strictly followed ethical guidelines, utilizing informed consent while ensuring the anonymity and confidentiality of all participants' data."

RESULTS

A total of 30 patients (mean corticosteroid treatment duration: 23.11 months) were recruited in this study conducted at the University Hospital Center (UHC) of Mostaganem over an 11-month period. The sex ratio was significantly higher among females (0.30). The most frequent therapeutic indications were systemic lupus erythematosus and sarcoidosis, which accounted for nearly a half of all cases. Fifty percent of the patients received prednisone as a first-line treatment, whereas 86.6% of them were prescribed a corticosteroid-sparing strategy associated with systematic adjuvant therapy. On the other hand, patients' lifestyles were rarely adapted to chronic glucocorticoid therapy: only 10% of them engaged in regular physical activity. After a comprehensive clinical examination, multiple adverse effects were identified. In particular, Cushing's syndrome was manifested by upper trunk weight gain (75% of patients) and typical signs such as insomnia (70%), irritability (66.7%), and anxiety (56.7%) (Figure 1) [27]



Fig1. photos of patients who developed cervico-facial lipodystrophy [27]

Besides, glucocorticoid-induced diabetes developed in 23.3% of cases, which was found to be positively correlated with sarcoidosis (Fisher's test, p = 0.006). Hypertension was another frequent metabolic complication that was noted in 16.7% of patients. Moreover, the analysis revealed a number of visceral and endocrine adverse effects, including menstrual irregularities (30.4%), hirsutism (60.8%) (Figure 2) [27]

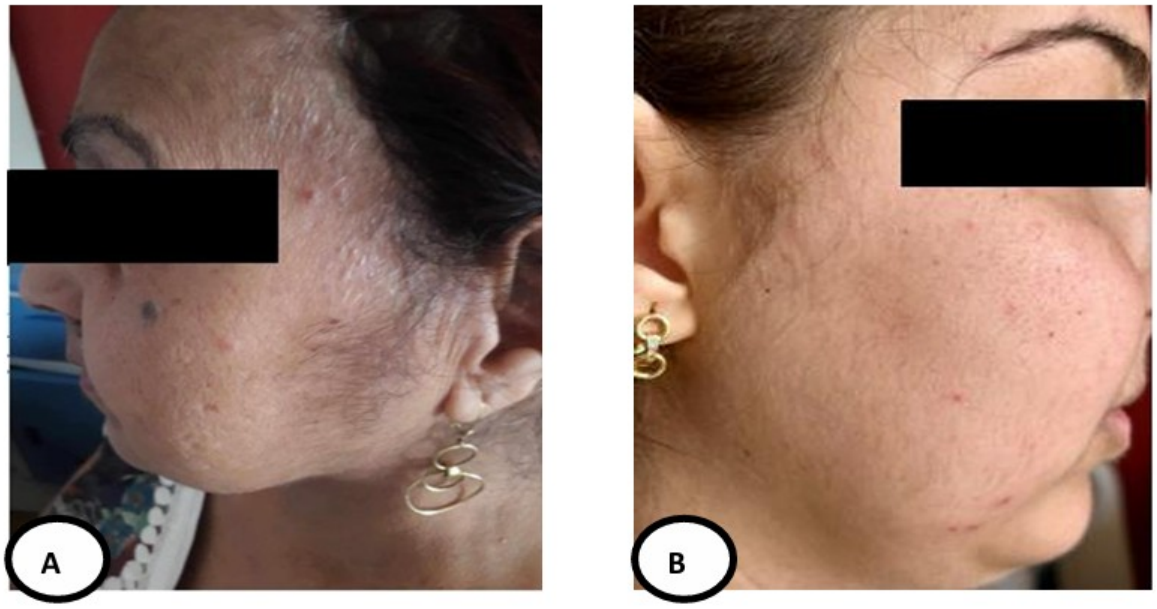


Fig 2. hirsutism secondary to prolonged corticosteroid therapy in female patients, A and B multiple localization, of the department) [27]

and acne (36.7%) (Figure 3) [27] .

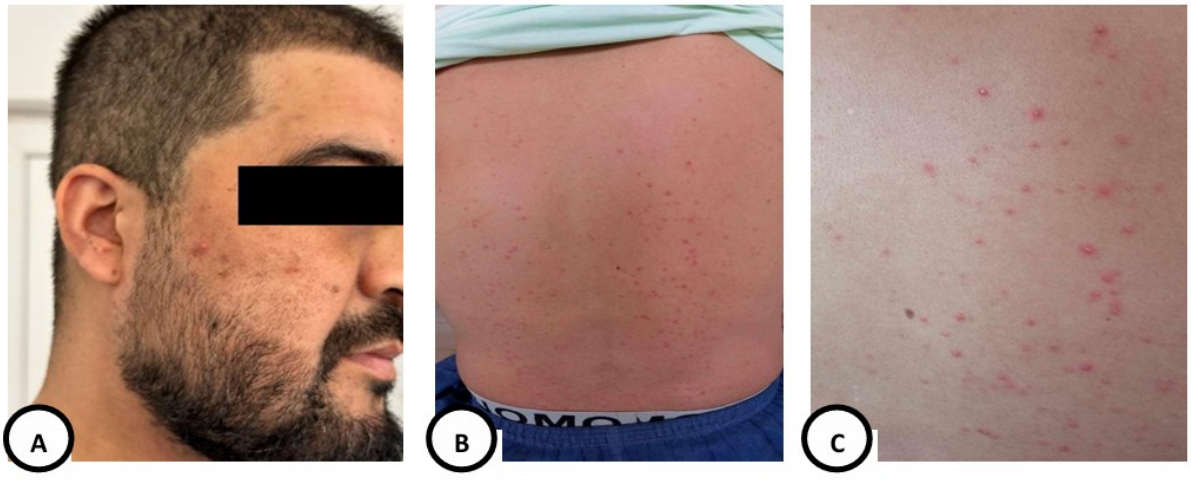


Fig 3. photos of patients known to the department who presented with steroid acne A. Face acne, B. and C. Back acne [27]

Osteoporosis was a typical complication of long-term prednisone treatment, which was documented in 16.7% of female patients, whereas aseptic necrosis of the femoral head was detected in one individual. The survey also reported a high incidence of infections, including fungal (53.3%) (Figure 4) [27],



Fig 4. photo of a female patient from the department who presented with oral thrush [27]

bacterial (43.3%) (Figure 5) [27] ,

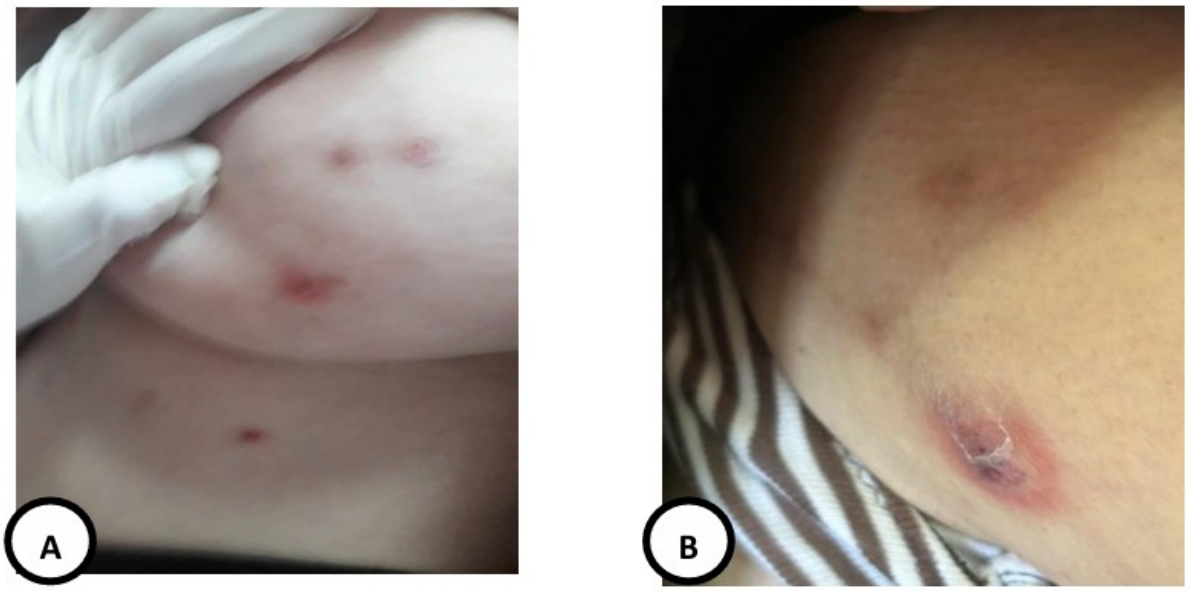


Fig5. photo of a female patient from the department who presented with corticosteroid-induced furunculosis. A. Mammary and inframammary region, B. Pelvic region. [27]

and viral (23.3%) ones. In addition, eye conditions such as cataracts (6.7%) and glaucoma (10%) were common adverse effects of glucocorticoid treatment. Finally, the study found that weight gain was the most debilitating adverse effect in 40% of patients (Figure 6) [27].

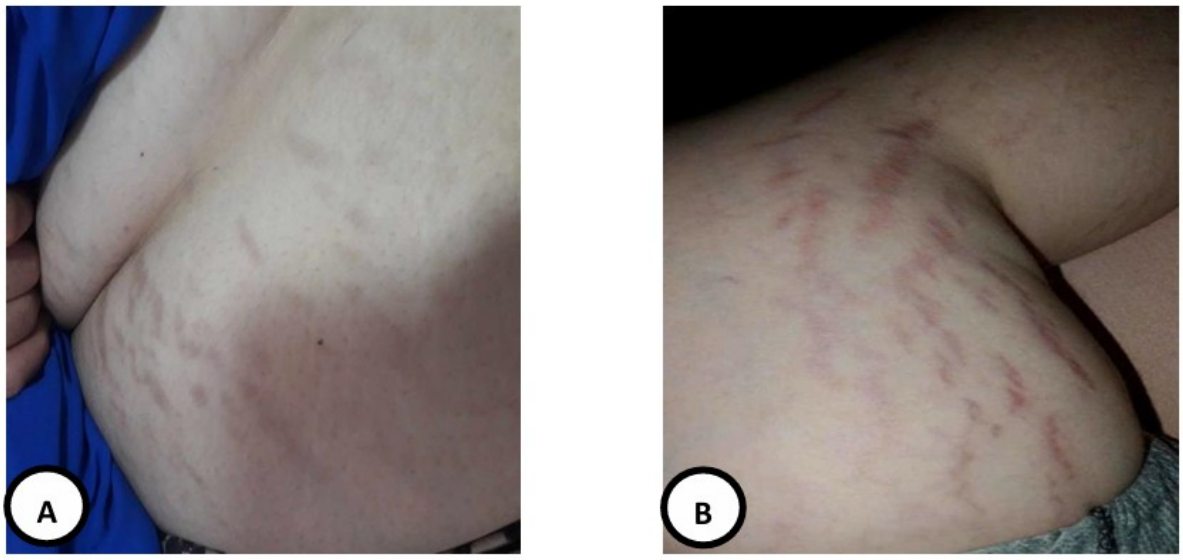


Fig 6. Photo of female patients from the department who presented with purplish striae A. Abdominal region, B. thigh region [27]

According to the Pearson chi-square test, female patients were significantly more likely to report sex-related adverse effects compared to males (chi2 = 20.726; p = 0.008).

DISCUSSION

The current monocentric observational study performed in the Internal Medicine Department of the CHU of Mostaganem on 30 patients aims to assess the tolerance of corticosteroids in long-term therapy in systemic diseases, bearing in mind that although glucocorticoids are the essential cornerstone in the management of these conditions due to their powerful anti-inflammatory and immunosuppressive properties [2], managing their long-term handling is characterized by major iatrogenic morbidity largely documented in the international literature. The analysis of our cohort underlines a clear female predominance and an age profile similar to that of the literature on systemic diseases, such as systemic lupus erythematosus or rheumatoid arthritis, affecting a vulnerable population to metabolic and trophic complications [8-10]. In our series, the initiation of corticosteroid therapy was dictated by the severity of visceral involvements threatening the functional or vital prognosis, with the preferential use of prednisone and prednisolone being in perfect accordance with international pharmacological standards of prescription of synthetic corticosteroids [9,11] whose intermediate half-life (between 12 and 36 hours) allows a single morning administration aiming to respect the nycthemeral rhythm of cortisol secretion and minimize, as far as possible, adrenal suppression, although the chronicity of treatments makes this suppression almost inevitable in the long term [12,13]. One of the major teachings of our work is the difficulty of weaning or reducing corticosteroid doses, with the literature confirming that dose reduction poses the risk of immunological relapse, where too rapid a decrease exposes patients to an inflammatory resurgence of the causal disease often requiring a re-escalation of doses [14,15], as well as iatrogenic chronic adrenal insufficiency resulting from the prolonged inhibition of the hypothalamic-pituitary-adrenal axis, which mandates a strict tapering regimen often supported by rigorous therapeutic education advocated in the reference manuals [13,16,17]. The richness of the

iatrogenic profile observed in our cohort matches point-for-point with the classical bibliographic data, whether considering metabolic and endocrine complications (cushingoid syndrome, weight gain, and corticosteroid-induced diabetes linked to the action of glucocorticoids on hepatic gluconeogenesis and peripheral insulin resistance) [7-9], osteoarticular complications (corticosteroid-induced osteoporosis and the risk of aseptic necrosis of the femoral head, justifying international prevention consensus by calcium and vitamin D supplementation, and bisphosphonates) [18-20], infectious vulnerability through alteration of cellular and humoral immunity [21,22], or trophic and ophthalmological complications (skin fragility, purpura, atrophy, and posterior subcapsular cataracts) requiring close multidisciplinary follow-up [8,23,24]. Finally, the statistical analysis of our series demonstrates a positive correlation between the cumulative duration of corticosteroid exposure and the overall iatrogenic load, validating observations on cumulative dose-dependent and duration-dependent toxicity [8,10], whereas bodily and morphological modifications, felt by patients as the most debilitating daily side effect, weigh heavily on therapeutic compliance and underline the vital importance of associating psychological support and active therapeutic patient education (TPE) with medical prescription [25, 26], demonstrating in conclusion of this confrontation with international references that the management of glucocorticoids requires the rigorous application of steroid-sparing strategies, the use of the minimum effective dose and the systematic prevention of their iatrogenicity [8,11].

CONCLUSION

In conclusion, despite the undeniable interest in treating various systemic, inflammatory and autoimmune diseases with glucocorticoids, the beneficial effects of corticosteroid therapy are inseparable from significant iatrogenic morbidity during prolonged or high-dose prescriptions. Although a wide range of corticosteroid-induced complications is well described, including various metabolic, bone, infectious, cardiovascular and psychiatric events, our work underlines a critical observation that their prevention and screening in the real world are in a large extent unsystematic, ranging from heterogeneous practices to sheer reliance on a single physician’s judgment, limited efficiency of evidence and the lack of specific randomized trials. Hence, a modern corticosteroid-treated patient with prolonged prescriptions needs more than a drug prescription: an integrated and multidisciplinary strategy is mandatory to optimize the benefit-to-risk ratio. In this context, therapeutic patient education (TPE) and combating «corticophobia» is of particular importance to improve the adherence to therapy, to understand the disease and better cope with all its psychosocial consequences of drug treatment. The optimization of this strategy may include the distribution of validated educational tools (dietary advice sheets, specific patient information booklets), strict individual tapering calendars and development of multidisciplinary educational programs as well as continuing education for professionals, which are the only guarantees for harmonizing practices and providing benefits to the patient.

REFERENCES

[1] F. Chast, "Histoire de la corticothérapie," La Rev. Médecine Interne, vol. 34, no. 5, pp. 258–263, May 2013.

[2] P. Roblot and D. Richard, Corticoïdes et corticothérapie, Paris: Hermann, 1997, 418 p.

[3] Protocole National de Diagnostic et de Soins (PNDS) : Dermatomyosite de l'enfant et de l'adulte, FAI2R, 2017.

[4] Protocole National de Diagnostic et de Soins (PNDS) : Syndrome de Sjögren, FAI2R, Mar. 2022.

[5] Protocole National de Diagnostic et de Soins (PNDS) : Maladie de Behcet, FAI2R, Dec. 2019.

[6] C. M. Spies, C. Strehl, M. C. van der Goes, J. W. J. Bijlsma, and F. Buttgereit, "Glucocorticoids," Best Pract. Res. Clin. Rheumatol., vol. 25, no. 6, pp. 891–900, Dec. 2011.

[7] M. Oray, K. Abu Samra, N. Ebrahimiadib, H. Meese, and C. S. Foster, "Long-term side effects of glucocorticoids," Expert Opin. Drug Saf., vol. 15, no. 4, pp. 457–465, Apr. 2016.

[8] L. Fardet, A. Kassar, J. Cabane, and P. Flahault, "Corticosteroid-induced adverse events in adults: frequency, screening and prevention," Drug Saf., vol. 30, no. 10, pp. 861–881, Oct. 2007.

[9] M. Pineton de Chambrun, B. Wechsler, and D. Saadoun, "Corticothérapie," EMC - Trait. Médecine AKOS, vol. 8, no. 1, pp. 1–7, Jan. 2013.

[10] J. B. Rice, A. G. White, L. M. Scarpati, G. Wan, and W. W. Nelson, "Long-term Systemic Corticosteroid Exposure: A Systematic Literature Review," Clin. Ther., vol. 39, no. 11, pp. 2216–2229, Nov. 2017.

[11] Haute Autorité de Santé (HAS), Bon usage des corticoïdes par voie systémique, Recommandations professionnelles, 2021.

[12] R. M. Paragliola, G. Papi, A. Pontecorvi, and S. M. Corsello, "Treatment with Synthetic Glucocorticoids and the Hypothalamus-Pituitary-Adrenal Axis," Int. J. Mol. Sci., vol. 18, no. 10, p. 2201, Oct. 2017.

[13] S. Hahner, R. J. Ross, and W. Arlt, "Adrenal insufficiency after glucocorticoid withdrawal: mechanisms, diagnosis and prevention," Lancet Diabetes Endocrinol., vol. 3, no. 6, pp. 469–479, Jun. 2015.

[14] N. A. Kennedy, B. Warner, E. L. Johnston, et al., "Relapse after withdrawal from corticosteroids in inflammatory bowel disease: a systematic review," Gut, vol. 63, no. 7, pp. 1255–1263, Jul. 2014.

[15] K. N. González, H. Lefebvre, and J. M. Kuhn, "Sevrage de la corticothérapie," Méd. Thérapeutique, vol. 5, no. 4, pp. 299–305, 1999.

[16] La Revue du Praticien, "Corticothérapie prolongée : prévenir l'insuffisance surrénalienne," Rev. Prat., vol. 67, no. 5, pp. 539–544, 2017.

[17] Société Française d'Endocrinologie (SFE), "Sevrage cortisonique chez l'adulte : mode d'emploi," Vidal [Internet], 2018. Available: https://www.vidal.fr.

[18] J. Compston, "Glucocorticoid-induced osteoporosis: an update," Endocrine, vol. 61, no. 1, pp. 7–16, Jul. 2018.

[19] J. P. Devogelaer, S. Goemaere, S. Boonen, et al., "Evidence-based guidelines for the prevention and treatment of glucocorticoid-induced osteoporosis: a consensus document," Osteoporos. Int., vol. 17, no. 1, pp. 8–19, Jan. 2006.

[20] P. Lafforgue, "Osteonecrosis of the femoral head," Rev. Rhum., vol. 76, no. 2, pp. 166–172, Feb. 2009.

[21] A. E. Stuck, C. E. Minder, and F. J. Frey, "Risk of infectious complications in patients taking glucocorticoids," Rev. Infect. Dis., vol. 11, no. 6, pp. 954–963, 1989.

[22] V. Noel, "Risk factors and prognostic influence of infection in a single cohort of 87 adults with systemic lupus erythematosus," Ann. Rheum. Dis., vol. 60, no. 12, pp. 1141–1144, Dec. 2001.

[23] B. Guillot, "Effets indésirables cutanés des glucocorticoïdes," La Rev. Médecine Interne, vol. 34, no. 5, pp. 310–314, May 2013.

[24] C. Haus, J. Collignon-Brach, and A. Galand, "Suivi ophtalmologique des patients sous corticothérapie," Rev. Med. Liège, vol. 52, no. 3, pp. 155–158, 1997.

[25] L. Fardet, A. Perdoncini-Roux, T. Blanchon, et al., "Perception par les médecins internistes de la fréquence et de la gêne induite par les effets indésirables d'une corticothérapie systémique prolongée," La Rev. Médecine Interne, vol. 30, no. 2, pp. 113–118, Feb. 2009.

[26] K. Nassar, S. Janani, C. Roux, et al., "La corticothérapie systémique au long cours : représentations des patients, perceptions des prescripteurs et observance thérapeutique," Rev. Rhum., vol. 81, no. 1, pp. 49–53, Jan. 2014.

[27] T. Bounzira, N. Belarbi, N.L. Gouaich et al. Internal Medicine Department, CHU Bensmaine Boumedien Mostaganem, Faculty of Medicine, University of Abdelhamid Ibn Badis Mostaganem, Algeria.

Renal Epidemiology

PREVALENCE OF CHRONIC KIDNEY DISEASE AMONG DIABETIC AND/OR HYPERTENSIVE PATIENTS IN THE LAGHOUAT DISTRICT, ALGERIA: A CROSS-SECTIONAL PRIMARY-CARE STUDY

DJENANE Ahmed[1,*]

1: Department of Nephrology and Haemodialysis, CHU Mostaganem, Algeria. Email: sab_dej@yahoo.fr.

***Corresponding Author:** DJENANE Ahmed, Department of Nephrology and Haemodialysis, CHU Mostaganem, Algeria. Email: sab_dej@yahoo.fr.*

***Received:** August 25, 2026 — **Accepted:** September 15, 2026 — **Published:** October 01, 2026*

***Citation:** DJENANE Ahmed. Prevalence of Chronic Kidney Disease among Diabetic and/or Hypertensive Patients in the Laghouat District, Algeria: A Cross-Sectional Primary-Care Study.*
OLCIAS Vol. 3, Issue 2.

ABSTRACT

Background: Chronic kidney disease (CKD) is a silent condition of rising global burden, particularly among patients with diabetes and hypertension, the two leading causes of end-stage renal disease worldwide. Data on CKD prevalence among high-risk patients in primary care remain scarce in North Africa.

Objective: To determine the prevalence of CKD, classified according to the 2012 KDIGO criteria, among diabetic and/or hypertensive patients in the Laghouat district of Algeria, and to identify independent factors associated with its presence.

Methods: We conducted a descriptive, cross-sectional prevalence study with prospective random recruitment at the Diabetes Care Centre, Public Hospital Establishment of Laghouat, between January 2018 and January 2019, among patients aged 18–70 years. CKD was defined as an estimated glomerular filtration rate (eGFR, MDRD equation) below 60 mL/min/1.73 m² and/or an abnormal urinary albumin- or protein-to-creatinine ratio, persisting beyond three months. Independent predictors of CKD were identified by multivariable logistic regression (odds ratio [OR], 95% confidence interval). Reporting followed the STROBE guidelines for cross-sectional studies.

Results: Of 420 patients screened, 302 met the inclusion criteria (249 type 2 diabetics, 44 hypertensive patients, 9 type 1 diabetics). Overall CKD prevalence was 40% (121/302): 39% in the diabetes-predominant subgroup and 49% in the hypertension-predominant subgroup. Patients with CKD had significantly higher mean blood pressure, urinary albumin-to-creatinine ratio (ACR), fasting glucose and HbA1c, and significantly lower eGFR and haemoglobin ($p < 0.05$ for all), with no significant difference in age or body mass index. On multivariable analysis, diabetic retinopathy (adjusted OR 13.05, 95% CI 6.84–24.88), anaemia (OR 2.23), a positive urine dipstick (OR 2.18) and antihypertensive treatment intensity (OR 1.52) were independently associated with CKD. Recommended screening measures (urine dipstick, serum creatinine, ACR) remained markedly underused in primary care before the study, having previously been performed in only 31.5%, 49.0% and 28.5% of patients, respectively.

Conclusion: CKD prevalence is high among diabetic and/or hypertensive patients in the Laghouat district, affecting a substantial proportion of relatively young patients. Diabetic retinopathy, anaemia, a positive urine dipstick and antihypertensive treatment intensity are readily identifiable predictors in routine general practice. Systematic, early CKD screening integrated into diabetes and hypertension care pathways, coupled with multidisciplinary management, appears essential to slow disease progression and reduce cardiovascular burden in this setting.

***Keywords:** chronic kidney disease; prevalence; diabetes mellitus; hypertension; glomerular filtration rate; screening; primary care ; cross-sectional study.*

1. INTRODUCTION

Chronic kidney disease (CKD) was long viewed primarily through the lens of its terminal stage, end-stage renal disease requiring renal replacement therapy. The classification proposed by the National Kidney Foundation in 2002, subsequently updated by the Kidney Disease: Improving Global Outcomes (KDIGO) 2012 guidelines, redefined CKD as any structural or functional kidney abnormality persisting for more than three months, stratified into five categories of estimated glomerular filtration rate (eGFR) and three categories of albuminuria [1–3].

This classification revealed the true scale of the problem: CKD affects an estimated 10–14% of adult populations in Western countries and constitutes an independent risk factor for cardiovascular mortality, even at early, asymptomatic stages [2,4]. A comprehensive analysis of the Global Burden of Disease study estimated that CKD affected over 697 million people worldwide in 2017 and was responsible for 1.2 million deaths that year, with its global burden projected to keep rising [5]. Management of CKD, particularly at its terminal stage, represents a considerable financial and human burden for health systems everywhere [6,7].

Diabetes mellitus and hypertension are the two leading causes of CKD worldwide and together account for more than half of all incident end-stage renal disease [3,5]. Because both conditions are most commonly followed in general practice, primary care represents the most logical setting for early, simple and low-cost screening, capable of triggering therapeutic measures that slow renal progression and improve cardiovascular prognosis.

Laghouat province, on the High Plateaus of Algeria some 400 km south of Algiers, illustrates the epidemiological transition under way across the country: communicable diseases historically linked to the region's pastoral vocation and climate are increasingly giving way to a rapid rise in non-communicable disease. In 2018, the province had approximately 12,000 known diabetic patients and 15,000 known hypertensive patients, and 37 patients started dialysis in 2017, 80% of them as unplanned emergencies without prior vascular access, with diabetes and hypertension implicated in 80% of cases [24]. This observation prompted a community-based screening survey targeting these high-risk populations.

The primary objective of this study was to estimate the prevalence of CKD, according to the 2012 KDIGO classification, among diabetic and/or hypertensive patients in the Laghouat district. Secondary objectives were to classify CKD by stage and to identify renal risk factors independently associated with its presence.

2. MATERIALS AND METHODS

2.1 Study design and setting

This was a descriptive, cross-sectional prevalence study with prospective, random recruitment, conducted over one year (January 2018 – January 2019) in a primary-care general medicine clinic at the Diabetes Care Centre, Public Hospital Establishment of Laghouat, a single-centre primary-care facility. Reporting follows the Strengthening the Reporting of Observational Studies in Epidemiology (STROBE) guidelines for cross-sectional studies [7].

2.2 Study population

The minimum sample size was calculated assuming a theoretical CKD prevalence of 25% among diabetic and/or hypertensive patients, with a 5% alpha risk and 5% precision, according to the formula $N = \varepsilon^2 \times P \times Q / i^2$, yielding a minimum requirement of 300 subjects.

Eligible participants were men and women aged 18–70 years with known diabetes and/or hypertension, resident in the Laghouat district, who provided informed consent. Exclusion criteria were acute kidney injury, prior dialysis or transplantation, pregnancy, and minor age. Of 420 randomly screened patients, 118 were excluded for not meeting these criteria; 302 patients were included in the final analysis.

2.3 Definition of chronic kidney disease

CKD was defined as the persistence, for more than three months, of biological, morphological or histological renal abnormalities and/or reduced kidney function, the latter characterised by an eGFR below 60 mL/min/1.73 m². eGFR was calculated using the four-variable Modification of Diet in Renal Disease (MDRD) equation ($eGFR = 186 \times \text{serum creatinine}^{-1.154} \times \text{age}^{-0.203} \times k$, with k = 0.742 for women), the equation recommended in national guidance at the time of data collection; we acknowledge that the CKD-EPI equation is now considered more accurate, particularly near-normal eGFR values [9]. Proteinuria was screened for by urine dipstick; a positive result prompted quantification of the urinary protein-to-creatinine ratio, while a negative result prompted screening for microalbuminuria by immunoturbidimetric assay with calculation of the albumin-to-creatinine ratio (ACR). Patients screening positive (eGFR < 60 mL/min and/or ACR > 30 mg/g) underwent confirmatory testing at three months.

2.4 Data collection

Each participant underwent a structured interview (personal and family history, cardiovascular and renal risk factors, smoking status), clinical examination (weight, height, body mass index [BMI], blood pressure measured with a validated electronic device), fasting biochemistry (venous glucose, lipid profile, serum creatinine, uric acid, urinary sediment) and renal ultrasonography. Target-organ damage was assessed by electrocardiography and echocardiography for left ventricular hypertrophy (LVH), and by fundoscopic examination for diabetic and/or hypertensive retinopathy. For each patient, prior performance of a urine dipstick, serum creatinine and ACR (before study inclusion), together with the usual treating practitioner (general practitioner, nephrologist, endocrinologist, cardiologist), was recorded by interview and medical record review.

2.5 Statistical analysis

Data were entered and analysed using SPSS version 19 and Microsoft Excel. Continuous variables are reported as means with 95% confidence intervals; categorical variables are reported as counts and percentages. Group means were compared using Student's t-test or analysis of variance (ANOVA); categorical variables were compared using the chi-square test (or Fisher's exact test where expected cell counts were below 5). Odds ratios (OR) with 95% confidence intervals were used to evaluate the association between candidate predictors and CKD; an OR was considered significant when its confidence interval excluded 1. Multivariable logistic regression, incorporating sex, age, BMI, diabetes, hypertension and dyslipidaemia treatment, disease duration, smoking status, HbA1c, haemoglobin, urine dipstick result, retinopathy, renal ultrasound findings and LVH, was used to

identify independent predictors of CKD. A two-sided p value < 0.05 was considered statistically significant.

2.6 Ethical considerations

The study was conducted after obtaining written informed consent from each participant, in accordance with the ethical principles applicable to observational clinical research and the Declaration of Helsinki. As an observational, non-interventional study, formal clinical trial registration was not required.

3. RESULTS

3.1 Population characteristics

Of 420 diabetic and/or hypertensive patients randomly screened, 302 met the inclusion criteria and were retained for analysis: 249 type 2 diabetic patients (82.5%), 44 hypertensive patients (14.6%) and 9 type 1 diabetic patients (3.0%). The female-to-male ratio was close to 1 (165 women, 137 men). Baseline characteristics by CKD status are presented in Table 1. CKD was more frequent with advancing age (46.3% among patients aged 50–70 years versus 29.4% among those under 29) and with longer disease duration (57.0% for a duration exceeding 10 years versus 24.0% for a duration under 5 years), yet remained common among younger patients: 56% of patients with CKD were under 50 years of age. No difference in prevalence was observed by sex (40.0% in women versus 40.1% in men).

Table 1. Demographic and disease-duration characteristics of the study population by CKD status (n = 302).

Variable	No CKD n = 181 (%)	CKD n = 121 (%)	Total n = 302 (%)
Female sex	99 (60.0%)	66 (40.0%)	165 (100%)
Male sex	82 (59.9%)	55 (40.1%)	137 (100%)
Age < 29 years	12 (70.6%)	5 (29.4%)	17 (100%)
Age 30–39 years	28 (58.3%)	20 (41.7%)	48 (100%)
Age 40–49 years	76 (65.5%)	40 (34.5%)	116 (100%)
Age 50–70 years	65 (53.7%)	56 (46.3%)	121 (100%)
Diabetes/hypertension duration < 5 years	76 (76.0%)	24 (24.0%)	100 (100%)
Diabetes/hypertension duration 5–10 years	56 (63.6%)	32 (36.4%)	88 (100%)
Diabetes/hypertension duration > 10 years	49 (43.0%)	65 (57.0%)	114 (100%)
Total population	**181 (59.9%)**	**121 (40.1%)**	**302 (100%)**

3.2 Overall prevalence of chronic kidney disease

According to the 2012 KDIGO classification, 121 of 302 patients had CKD, an overall prevalence of 40%. This prevalence was 39% in the diabetes-predominant subgroup (type 2 diabetes and/or hypertension) and 49% in the hypertension-predominant subgroup (hypertension and/or diabetes). The

distribution by KDIGO stage (eGFR category by albuminuria category) is presented in Table 2. Early stages (G1–G2) accounted for 79% of the cohort, while a marked reduction in eGFR (<60 mL/min/1.73 m², stages G3–G5) affected 20% of patients.

Table 2. Classification of 302 patients by 2012 KDIGO stage (eGFR category × albuminuria category).

Stage (eGFR)	A1	A2	A3	Total
G1 (≥90 mL/min/1.73 m²)	80 (76.2%)	17 (16.2%)	8 (7.6%)	105 (100%)
G2 (60–89 mL/min/1.73 m²)	101 (75.4%)	16 (11.9%)	17 (12.7%)	134 (100%)
G3a (45–59 mL/min/1.73 m²)	17 (50.0%)	14 (41.2%)	3 (8.8%)	34 (100%)
G3b (30–44 mL/min/1.73 m²)	4 (25.0%)	4 (25.0%)	8 (50.0%)	16 (100%)
G4 (15–29 mL/min/1.73 m²)	5 (41.7%)	2 (16.7%)	5 (41.7%)	12 (100%)
G5 (<15 mL/min/1.73 m²)	0 (0.0%)	1 (100%)	0 (0.0%)	1 (100%)
Total	**207 (68.5%)**	**54 (17.9%)**	**41 (13.6%)**	**302 (100%)**

3.3 Comparison of clinical and biological parameters

Compared with patients without CKD, patients with CKD had significantly higher mean systolic and diastolic blood pressure, ACR, fasting glucose, and HbA1c, and significantly lower mean eGFR and haemoglobin (Table 3). No significant difference was found for age or BMI.

Table 3. Comparison of clinical and biological parameters between patients with and without CKD (Student's t-test).

Parameter	CKD patients (n = 121)	No-CKD patients (n = 181)	p value
Age (years)	58.53	56.50	0.070
BMI (kg/m²)	28.80	28.33	0.417
Systolic BP (mmHg)	147.14	134.17	<0.001
Diastolic BP (mmHg)	85.25	79.39	<0.001
ACR (mg/g)	548.08	9.48	<0.001
Fasting glucose (g/L)	1.85	1.57	<0.001
eGFR (mL/min/1.73 m²)	64.62	89.26	<0.001
HbA1c (%)	8.22	7.56	0.005
Haemoglobin (g/dL)	11.96	12.97	<0.001

3.4 Independent predictors of chronic kidney disease

On multivariable logistic regression, four variables were retained as independent predictors of CKD: diabetic retinopathy, anaemia (low haemoglobin), a positive urine dipstick, and antihypertensive treatment intensity (Table 4).

Table 4. Independent predictors of CKD after multivariable logistic regression.

Variable	Adjusted OR	95% CI	p value
Antihypertensive treatment	1.52	1.17–1.98	0.002
Positive urine dipstick	2.18	1.20–3.97	0.010
Anaemia (low haemoglobin)	2.23	1.19–4.19	0.013
Diabetic retinopathy	13.05	6.84–24.88	<0.001

3.5 Associated complications and prior screening practices

Inadequate blood pressure control was observed in 82.6% of patients, and 52.9% required at least two antihypertensive drug classes to reach target blood pressure. Glycaemic imbalance (HbA1c > 7%) was present in 71.1% of patients with CKD. Obesity affected 42.1% of patients with CKD and overweight a further 30.6%. Diabetic retinopathy was found in 61.2% of patients with CKD and hypertensive retinopathy in 34.7%; LVH was present in 35.5% of patients. Renal ultrasonography, performed for the first time in the majority of patients, was abnormal in 39.7% of cases.

Recommended CKD screening remained markedly underused before the study: a urine dipstick had previously been performed in only 31.5% of patients (28.9% of those with CKD, 33.1% of those without), serum creatinine in 49.0% (46.3% versus 50.8%), and ACR in 28.5% (29.8% versus 27.6%) — proportions that did not differ meaningfully by eventual CKD status, indicating that prior screening had not been preferentially directed at patients later found to have CKD. Medical follow-up was provided by a general practitioner in 91.1% of patients, by a nephrologist in only 12.6–16.6% (depending on calculation method), by an endocrinologist in 36.8%, and by a cardiologist in 23.8%.

4. DISCUSSION

This community-based, primary-care study, conducted in a southern Algerian region undergoing rapid epidemiological transition, demonstrates a high prevalence of CKD — 40% — among diabetic and/or hypertensive patients, exceeding the theoretical 25% prevalence used for sample-size calculation and figures reported in several Western cohorts, where CKD affects 10–14% of the general population but 25–40% of diabetic or hypertensive subgroups depending on the series [2,4,5,10]. It approaches data reported elsewhere in the Maghreb, notably in Morocco, where Benghanem Gharbi et al. observed a high prevalence of CKD associated with diabetes, hypertension and obesity in the general adult population [11], and is broadly consistent with an Algerian cohort study linking hypertension to diabetic nephropathy [23], as well as with the substantial burden of CKD documented across the Global Burden of Disease framework [5].

The higher prevalence observed in the hypertension-predominant subgroup (49%) than in the diabetes-predominant subgroup (39%) is consistent with literature emphasising the central role of blood pressure control in preserving kidney function, including among diabetic patients [12,13]. That antihypertensive treatment intensity — an indirect marker of hypertension severity and the number of drug classes required for control — emerged as an independent predictor on multivariable analysis supports this interpretation: the more difficult hypertension is to control, the greater the associated risk of renal involvement appears to be, a pattern also demonstrated in landmark trials of intensive blood-pressure control [14].

Diabetic retinopathy was, in our series, the factor most strongly associated with CKD (OR 13.05). This association, extensively documented, reflects the shared microvascular pathophysiology of diabetic retinopathy and nephropathy; the presence of retinopathy can therefore be regarded as a simple clinical marker of systemic microvascular damage, including renal involvement [15]. Similarly, anaemia — common from early CKD stages owing to relative erythropoietin deficiency — emerged as an independent predictor, consistent with established pathophysiology and with evidence that anaemia correction is closely linked to CKD progression [16].

Urine dipstick positivity, a simple, rapid and inexpensive test, also emerged as an independent predictor, underscoring its potential value as a first-line screening tool in general practice — particularly since this test remained markedly underused in our population, performed in fewer than one-third of patients before the study. More broadly, this study reveals a substantial deficit in the application of recommended CKD screening in primary care (urine dipstick, eGFR, ACR), with nephrology follow-up remaining marginal (12.6–16.6% of patients), despite diabetes and hypertension together accounting for the majority of end-stage renal disease causes in the region [8,9]. This pattern is consistent with international evidence that primary-care CKD screening frequently falls short of guideline recommendations and that patient and provider awareness of CKD often remains low even when laboratory markers of dysfunction are present [17–20], despite explicit care-pathway guidance assigning general practitioners a central role in CKD screening and monitoring [22].

These results should be interpreted in light of several methodological limitations. This was a single-centre study conducted in a reference facility for diabetes care, which may introduce selection bias toward patients followed more regularly or with more pronounced comorbidity than the general population of diabetics and hypertensives in the district. The cross-sectional design does not permit causal inference between the identified factors and CKD occurrence, only association. Estimation of eGFR using the MDRD equation, although widely used at the time of data collection, is now recognised as less accurate than the CKD-EPI equation, particularly near-normal eGFR values, which may have led to some misclassification of prevalence across eGFR strata [9]. Finally, confirmation of CKD at three months, although performed for patients screening positive, represents a pragmatic community-based approach rather than strict confirmation against every KDIGO criterion.

Strengths of this work include its community-based, prospective design, random patient recruitment within a primary-care facility, the comprehensiveness of the biological, morphological and target-organ assessment performed, and a sample size exceeding the a priori calculated minimum. These elements lend good internal validity to the prevalence estimates reported for this specific region of Algeria, where epidemiological data on CKD had previously been limited.

5. CONCLUSION

This community-based cross-sectional study shows that CKD prevalence is high — 40% — among diabetic and/or hypertensive patients in the Laghouat district, affecting a substantial proportion of relatively young patients. Diabetic retinopathy, anaemia, urine dipstick positivity, and antihypertensive treatment intensity are independent predictors of CKD, readily identifiable during a routine general practice consultation.

The deficit observed in the application of recommended screening measures (urine dipstick, eGFR, ACR) and in the use of specialised nephrology follow-up underscores the need to integrate systematic, early CKD screening — based on simple, low-cost tools — into diabetes and hypertension

management programmes in primary care. Multidisciplinary care combining general practitioners, nephrologists, diabetologists and cardiologists, supported by nephro-cardioprotective measures, appears essential to slow the progression of chronic kidney disease and reduce its cardiovascular impact and societal cost.

DECLARATIONS

Funding

This work did not receive any specific grant from funding agencies in the public, commercial, or not-for-profit sectors.

Conflicts of interest

The author declares no conflicts of interest relevant to this article.

Ethics approval and consent to participate

The study was conducted after obtaining written informed consent from each participant, in accordance with the ethical principles applicable to observational clinical research and the Declaration of Helsinki. As an observational, non-interventional study, no clinical trial registration was required.

Availability of data and materials

The datasets analysed during the current study are derived from the author's academic dissertation [23] and are available from the corresponding author on reasonable request.

Acknowledgements

The author thanks the medical and paramedical staff of the Diabetes Care Centre, Public Hospital Establishment of Laghouat, for their assistance with patient recruitment and data collection.

REFERENCES

1. National Kidney Foundation. K/DOQI clinical practice guidelines for chronic kidney disease: evaluation, classification, and stratification. Am J Kidney Dis. 2002;39(2 Suppl 1):S1–266.

2. Levey AS, Coresh J. Chronic kidney disease. Lancet. 2012;379(9811):165–80.

3. Kidney Disease: Improving Global Outcomes (KDIGO) CKD Work Group. KDIGO 2012 clinical practice guideline for the evaluation and management of chronic kidney disease. Kidney Int Suppl. 2013;3(1):1–150.

4. Chronic Kidney Disease Prognosis Consortium, Matsushita K, van der Velde M, Astor BC, Woodward M, Levey AS, et al. Association of estimated glomerular filtration rate and albuminuria with all-cause and cardiovascular mortality in general population cohorts: a collaborative meta-analysis. Lancet. 2010;375(9731):2073–81.

5. GBD Chronic Kidney Disease Collaboration. Global, regional, and national burden of chronic kidney disease, 1990–2017: a systematic analysis for the Global Burden of Disease Study 2017. Lancet. 2020;395(10225):709–33.

6. United States Renal Data System. USRDS Annual Data Report: Epidemiology of Kidney Disease in the United States. Bethesda, MD: National Institute of Diabetes and Digestive and Kidney Diseases; 2021.

7. Mujais SK, Story K, Brouillette J, Takano T, Soroka S, Franek C, et al. Health-related quality of life in CKD patients: correlates and evolution over time. Clin J Am Soc Nephrol. 2009;4(8):1293–301.

8. von Elm E, Altman DG, Egger M, Pocock SJ, Gøtzsche PC, Vandenbroucke JP; STROBE Initiative. The Strengthening the Reporting of Observational Studies in Epidemiology (STROBE) statement: guidelines for reporting observational studies. Lancet. 2007;370(9596):1453–7.

9. Levey AS, Stevens LA, Schmid CH, Zhang YL, Castro AF 3rd, Feldman HI, et al.; CKD-EPI (Chronic Kidney Disease Epidemiology Collaboration). A new equation to estimate glomerular filtration rate. Ann Intern Med. 2009;150(9):604–12.
10. Stengel B, Metzger M, Froissart M, Rainfray M, Berr C, Tzourio C, et al. Epidemiology and prognostic significance of chronic kidney disease in the elderly – the Three-City prospective cohort study. Nephrol Dial Transplant. 2011;26(10):3286–95.
11. Benghanem Gharbi M, Elseviers M, Zamd M, Belghiti Alaoui A, Benghanem M, Ramdani B, et al. Chronic kidney disease, hypertension, diabetes, and obesity in the adult population of Morocco: how to avoid 'over'- and 'under'-diagnosis of CKD. Kidney Int. 2016;89(6):1363–71.
12. Bakris GL, Weir MR, Shanifar S, Zhang Z, Douglas J, van Dijk DJ, et al.; RENAAL Study Group. Effects of blood pressure level on progression of diabetic nephropathy: results from the RENAAL study. Arch Intern Med. 2003;163(13):1555–65.
13. Pohl MA, Blumenthal S, Cordonnier DJ, De Alvaro F, Deferrari G, Eisner G, et al. Independent and additive impact of blood pressure control and angiotensin II receptor blockade on renal outcomes in the Irbesartan Diabetic Nephropathy Trial: clinical implications and limitations. J Am Soc Nephrol. 2005;16(10):3027–37.
14. SPRINT Research Group, Wright JT, Williamson JD, Whelton PK, Snyder JK, Sink KM, et al. A randomized trial of intensive versus standard blood-pressure control. N Engl J Med. 2015;373(22):2103–16.
15. Knowler WC, Bennett PH, Ballintine EJ. Increased incidence of retinopathy in diabetics with elevated blood pressure: a six-year follow-up study in Pima Indians. N Engl J Med. 1980;302(12):645–50.
16. Ritz E, Laville M, Bilous RW; ACORD Investigators and Coordinators. Target level for hemoglobin correction in patients with diabetes and CKD: primary results of the Anemia Correction in Diabetes (ACORD) study. Am J Kidney Dis. 2007;49(2):194–207.
17. de Lusignan S, Chan T, Stevens P, O'Donoghue D, Hague N, Dzregah B, et al. Identifying patients with chronic kidney disease from general practice computer records. Fam Pract. 2005;22(3):234–41.
18. Allen AS, Forman JP, Orav EJ, Bates DW, Denker BM, Sequist TD. Primary care management of chronic kidney disease. J Gen Intern Med. 2011;26(4):386–92.
19. Plantinga LC, Boulware LE, Coresh J, Stevens LA, Miller ER 3rd, Saran R, et al. Patient awareness of chronic kidney disease: trends and predictors. Arch Intern Med. 2008;168(20):2268–75.
20. Tuot DS, Plantinga LC, Hsu CY, Jordan R, Burrows NR, Hedgeman E, et al.; Centers for Disease Control and Prevention Chronic Kidney Disease Surveillance Team. Chronic kidney disease awareness among individuals with clinical markers of kidney dysfunction. Clin J Am Soc Nephrol. 2011;6(8):1838–44.
21. Djenane A. Prevalence of chronic kidney disease among diabetic and/or hypertensive patients in the Laghouat district [dissertation]. Algiers: Faculty of Medicine Benyoucef Benkhedda, University of Algiers; 2020.
22. Haute Autorité de Santé (HAS). Guide du parcours de soins: maladie rénale chronique de l'adulte [Care pathway guide: chronic kidney disease in adults]. Saint-Denis: HAS; 2012.
23. Nebti N, Si Youcef H, Zenati N, Mezeghrani K, Ghermoule H, Djoghane H, et al. Hypertension and diabetic nephropathy. Diabetes Metab. 2013;39(Suppl 1).
24. Direction de la Santé et de la Population de la wilaya de Laghouat (DSP Laghouat). Health situation report, 31 December 2018.

Academic Mental Health

WHEN SUPERVISION BECOMES A SOURCE OF DISTRESS: A Pilot Study of Academic Mobbing, Anxiety, and Perceived Stress Among Postgraduate Students in Türkiye

SENGUL Pinar[1], PhD

1: Independent Researcher

***Corresponding Author:** SENGUL Pinar, PhD, Independent Researcher.*

***Received:** September 20, 2026 — **Accepted:** September 25, 2026 — **Published:** October 01, 2026*

***Citation:** SENGUL Pinar. When Supervision Becomes a Source of Distress: A Pilot Study of Academic Mobbing, Anxiety, and Perceived Stress Among Postgraduate Students in Türkiye.*
OLCIAS Vol.3, Issue 2.

ABSTRACT

Academic supervision involves an inherent power asymmetry that can affect degree progress, resources, opportunities, and future careers. This pilot study examined negative supervisory behaviours and psychological outcomes among 10 postgraduate students in Türkiye (six PhD and four master's students). Nine rated a current primary supervisor and one a former primary supervisor. Three participants (30%) explicitly identified systematic bullying or mistreatment, whereas nine (90%) endorsed at least one of 18 negative supervisory behaviours. Behaviour burden was strongly associated with anxiety (Spearman's $\rho = .874$, $p \approx .001$) and positively associated with perceived stress ($\rho = .638$, $p \approx .047$). Associations with cognitive failures ($\rho = .482$, $p \approx .159$) and perceived institutional safety ($\rho = -.543$, $p \approx .105$) were not statistically significant. Participants self-identifying bullying/mistreatment had a median behaviour score of 40/72 versus 3/72 in the remaining participants (exact Mann–Whitney $p \approx .017$). Qualitative responses highlighted dependency, fear of disagreement, costly supervisor change, control over thesis or defence processes, micromanagement, and control of resources or opportunities. Because the sample is extremely small and cross-sectional, these findings cannot estimate prevalence or establish causality. They provide preliminary signals for a larger study of supervisory power, psychological safety, and postgraduate mental health.

***Keywords:** academic bullying, mobbing, postgraduate supervision, anxiety, perceived stress, Türkiye*

INTRODUCTION

Postgraduate supervision is both an educational relationship and a relationship of institutional power. Supervisors may influence research progress, authorship, professional networks, funding, recommendations, resources, and degree completion. This dependence can make conflict or mistreatment difficult to challenge without fear of academic or career consequences.

Academic bullying is generally characterised by repeated hostile, intimidating, humiliating, or harmful conduct within a power structure. A global investigation of academic science documented abusive supervision as an important concern with consequences for individuals and research environments (Moss et al., 2021). More recently, Zheng (2026) analysed 6,356 PhD students from 34 countries and reported that 22.34% experienced bullying; supervisors were the most frequently identified perpetrators among those reporting bullying.

Supervision is also relevant to postgraduate mental health. Research in doctoral students has linked supervisory relationship characteristics with depression, anxiety, and stress (Jackman et al., 2024). Qualitative work has described abusive supervision, micromanagement, intimidation, threats, and coercion among negative mentoring experiences (Moss et al., 2022). In Türkiye, Öztürk and Şahbudak (2017) documented mobbing as an academic workplace concern among research assistants.

An important measurement problem is that students may experience controlling, humiliating, threatening, or obstructive behaviours without calling the experience “bullying” or “mobbing.” The present pilot therefore separated behaviour-based exposure from self-identification. It examined associations between cumulative negative supervisory behaviour and anxiety, perceived stress, cognitive failures, and institutional safety. The study was exploratory and was not designed to estimate prevalence or establish causality.

METHOD

Design and participants. This cross-sectional anonymous pilot included 10 postgraduate students studying in Türkiye: six doctoral students and four master’s students. Nine answered about a current primary supervisor and one about a former primary supervisor.

Measures. Participants completed a study-specific 18-item negative supervisory behaviour inventory. Frequency ratings were summed to produce a 0–72 exposure score; higher scores indicated greater behavioural burden. Items addressed experiences including belittling or humiliation, fear in communication or disagreement, supervisor control over resources or opportunities, dependence on supervisory approval, and the perceived cost of changing supervisor. Because this was a pilot instrument, it should be regarded as an exploratory exposure index rather than a validated diagnostic measure of mobbing.

Participants separately indicated whether they considered their experience systematic bullying or mistreatment. Anxiety was assessed with the Generalised Anxiety Disorder-7 (GAD-7; Spitzer et al., 2006). Perceived stress was assessed with the Perceived Stress Scale (PSS; Cohen et al., 1983). Cognitive failures were assessed with the Cognitive Failures Questionnaire (CFQ; Broadbent et al., 1982). Exploratory items assessed perceived institutional safety, and open-ended responses addressed dependency and barriers to responding to mistreatment.

Analysis. Spearman rank correlations examined associations between behavioural exposure and outcome measures. An exact Mann–Whitney comparison contrasted behaviour scores between participants who did and did not self-identify systematic bullying/mistreatment. Qualitative responses were reviewed descriptively for recurrent themes. Given n = 10, inferential statistics are treated as preliminary signals.

Ethics and consent. SUBMISSION CHECK: The actual ethics approval or exemption, consent procedure, recruitment wording, and data-protection statement must be inserted from the study documentation before submission. These details have deliberately not been invented in this manuscript.

RESULTS

Three participants (30%) identified systematic bullying or mistreatment, while nine (90%) endorsed at least one negative supervisory behaviour. The most common experiences were dependence of career/progress on supervisor approval (6/10), fear or tension in communication (6/10), and perceiving supervisor change as costly or difficult (6/10). Five participants reported fear of consequences for disagreement; five reported supervisor control over resources or opportunities; and four reported belittling or humiliation.

The median negative-behaviour score was 40/72 among participants self-identifying bullying/mistreatment and 3/72 among the other participants. The groups showed complete rank separation in this pilot dataset; the exact Mann–Whitney comparison yielded $p \approx .017$, with a rank-biserial estimate of 1.00. This effect estimate is unstable because the groups contained only three and seven participants.

Negative supervisory behaviour burden was strongly associated with GAD-7 anxiety ($\rho = .874$, $p \approx .001$) and positively associated with perceived stress ($\rho = .638$, $p \approx .047$). The association with cognitive failures was positive but not statistically significant ($\rho = .482$, $p \approx .159$), while institutional safety showed a negative, non-significant association ($\rho = -.543$, $p \approx .105$). Median anxiety was 21 in the self-identified bullying/mistreatment group versus 10 in the remaining participants; median perceived stress was 27 versus 20.

Qualitative responses highlighted supervisory dependency, fear of disagreement, the perceived cost of changing supervisor, control over thesis or defence timing, micromanagement, and control over resources or opportunities. Confidential reporting and independent institutional channels were proposed as possible safeguards.

DISCUSSION

The pilot produced two notable signals. First, concrete negative behaviours were reported more often than participants explicitly labelled their experience bullying or mistreatment. This discrepancy may partly reflect the difference between isolated difficult interactions and repeated bullying. It may also reflect normalisation, uncertainty about definitions, or reluctance to adopt a stigmatised label while dependent on a supervisor. Larger studies should therefore retain both behaviour-based and self-label approaches.

Second, greater behavioural exposure was associated with higher anxiety and perceived stress. This pattern is consistent with broader evidence connecting supervisory relationships with doctoral mental health (Jackman et al., 2024) and with studies describing the psychological and professional consequences of academic bullying (Moss et al., 2021; Zheng, 2026). However, the present cross-sectional data cannot determine direction. Negative supervision may contribute to distress, distress may affect perceptions of interactions, or both may reflect other contextual factors.

The qualitative findings underline the importance of power asymmetry. A postgraduate student may be encouraged to communicate concerns directly while simultaneously believing that the supervisor controls degree progress, resources, recommendations, or opportunities. Direct confrontation is therefore not structurally neutral. Recent work on dependency and vulnerability in doctoral supervision similarly emphasises how supervisory power can magnify the consequences of conflict (Joxe, 2026).

Academic rigor must also be distinguished from harmful supervision. Critical feedback, high standards, disagreement, and rejection of weak work are legitimate components of research training. Concern arises when power is exercised through repeated humiliation, intimidation, retaliation fears, obstruction, coercive control, or conditions that make reasonable disagreement unsafe.

Possible institutional safeguards include meaningful access to secondary supervisors or independent postgraduate tutors, confidential reporting outside the supervisory chain, behaviourally specific definitions of unacceptable conduct, anti-retaliation protections, and workable procedures for changing supervisors. These mechanisms can protect both students and supervisors by distinguishing harmful patterns from ordinary academic disagreement.

The Turkish context deserves further study. Existing Turkish research has examined mobbing among academic employees (Öztürk & Şahbudak, 2017), but postgraduate supervision crosses educational and employment boundaries. Larger research could examine discipline, institutional type, funding dependence, employment status, degree stage, supervisory structure, and access to independent support.

LIMITATIONS

This pilot has substantial limitations. The sample contained only 10 participants, so percentages cannot be interpreted as prevalence estimates. The cross-sectional design prevents causal inference, and non-probability recruitment may introduce selection bias. The 18-item behaviour inventory was study-specific and has not undergone psychometric validation. All variables were self-reported. The study was not powered for inferential hypothesis testing, subgroup comparisons involved only three self-identified cases, and the qualitative component was brief. A definitive study should use a substantially larger preregistered sample, psychometrically evaluated measures, longitudinal assessment where feasible, and a pre-specified analysis plan.

CONCLUSION

In this 10-participant pilot, negative supervisory behaviours were more frequently endorsed than the explicit label of systematic bullying or mistreatment. Greater behavioural exposure was associated with higher anxiety and perceived stress, while qualitative responses emphasized dependency, fear of disagreement, costly supervisor change, and supervisory control over progression or opportunities. These findings neither estimate prevalence nor establish causality. They identify a coherent signal worth testing at scale: postgraduate mental health may be intertwined with the power structure of supervision.

REFERENCES

Broadbent, D. E., Cooper, P. F., FitzGerald, P., & Parkes, K. R. (1982). The cognitive failures questionnaire (CFQ) and its correlates. British Journal of Clinical Psychology, 21(1), 1–16. https://doi.org/10.1111/j.2044-8260.1982.tb01421.x

Cohen, S., Kamarck, T., & Mermelstein, R. (1983). A global measure of perceived stress. Journal of Health and Social Behaviour, 24(4), 385–396. https://doi.org/10.2307/2136404

Jackman, P. C., et al. (2024). The supervisory relationship as a predictor of mental health outcomes in doctoral students in the United Kingdom. PLOS ONE.

Joxe, L. (2026). Dependency, vulnerability and bullying in university: Doctorate supervision through the lens of care. Canadian Journal for the Study of Adult Education, 37(2). https://doi.org/10.56105/cjsae.v37i02.5734

Moss, S. E., et al. (2021). STEM the bullying: An empirical investigation of abusive supervision in academic science. EClinicalMedicine, 40, 101121. https://doi.org/10.1016/j.eclinm.2021.101121

Moss, S. E., et al. (2022). The dark side of development: A systems characterization of the negative mentoring experiences of doctoral students. CBE—Life Sciences Education.

Öztürk, M., & Şahbudak, E. (2017). İşyerinde psikolojik taciz (mobbing) ve iş doyumu: Cumhuriyet Üniversitesindeki araştırma görevlileri üzerine bir çalışma. Sosyoloji Araştırmaları Dergisi, 20(2), 200–228. https://doi.org/10.18490/sosars.345512

Spitzer, R. L., Kroenke, K., Williams, J. B. W., & Löwe, B. (2006). A brief measure for assessing generalised anxiety disorder: The GAD-7. Archives of Internal Medicine, 166(10), 1092–1097. https://doi.org/10.1001/archinte.166.10.1092

Zheng, L. (2026). The arduous journey: Experiences and consequences of bullying and discrimination for PhD students from 34 countries. British Educational Research Journal. https://doi.org/10.1002/berj.70168